

University of Montana

ScholarWorks at University of Montana

Graduate Student Theses, Dissertations, &
Professional Papers

Graduate School

1998

Hydrothermal copper and platinum group element mineralization in the Revais Creek Intrusion : Flathead Indian Reservation west- central Montana

Daniel David Lauer
The University of Montana

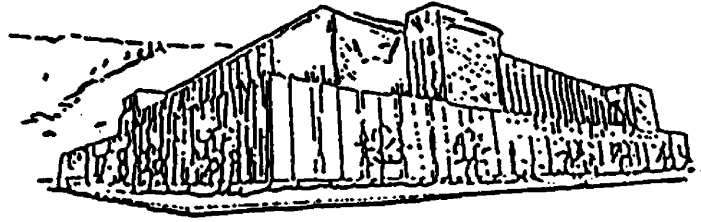
Follow this and additional works at: <https://scholarworks.umt.edu/etd>

Let us know how access to this document benefits you.

Recommended Citation

Lauer, Daniel David, "Hydrothermal copper and platinum group element mineralization in the Revais Creek Intrusion : Flathead Indian Reservation west-central Montana" (1998). *Graduate Student Theses, Dissertations, & Professional Papers*. 7129.
<https://scholarworks.umt.edu/etd/7129>

This Thesis is brought to you for free and open access by the Graduate School at ScholarWorks at University of Montana. It has been accepted for inclusion in Graduate Student Theses, Dissertations, & Professional Papers by an authorized administrator of ScholarWorks at University of Montana. For more information, please contact scholarworks@mso.umt.edu.



Maureen and Mike
MANSFIELD LIBRARY

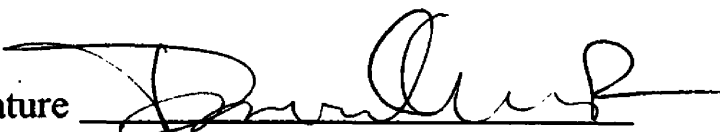
The University of **MONTANA**

Permission is granted by the author to reproduce this material in its entirety,
provided that this material is used for scholarly purposes and is properly cited in
published works and reports.

*** Please check "Yes" or "No" and provide signature ***

Yes, I grant permission

No, I do not grant permission

Author's Signature 

Date 12/11/98

Any copying for commercial purposes or financial gain may be undertaken only with
the author's explicit consent.

**Hydrothermal Copper and Platinum Group Element Mineralization
in the Revais Creek Intrusion.
Flathead Indian Reservation, West-Central Montana**

By
Daniel David Lauer

Presented in partial fulfillment of the requirements
for the degree of
Master of Geology

University of Montana
1998

Approved by


Chairman, Board of Examiners


Dean, Graduate School

12-22-98

Date

UMI Number: EP37930

All rights reserved

INFORMATION TO ALL USERS

The quality of this reproduction is dependent upon the quality of the copy submitted.

In the unlikely event that the author did not send a complete manuscript and there are missing pages, these will be noted. Also, if material had to be removed, a note will indicate the deletion.



UMI EP37930

Published by ProQuest LLC (2013). Copyright in the Dissertation held by the Author.

Microform Edition © ProQuest LLC.

All rights reserved. This work is protected against unauthorized copying under Title 17, United States Code



ProQuest LLC.
789 East Eisenhower Parkway
P.O. Box 1346
Ann Arbor, MI 48106 - 1346

Hydrothermal Copper and Platinum Group Element Mineralization in the Revais Creek Intrusion, Flathead Indian Reservation, West-Central Montana

Director: Ian M. Lange



Palladium, platinum, copper, and gold exist within the Revais Creek Intrusion (RCI). The RCI is a mafic intrusive dike-sill body located in the Revais Creek Mining district on the Flathead Indian Reservation in west-central Montana. This study included mapping, geochemical analysis, scanning electron microscopy (SEM), reflected light and transmitted light microscopy, Nd-Sm and Rb-Sr isochron age dating ($687 \pm 6\text{Ma}$), sulfur isotopy, and a fluid inclusion study.

Platinum and palladium have been detected throughout the body with a combined average of about 50 ppb. These metals are concentrated up to 12,483 ppb in one sample. Copper averages about 400 ppm and is concentrated to more than eleven percent. Gold is concentrated to as much as 2,250 ppb and has a background average of about seven ppb. All of these metals occur in anomalous amounts in five areas within the RCI.

The elements appear to be concentrated by post-magmatic hydrothermal processes. Several platinum group minerals (PGM) were semi-quantitatively identified including mertieite, stibiopalladinite, michnerite, atokite, sperrylite, kotulskite, isoferroplatinum, tulameenite and hollingworthite. The majority of the PGM were found on sulfide/silicate grain boundaries. A few of the PGM are completely surrounded by sulfide grains. Some PGM grains exhibit vein-like textures and are spatially associated with hydrothermally introduced quartz and other alteration minerals. High $\text{Cu}/(\text{Cu}+\text{Ni})$ ratios (0.99) and low $\text{Pt}/(\text{Pt}+\text{Pd})$ ratios (0.28) are comparable to known hydrothermal PGE deposits. The predominance of more soluble Cu, Pd, and Pt with respect to Ni, Ir, Os, Ru, and Rh also supports a hydrothermal origin.

The primary process of Cu, Pd, and Pt concentration in the RCI is believed to be aqueous transport of the metals as bisulfide complex ions in reducing, neutral, hydrothermal fluids.

TABLE OF CONTENTS

Abstract	ii
Table of Contents	iii
Acknowledgments	vi
List of Tables	vii
List of Figures	viii
Introduction	1
<i>Method and Scope of Investigation</i>	2
<i>Location and Access</i>	4
<i>Previous Studies</i>	6
<i>Exploration and Mining History</i>	6
Regional Geology	8
<i>Introduction</i>	8
<i>Tectonic Development</i>	8
<i>Prichard Formation</i>	12
<i>Ravalli Group</i>	13
<i>Burke Formation</i>	13
<i>Revett Formation</i>	13
<i>St. Regis Formation</i>	14
Geology of the Revais Creek Mining District	15
<i>Introduction</i>	15
<i>Mafic Intrusions of the Revais and Seepay Creek Areas</i>	15
<i>Older Mafic Generation</i>	17
<i>Younger dikes and related sill-like intrusions</i>	19
Metal Concentration Within the Revais Creek Intrusion	24
<i>Introduction</i>	24
<i>Green Mountain Mine</i>	25
<i>Bayhorse Prospect</i>	26
Petrography of the Revais Creek Intrusion	27
<i>Introduction</i>	27
<i>Unmineralized Gabbro</i>	27
<i>Weakly Altered</i>	27

<i>Strongly altered</i>	29
Mineralized Gabbro	30
<i>Partially Altered</i>	30
<i>Strongly Altered, mineralized</i>	36
<i>Oxidized, mineralized</i>	36
<i>High Copper, Low PGE Bearing RCI</i>	36
Geochemistry of the Revais Creek Intrusion	38
Scanning Electron Microscope Study	41
<i>Introduction</i>	41
<i>SEM Findings</i>	41
Sulfur Isotope Study of the Revais Creek Mining District	50
Fluid Inclusions in the Revais Creek Intrusion	54
Rb-Sr and Sm-Nd Isochron Dates of the Revais Creek Intrusion	57
<i>Introduction</i>	57
<i>Procedures</i>	57
<i>Results</i>	58
<i>Implications of the 687 ± 6 - 676 ± 14 Ma ages of the RCI</i>	61
Environment of Formation and Model of the Revais Creek Intrusion	63
<i>Partial Melting</i>	63
<i>Crustal Assimilation</i>	64
<i>Partial Melting of an Enriched Source</i>	64
Discussion	66
<i>Magmatic Concentration Processes</i>	67
<i>Sulfur Assimilation</i>	68
<i>Sialic Assimilation</i>	69
<i>Fe⁺⁺ Effect</i>	70
<i>S₂ and O₂ Fugacities (f)</i>	71
<i>Pressure and Temperature</i>	71
<i>Hydrothermal Concentration of Precious Metals</i>	72
<i>Comparison to PGE deposits of documented hydrothermal origin</i>	73
<i>Ore-gangue textures</i>	75
<i>Hydrothermal alteration</i>	76
<i>Hydrothermal Transport</i>	79
<i>Copper, Nickel and PGE behavior in hydrothermal solutions</i>	81
<i>Comparison of the RCI with Other Similar Deposits</i>	82
<i>Combined Magmatic and Hydrothermal Processes</i>	84

Conclusions	85
Appendix A	87
References	89

ACKNOWLEDGMENTS

This study would not have been possible without the financial support, advice and patience of many individuals and organizations. Thanks goes to the Confederated Salish and Kootenai Tribes of the Flathead Indian Reservation for funding the fieldwork and analysis costs. I also thank Ian Lange for providing advice and guidance throughout the study as well as reviewing several drafts. Don Hyndman and George Woodbury also provided useful comments and suggestions for the final draft. Steve Buckley provided me with the means and the ambition to study this deposit. Steve also provided indispensable field guidance without which I could have spent all my fieldwork time mired in the stratigraphy of the Lower Belt Supergroup. Advice and references from Michael Zientek of the USGS was extremely helpful in sorting out the PGE literature. Oscar Robertson, also of the USGS examined some additional samples with the SEM to confirm that I was not missing anything. Thanks also goes to Ken Foland for isotope work performed for me and the background support that came with it.

My parents, Christopher and Margaret Lauer, my grandparents, Bo and Ellie Wright, and my wife, Andrea Lauer also deserve my utmost gratification for supporting me in many uncountable ways.

List of Tables

Table 1.	Average Major (normalized to 100%) and Trace Element Geochemistry for Mafic Intrusives in The Revais Creek Area	16
Table 2.	Average Major and Trace element Geochemistry for different rock types within the RCI	22
Table 3.	Typical Mineralogy of partially altered samples from the RCI	28
Table 4.	Typical Alteration Assemblage of Highly Altered RCI.	30
Table 5.	PGE and other precious metal minerals in the RCI located and identified using the JEOL-6100 SEM at Montana State University	37
Table 6.	Sulfur isotope analysis results from the Revais Creek district and selected other mineralized areas for comparison	51
Table 7.	Fluid inclusion data from 2 mineralized samples	55
Table 8.	Rb-Sr and Sm-Nd analytical data for sample of the RCI	58
Table 9.	Geochemistry of Windermere Age Rocks Including the RCI	62
Table 10.	Evidence for magmatic and hydrothermal concentration in enriched zones within the RCI	66
Table 11.	Evidence for magmatic and hydrothermal concentration in enriched zones within the RCI	74

List of Figures

Figure 1.	Location of the study area	5
Figure 2.	Generalized geology of the Revais Creek and Seepay Creek mining districts, Flathead Indian Reservation, Montana	10
Figure 3.	Idealized stratigraphic column of the Revais Creek and Seepay Creek Mining districts, Flathead Indian Reservation, Montana	11
Figure 4.	FeO*-Na ₂ O+K ₂ O-MgO ternary diagrams for the a)Paradise Sill, b)Plains Sill, and c) Whiskey Gulch Sill	19
Figure 5.	FeO*-(Na ₂ O+K ₂ O)-MgO Ternary diagram of unmineralized samples from the Revais Creek Intrusive	20
Figure 6.	Photomicrograph of slightly altered Revais Creek Intrusion	29
Figure 7.	Crossed nicols photomicrograph of RCI gabbro that has undergone strong hydrothermal alteration. Blue mineral is probably chlorite and/or other hydrosilicate mineral.	31
Figure 8.	Two photomicrographs. a) Photomicrograph of partially altered, mineralized RCI. Note presence of partially altered clinopyroxene (cp). Crossed nicols. b) Reflected light photomicrograph of same region as 'a'.	32
Figure 9.	Two photomicrographs. a) Crossed nicols photomicrograph of relationship between relict plagioclase(plg) and chalcopyrite-chalcocite (cp-cc) grain. Note cp-cc grain infilling of 'tattered' end of plagioclase lath. b) Same view as 'a' in reflected light.	33
Figure 10.	Two photomicrographs of examples (a & b) of magnetite(mg) embayed by chalcopyrite-chalcocite (cp-cc) grains. Note skeletal magnetite/ilmenite (mg-il) in upper right hand corner of 'b'. Both are reflected light photomicrographs.	34
Figure 11.	a) Crossed nicols photomicrograph of strongly altered, mineralized RCI. b) Same view as 'a' in reflected light.	35

Figure 12.	Crossed nicols photomicrograph of a strongly oxidized sample from the RCI. The red and orange grain dominating the photo is composed of cuprite and possibly goethite and was formerly a chalcopyrite-bornite mixture. The opaque masses are magnetite	37
Figure 13.	Sulfur log vs. metal log plots. Lines and r ² values are from linear regression	39
Figure 14.	Palladium vs. Au, Cu, Pt, and Ni log plots of mineralized samples from the RCI	40
Figure 15.	SEM BEI showing sperrylite (sp) grain with hollingworthite (ho) in the center	43
Figure 16.	SEM BEI showing small sperrylite (sp) grain on chalcocite (cc) grain boundary. Dark area surrounding sperrylite is possibly biotite (bi) or another hydrosilicate.	43
Figure 17.	SEM BEI of same area as in Figure 33a & b. Note chalcopyrite-bornite (cp-bn) grain rimmed with chalcocite (cc) with sperrylite (sp) grain on boundary. Also note abundance of bright mertieite (mr) grains scatted in the center of the photo. Much of the dark area is quartz (qz) with granoblastic texture.	44
Figure 18.	SEM BEI closeup of bright mertieite grains seen in Figure 13.	44
Figure 19.	SEM BEI of large double grain of atokite (at) adjacent to chalcopyrite (cp) grain rimmed by chalcocite (cc). This atokite grain can also be seen in Figure 6. Surrounding dark area is silicate (si), possibly pyroxene	45
Figure 20.	SEM BEI closeup of sperrylite (sp) grain along chalcocite (cc)-quartz (qz) grain boundary. Along this boundary is a hydrosilicate possibly chlorite (cl) or epidote.	45
Figure 21.	SEM BEI showing long vein-like stibiopalladinite (st) grain in mass of very fine grained hydrosilicate minerals (chlorite and or epidote)	46
Figure 22.	SEM BEI showing mertieite (mt) grain in hydrothermal quartz	46
Figure 23.	SEM BEI showing diamond shaped kotulskite (kt) grain in chalcocite (cc). Dark rim around diamond is an unidentified silicate mineral, possibly chlorite.	47

Figure 24.	SEM BEI showing isoferroplatinum (ip) grain in chalcocite (cc) altered from chalcopyrite (cp). Dark veins are unidentified silicate mineral, possibly chlorite.	47
Figure 25.	SEM BEI showing two small tulameenite (tu) grains on chalcocite (cc)-silicate grain boundary	48
Figure 26.	SEM BEI showing a michnerite (mi) grain in quartz (?) (qz) between chalcocite (cc) and magnetite (?) (mg).	48
Figure 27.	SEM BEI showing conglomerate of at least four different precious metal phases including Sperrylite (?) (Sp), silver-rich electrum (el), kotulskite (kt) and telluropalladinite (?) (Tp). Most surrounding material is chalcocite (cc) with veins of unidentified silicate (chlorite or epidote). Note "Si-Te" grain, this grain contains silicon and tellurium	49
Figure 28.	Sm-Nd isochron based on three mineral fractions, whole rock residue, and whole rock from the RCI. The age calculated from this plot is 745 ± 23 Ma and the initial $^{143}\text{Nd}/^{144}\text{Nd}$ ratio is 0.511820 ± 0.000028	59
Figure 29.	Sm-Nd isochron based on two mineral fractions, whole rock residue, and whole rock from the RCI. The age calculated from this plot is 676 ± 14 Ma and the initial $^{143}\text{Nd}/^{144}\text{Nd}$ ratio is 0.511907 ± 0.000018	59
Figure 30.	Rb-Sr isochron based on three mineral fractions, whole rock residue, and whole rock from the RCI (pyroxene excluded). The age calculated from this plot is 687 ± 6 Ma and the initial ($^{87}\text{Sr}/^{86}\text{Sr}$) ratio is 0.70487 ± 0.00004	60
Figure 31.	Stages in the formation of a typical magmatic ore and subsequent remobilization	67
Figure 32.	Ternary diagram illustrating the effect of silica contamination of a FeO-FeS melt.	69
Figure 33.	a) Crossed nicols photomicrograph of recrystallized quartz. Note 120° annealed quartz grain intersections. b) Same view as 'a' in plane light. Large opaque grain on right side of photo is chalcopyrite and bornite (cp-bn). Several of the small opaque grains dotting the photo are mertieite (Pd_3Sb_2) (mr). Note the small grain of sperrylite (sp) on the boundary of the cp-bn grain. These PGM grains can also be seen in Figures 17 and 18.	77

Figure 34. Log f_{O_2} - pH diagrams for the system Pt(Pd)-H-O-S showing the stability of various Pt(Pd) phases and their solubility as bisulfide complex. **a)** The Pt-H-O-S system. **b)** The Pd-H-O-S system 80

Introduction

The Revais Creek Intrusion is a quartz-normative, gabbroic intrusive body of continental tholeiite affinity located in the Revais Creek and Seepay Creek mining districts on the Flathead Indian Reservation, Montana. The Revais Creek intrusion (RCI) is the largest of several small dikes and sills in the area. Platinum (Pt) and palladium (Pd) have been detected throughout the RCI. The combined (Pt + Pd) average from unmineralized samples of 50 (range 13-171, STD = 26) parts per billion (ppb). Pt + Pd concentrations are as high as 12,483 (range 467-12,483, STD = 3,288) ppb in altered gabbro. Copper occurs throughout the RCI in unmineralized samples averaging 409 (range 176-801, STD = 118) parts per million (ppm), and is concentrated in the same areas as the PGE to more than 11 percent. Gold has a background average of 12 (range 2-128, STD 21) ppb, and is concentrated in the same zones as the other metals to as much as 2,250 (range 30-2,250, STD 511) ppb.

The age of the RCI is 687 ± 6 Ma (Rb-Sr isochron). The intrusion is hosted by the Prichard, Burke, and Revett formations of the Lower Belt Supergroup. Stratigraphically, the lowest portion of the RCI is hosted by the Prichard Formation where the RCI cuts across bedding at a steep angle. The intrusion becomes less discordant, roughly paralleling bedding, as it enters the overlying Burke and Revett formations. At least five zones of disseminated copper sulfide and anomalous concentrations of Cu and PGE occur in the less discordant portion of the RCI. The spatial location and the size of these zones are difficult to quantify. Poor mine records and collapsed workings do not allow for a detailed evaluation of the spatial locations or other details of the ore distribution. No

anomalously high metal concentrations are known to occur in the lower, more discordant, portion of the intrusion.

All of the zones with concentrated metal values have varying degrees of shearing and hydrothermal alteration, low Pt:Pd ratios (1:2.6) and up to six percent chalcopyrite + bornite + supergene chalcocite. In part of at least one of the zones of anomalously high metal concentrations, the RCI is strongly sheared and oxidized with varying degrees of supergene gossan. This oxidized area is characterized by higher Pt:Pd ratios (1:1.6), contains supergene chalcocite, and copper sulfides replaced by copper oxides. In the partially altered, high-grade zones, several platinum group minerals (PGM) have been identified. Most commonly, PGM occur spatially associated with chalcocite, chalcopyrite and bornite. Other PGM are found in small grains and vein-like “conglomerates” possibly associated with hypogene alteration mineralogy including quartz showing granoblastic texture indicating that it was hydrothermally introduced. Only one small PGM, a 5 micron mertieite grain, was found in the oxidized samples.

Method and Scope of Investigation

This study describes the Cu-PGE mineralization in the mafic dikes, specifically the RCI, intruding the Prichard Formation and Ravalli Group in and around the Revais Creek mining district.

The goals of this study were to:

- Determine the age and origin of the RCI and its relationship with the sills and the rocks of the Belt Supergroup
- petrographically describe the RCI

- ascertain the mode of occurrence of the PGE
- develop a model(s) of copper and precious metals mineralization of the RCI

Methods used in this study included:

- Geologic mapping and float soil sampling to determine the extent of the Revais Creek intrusion
- Sm-Nd and Rb-Sr isochron age dating of the intrusion
- major and trace element geochemical analyses
- thin section petrography
- scanning electron microscope (SEM) semiquantitative PGE mineral analysis
- sulfur isotopy
- mineral fluid inclusion determinations.

Field mapping and sampling of the RCI was conducted in the summer of 1993.

Thin section petrography of approximately twenty samples was completed using transmitted and reflected, polarizing, light microscopy. Thin section data and petrography were combined with the work of Kell (1992). Scanning electron microscope work was accomplished with a JEOL-6100 Scanning Electron Microscope and NORAN Energy Dispersive X-Ray Detector, supported by a SUN workstation and semi-quantitative analysis software at Montana State University. X-Ray scans, elemental maps, and phase analyses helped identify particular PGE and other precious metal phases. Backscattered electron images (BEI) were also obtained for most of the PGE phases identified. Sm-Nd and Rb-Sr age date analyses were performed by Dr. Ken Foland at Ohio State University. He obtained a five point isochron using mineral separates of pyroxene, hornblende, whole-rock, leached whole-rock, and whole-rock leachate. The isochron yields a mean square weighted deviation (MSWD) of 1.2 suggesting that the age date is valid.

Geochemical analyses were performed by Bondar-Clegg & Company Ltd. As

many as fifty different major oxide and trace elements analyses were obtained per sample. Lower detection limits, extraction, and technique for all types of analyses are listed in Appendix A.

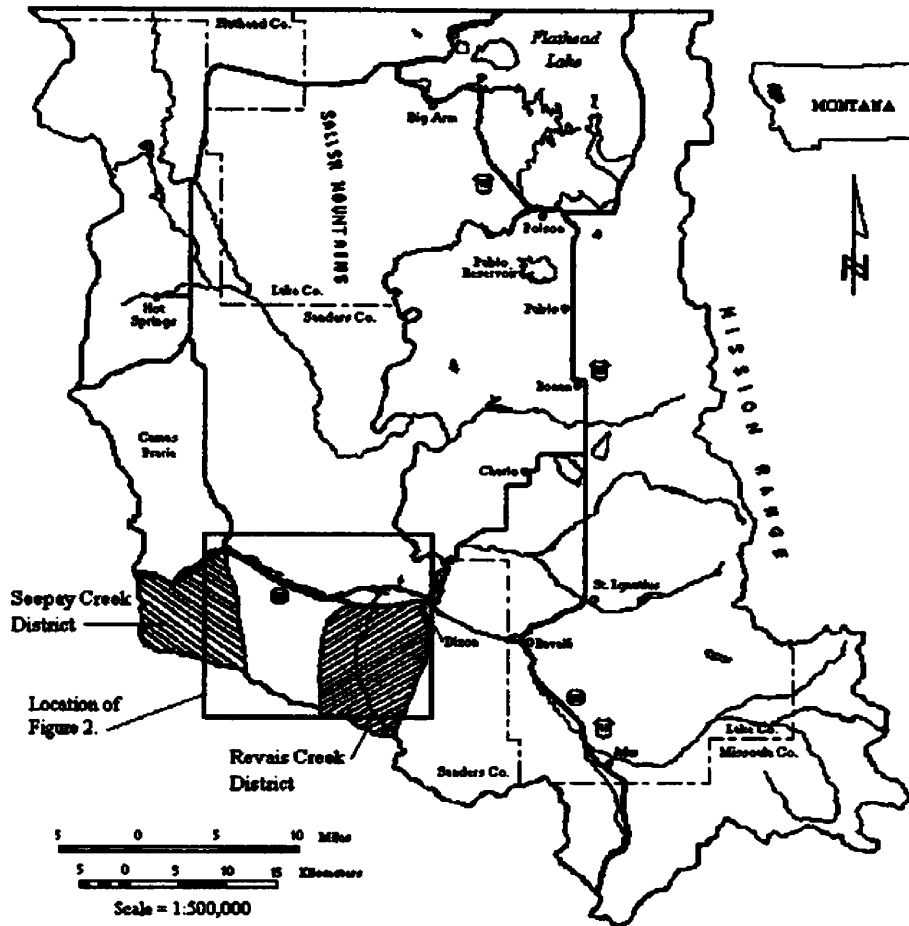
Twelve samples were analyzed by Dr. Ed Ripley at Ohio State University for sulfur isotope ratios. Six samples were from the RCI and six were from sedimentary rocks hosting the intrusion.

This paper describes the results of each of these methods. The data gathered from the study are then used to develop models for the formation of the RCI and concentration of the metals.

Location and Access

The Revais Creek mining district lies in the southern part of the Flathead Indian Reservation in north-western Montana about nine kilometers south-west of the town of Dixon. Montana Highway 200 provides access to logging roads that cover the entire area. The Confederated Salish and Kootenai Tribes (CSKT) of the Flathead Indian Reservation control all the mineral rights in the Revais Creek district. Figure 1 shows the general locations of the Flathead Indian Reservation and the Revais Creek area. The area covered in this study includes the Revais Creek mining district, the western half of the Seepay Creek mining district, and the area between. The RCI outcrop trace extends the length of the study area but mineralization occurs only in the Revais Creek district.

Topographic relief in the study area is about 740 meters (1,060 to 1,800 meters). Slopes of 25-35 degrees are common. Except for a few clear cuts, the district is heavily



FLATHEAD INDIAN RESERVATION

Figure 1. Location of the study area.

forested with lodge-pole pine, larch, and ponderosa pine. The undergrowth and soil development varies within the district but is typically strong. Despite the dense flora, some well-used logging roads provide relatively easy access to all parts of the study area. However, due to surface weathering and soil development, outcrops of the PGE-bearing intrusion, especially fresh ones, are few.

Previous Studies

The geology and ore deposits of the Revais Creek district have been studied by several investigators. Mineral resource status information for the Flathead Indian Reservation compiled by the U.S. Geological Survey and the U.S. Bureau of Mines (Mudge *et al.*, 1976) contains information on mining in the Green Mountain area within the RCI. Older reports by Sahinen (1936) and Sample (1942) describe the mine workings and general geology of the Revais Creek mining district. Recent studies by Dahy (1986) and Kell (1992) address the mineralogy and petrography of the RCI. Dahy (1986), described the mineralogy of the dike whereas Kell (1992) carefully studied the mineralogy, petrography, and geochemistry of the RCI. Kell (1992) is the only investigator who concentrated on the PGE occurrence.

Several Belt Supergroup investigators discuss the rocks in the study area. Cressman (1989) reported on the stratigraphy of the Prichard Formation exposed to the west of the Revais Creek district. Ryan and Buckley (1993) described stratabound Cu-Ag mineralization in the Revett Formation adjacent to the RCI, and Mauk (1983) described the stratigraphy and sedimentation of the local Burke and Revett formations.

Exploration and Mining History

Mudge *et al.* (1976), estimated that between 1910 and 1949 more than nine thousand tons of ore were shipped from the Revais Creek district, mostly from the RCI. It included 1,392,791 pounds of copper, 5,752 ounces of silver, and 1,277 ounces of gold. Mudge *et al.* (1976) also noted that there is as much as 0.10 ounces per ton (OPT) PGE in

the gabbro. Most of this production came from the Green Mountain Mine. Presently, all of the land in the district is under the jurisdiction of the Confederated Salish and Kootenai Tribes, and no active mines or mills exist (Mudge *et al.*, 1976).

Exploration work done in the early 1970's suggests that the higher grade Cu-PGE deposits are restricted to the contacts between the Belt Supergroup rocks and the gabbroic intrusions, and that disseminated copper minerals occur throughout the dike. Several core holes were drilled across a contact in the Green Mountain mine area. One hole cuts a 2 meter vein containing more than 7 percent copper, 0.83 ounces per ton (OPT) silver, and trace amounts of gold. Another hole contains a 2.5 meter "sludge" sample from the contact zone which assayed 0.45% copper, 4.6 OPT silver, 40.64 OPT gold, and 0.085 OPT platinum (Mudge *et al.*, 1976). However, this hole was plagued by poor core recovery.

Recent work done by the CSKT includes six reverse-circulation (RVC) drill holes, grid soil sampling, and geophysical studies gathering very low frequency (VLF) electromagnetic, magnetic, and induced polarity (IP) data along the soil grids. One of the six RVC holes intercepted a forty-foot interval containing elevated copper and PGE values. The soil sampling and geophysical studies were useful in determining the location of the RCI in areas plagued by poor exposure. No new mineralized zones were located during this study.

Regional Geology

Introduction

Most of the Flathead Indian Reservation is underlain by rocks of the Precambrian Belt Supergroup. Figure 2 is a geologic map of the study area showing the units of the Belt Supergroup. Figure 3 contains a stratigraphic column from this area. These rocks have been regionally metamorphosed to greenschist facies by compression (burial) and heat, and subsequently folded and thrust during Laramide compression (Norwick, 1972; Cressman, 1989; Porder, 1997). The Belt Supergroup contains fine-grained quartzite, red and green argillite, argillaceous carbonate, dark grey laminated argillite and quartzite of Middle Proterozoic age. It is about 15 kilometers thick in the Plains area (Winston and Link, 1986). Large mafic sills account for about 2 kilometers (or 13%) of the stratigraphic column (Winston and Link 1993). Most of these sills are within the Prichard Formation and some are thought to be contemporaneous with sedimentation. There is evidence that the sills intruded into saturated, unlithified, sediment (Buckley and Sears, 1992; Höy, 1989). The intrusions are typically conformable to bedding, but in some locations, they cut bedding at low angles.

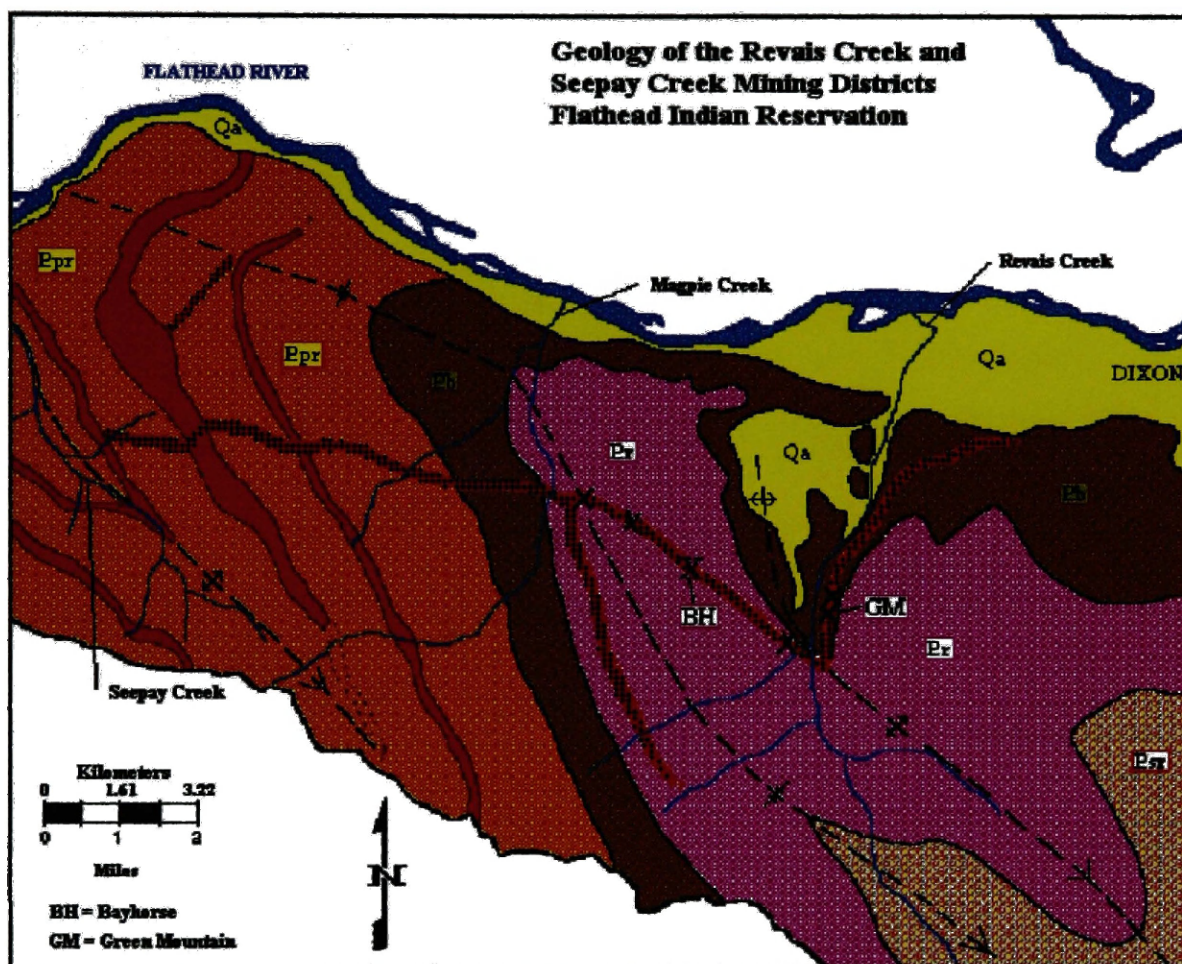
Tectonic Development

An intracratonic rift basin, a marine-trailing continental margin, an episutural basin, and a meteorite impact basin have all been proposed for the origin of the Belt basin (Winston and Link 1993). Recent mapping and U-Pb dates by Sears et al, (1998) supports continental rifting beginning about 1470Ma. However, most workers agree that

the Belt basin was formed by block faulting and subsidence of the continental crust beginning in the Middle Proterozoic time. The sedimentary rocks of the Prichard Formation were deposited into the deep basin in a shallowing upward sequence (Cressman, 1988). The Burke and Revett formations were deposited as alluvial apron progradations and retreats. The St. Regis Formation was deposited as sand flats and mud flats (Winston and Link 1993). Large mafic sills were emplaced in the Prichard Formation as the basin subsided and the Middle Belt Carbonate and the Missoula Group were deposited (Winston and Link 1993).

Following deposition of the Belt Supergroup, the East Kootenay orogeny, at 1,300-1,350 Ma (McMechan and Price, 1982), subjected the basin to east to northeast trending compression resulting in gentle folding. The East Kootenay orogeny was possibly the result of convergence of the Siberian and North American cratons (Cressman, 1988). The Goat River orogeny caused block faulting through the Belt Basin at about 800 to 900 Ma (Winston & Link 1993).

Windermere age (780 - 730 Ma) volcanism accompanying rifting in western North America produced the mafic igneous rocks found in the Mackenzie Mountains to the north in Canada (Jefferson and Parrish, 1988). The Mackenzie Mountains mafic rocks are of similar age and composition to the RCI (Table 9) suggesting that the RCI could be related to Windermere tectonism. Despite an age difference of 45 to 95 million years, it seems that similar conditions created the mafic igneous rocks of the Mackenzie Mountains and the RCI. It is possible that the RCI intruded the Belt Supergroup after the gentle folding of the East Kootenai Orogeny. The sill-like section of the RCI does not completely



- Qa Quaternary alluvium
- Revais Creek Intrusion
- Prichard Formation Sills
- Proterozoic St. Regis Formation
- Proterozoic Revett Formation
- Proterozoic Burke Formation
- Proterozoic Prichard Fo. (Undifferentiated)

Figure 2. Generalized geology of the Revais Creek and Seepay Creek mining districts, Flathead Indian Reservation, Montana (This study; Buckley, 1993 personal communication).

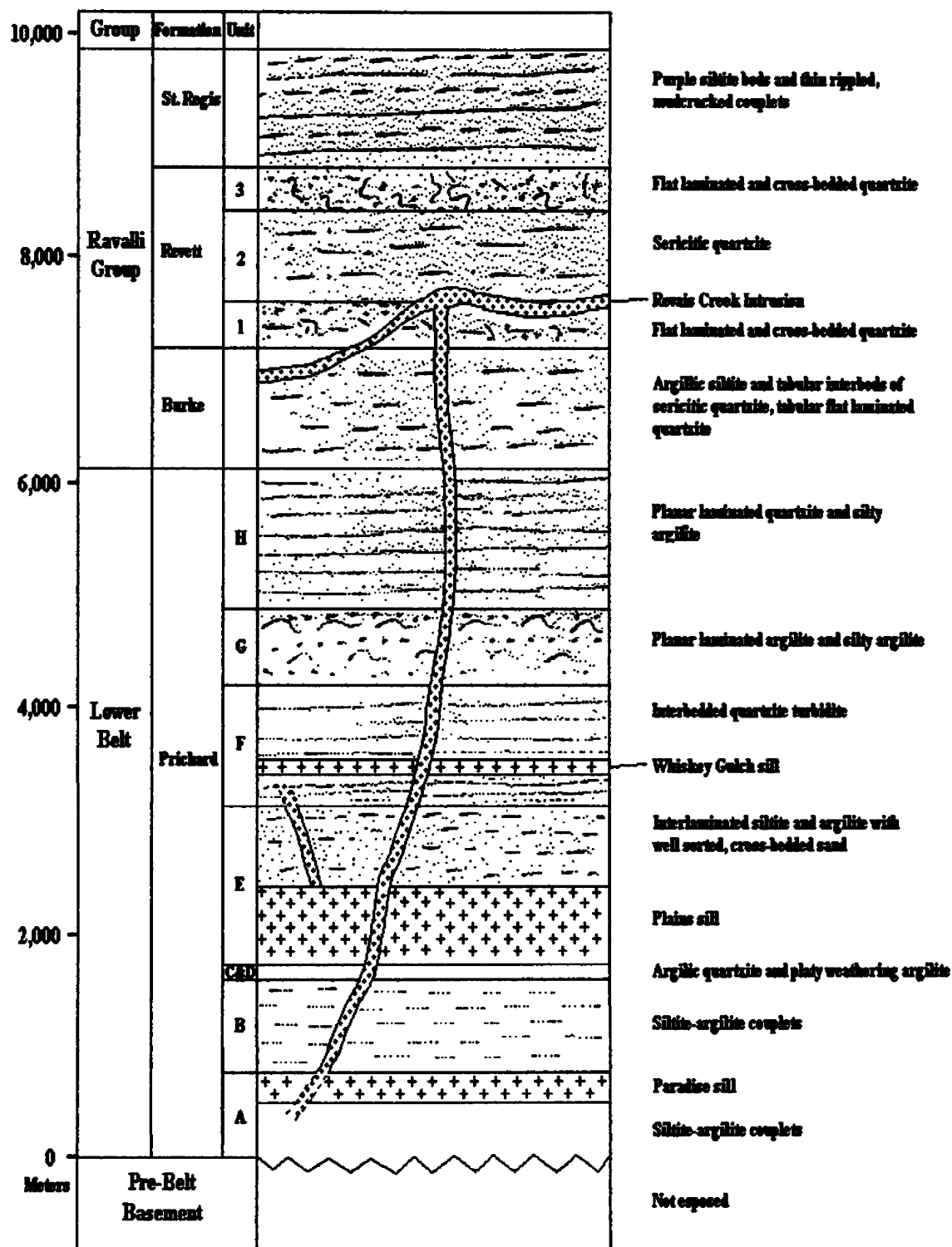


Figure 3. Idealized stratigraphic column of the Revais Creek and Seepay Creek Mining districts, Flathead Indian Reservation, Montana (Compiled from this study, Cressman, 1989, Sears, 1992, Herberger, 1990).

conform to bedding which suggests that it intruded into slightly folded sediments.

However, it is possible that the intrusion cut up section through horizontal, unfolded sediments.

Prichard Formation

Cressman (1989) described the Prichard Formation in detail. Other recent works include those by Mudge *et al* (1976) and Winston and Link (1986). The Prichard Formation is the oldest of the Belt Supergroup, and comprises the bottom one-fourth to one-third of the Supergroup. The Prichard Formation is divided into eight members named A through H, from oldest to youngest. The thickness of the exposed Prichard Formation in the study area is approximately six kilometers. The bottom of the Prichard Formation is not exposed here or anywhere else. The stratigraphic column in Figure 3 details the units of the Prichard Formation.

In the Seepay Creek area, 1,160 meters of exposed members A and B consist of siltite-argillite turbidite couplets. Member C is 60 meters thick and is characterized by argillic quartzite turbidite. Member D is a platy-weathering argillite 60 meters thick. Member E exhibits shallow water features such as hummocky cross-stratification and desiccation cracks. The member consists of about 730 meters of interlaminated siltite and argillite with the occasional well-sorted cross bedded quartzite. Member F is 915 meters thick and consists of planar laminated argillite and silty argillite that contain abundant iron sulfide laminae. Member G, 670 meters thick, is characterized by interbedded quartzite turbidite. Member H has similar lithology as member F and it is approximately 1,220 meters

thick (Cressman 1989; Mudge *et al* 1976; Winston and Link 1993).

At least three large mafic sills intrude the Prichard Formation in the Seepay Creek area. The Paradise sill is about 275 meters thick and intrudes along the A-B contact. The 640 meter thick Plains sill intrudes along the D-E contact. The Whiskey Gulch sill is 120 meters thick and intrudes the lower part of Member F. These sills are described in a following section.

Ravalli Group

Overlying the Prichard Formation are three units of purple to green argillite and light grey to lavender quartzite of the Ravalli Group. These three units, from youngest to oldest, are the St. Regis, Revett, and Burke Formations with thicknesses of: 940 meters (3,100 feet), 1,606 meters (5,300 feet), and 1,060 meters (3,500 feet), respectively (Ryan and Buckley, 1993).

Burke Formation

The lower part of the Burke Formation is characterized by tabular, flat-laminated quartzite and siltite beds. The upper part is composed of argillic siltite and tabular interbeds of sericitic quartzite that thicken upward (Winston and Link, 1986).

Revett Formation

The Revett Formation is divided into lower, middle, and upper members. A gradational contact separates the Burke Formation from the lower member of the Revett Formation. The lower and the upper members are characterized by flat-laminated and cross-bedded quartzite while the middle member consists of sericitic quartzite (Winston and Link, 1986). In some areas adjacent to the RCI, the Revett Formation contains

stratabound Cu-Ag minerals which occur at interfaces between oxidized and reduced beds (Ryan and Buckley, 1993).

The Cu-Ag mineralization adjacent to the RCI is similar to that found in large Cu-Ag deposits, such as the Spar Lake (or Troy) deposit located in the Revett Formation in northwestern Montana, (Ryan and Buckley, 1993). Lange and Sherry (1983) contend that these Revett-hosted Cu-Ag deposits were formed as oxidizing, metal-rich fluids which migrated up syndepositional basement-controlled faults. These metal-bearing fluids traveled laterally along permeable horizons and deposited sulfide minerals when reducing, sulfur-bearing zones were encountered. Ryan and Buckley (1993) suggest that the Cu-Ag occurrences exist along an east-west trending fault. This fault, known as The Jocko Line, was proposed by Winston (1986) as a syndepositional, basement-controlled fault.

St. Regis Formation

The St. Regis Formation overlies the Revett Formation of the Ravalli Group. Purple siltite beds and thin, rippled, and mud-cracked couplets distinguish the St. Regis Formation. The Middle Belt Carbonate and the Missoula Group overlie the St. Regis Formation (Winston and Link, 1986).

Geology of the Revais Creek Mining District

The general geology of the greater Revais Creek Mining district is shown in Figure 2. An idealized stratigraphic column of the area is shown in Figure 3. Most of the district is underlain by Ravalli Group quartzite and argillite (Sahinen, 1936; Sample, 1942). About 5,915 meters (19,400 feet) of the Prichard Formation is exposed in the Seepay Creek mining district. The base of the Prichard is not exposed but the formation is believed to exceed 6,060 meters (20,000 feet) thick (Mudge *et al* 1976).

At least three mafic sills with a combined thickness of 1 kilometer intrude the Prichard Formation. These sills account for sixteen percent of the exposed 6 kilometer thickness. Mafic dikes and related sill-like bodies, including the RCI, cut all of the formations in the area including the upper-most sill. The sedimentary rocks and sills of the Belt Supergroup have been regionally metamorphosed and folded into northwest-trending folds.

Mafic Intrusions of the Revais and Seepay Creek Areas

There are at least two distinct generations of mafic intrusions in the Revais and Seepay Creek areas. The older generation is characterized by regionally extensive, tholeiitic sills intruding the Lower Belt formations. At least three are exposed in the Seepay Creek Anticline (Figure 2). Many small tholeiitic dikes and related sill-like bodies scattered through the formations typify the younger generation. The largest and most extensive of the younger intrusions is the RCI.

Table 1. Average Major (normalized to 100%) and Trace Element Geochemistry for Mafic Intrusions in The Revais Creek Area (see Appendix A for analytical information).

Samples	RCI (Un-Min.) ¹	Paradise Sill ^{1,2}	Plains Sill ^{1,2}	Whiskey G. Sill ^{1,2}	Avg. C.T. ³
n	64	32	87	21	946
SiO ₂ Wt. %	50.38	55.80	56.10	51.31	51.50
TiO ₂	2.75	0.81	0.98	1.17	1.20
Al ₂ O ₃	12.53	14.91	14.47	14.05	16.30
Fe ₂ O ₃ *	16.77	10.59	11.12	13.54	11.60
MnO	0.23	0.15	0.16	0.20	0.17
MgO	4.92	4.74	5.01	6.62	5.90
BaO	0.02	nd	nd	nd	nd
CaO	8.50	7.68	7.62	8.14	9.80
Na ₂ O	2.33	1.72	2.19	2.51	2.50
K ₂ O	0.77	1.38	0.93	0.23	0.86
P ₂ O ₅	0.12	0.05	0.06	0.01	0.21
Cr ₂ O ₃	0.01	nd	nd	nd	nd
LOI	0.66	2.15	1.32	2.04	0.81
Total	100	100	100	100	100
Au (ppb)	12	<1 (7) ⁴	<1 (16)	nd	nd
Pt (ppb)	22	<5 (7)	<5 (16)	nd	nd
Pd (ppb)	28	<1 (7)	<1 (16)	nd	8.3 ⁵
Ag (ppm)	<0.2	<0.2	<0.2	<0.2	nd
Cu	409	28	76	138	141 (83)
Pb	5	4	1.15	7	nd
Zn	48	64	64	45	nd
Mo	<1	<1	<1	<1	nd
Ni	24	12	23	39	77 (158)
Co	19	18	16	20	35 (156)
Cd	<1	<1	<1	<1	nd
Bi	<1	<1	<1	<1	nd
As	2.8	4.4	-0.1	-0.1	nd
Sb	0.24	1.1	0.65	1.5	nd
Fe (%)	3.89	3.62	3.77	3.3	nd
Mn (ppm)	355	505	573	573	nd
La	8	4	6	1	nd
Te	<0.2	<0.2	<0.2	<0.2	nd
Ba	107	105	133	44	200 (146)
Cr	29	66	53.2	63	153 (151)
V	208	84	116	109	250 (151)
Hg	<0.01	<0.01	<0.01	<0.01	nd

nd = not determined

n = number of samples

¹ All samples are unmineralized but have undergone varying degrees of alteration

² Samples from sills collected by Buckley, (1993). Additional analyses can be found in Poage, (1997).

³ Average continental tholeiite (Prinz, 1967; Manson, 1967)

⁴ Parenthesis indicates number of samples for individual elements.

⁵ Crocket, (1981)

The two generations of mafic intrusions are quite similar geochemically but they do have some distinct differences: the older amphibole-bearing sills appear to have hydrated before crystallization (Sims *et al*, 1994; Poage, 1997) while the younger clinopyroxene-bearing RCI remained dry. Also, the RCI contains significantly more Fe₂O₃ and TiO₂ and less SiO₂ than the older Prichard sills (Table 1). Trace element geochemistry also distinguishes the RCI from the sills. Specifically, the RCI contains elevated amounts of copper, vanadium, gold, and PGE's and significantly less Cr and Sb with respect to the sills.

Older Mafic Generation

The three large sills exposed in the Seepay Creek anticline, from lowest to highest stratigraphically, are the Paradise, Plains, and Whiskey Gulch. Their thicknesses are 275, 640, and 120 meters respectively. U-Pb ages of 1469 ± 2.5 and 1457 ± 2 Ma for the Plains and Paradise sills respectively were obtained by Sears *et al*, (1998). Similar Lower Belt formation sills have been dated elsewhere. A granophyric differentiate from the Crossport sill near Eastport, Idaho yielded a concordant U-Pb (zircon) date of $1,433 \pm 10$ Ma and a Rb-Sr (whole rock) date of $1,285 \pm 165$ Ma (Zartman *et al*, 1982). Correlative sills in the Moyie Lake region were dated using three different isotope systems. They include discordant U-Pb (zircon) with an intercept of $1,445 \pm 10$ Ma, K-Ar (hornblende) 836-1,918 Ma, and Sm-Nd tCHUR model ages of 1.43, 1.44, and 1.55 Ga (Burwash and Wagner, 1989). Sills stratigraphically higher in the Belt section range from 1,165 to 1,345 Ma (Burwash, 1993).

The sills in the Seepay Creek Anticline are composed of tholeiitic actinolite-

bearing gabbro and are widespread throughout the Belt Supergroup (Sims *et al*, 1994; Sears *et al*, 1998). Sims *et al*, (1994) and Poage, (1997) suggest that, due to the lack of relict pyroxene, the sills may have taken on water from the sediments during intrusion and crystallized as amphibole-bearing gabbro. Sims *et al* (1994) also observed that the sills were later recrystallized, during regional metamorphism, to the greenschist facies while preserving primary igneous textures. The Paradise and Plains sills are geochemically differentiated; the thinner Whiskey Gulch sill is not. The Paradise sill shows a gradual geochemical differentiation upward from quartz tholeiite to quartz diorite. Conversely, the Plains sill exhibits a relatively constant tholeiitic geochemistry for the bottom two-thirds of the sill; the top one-third is a miarolitic granophyre.

Differences in physical appearance, major oxide, and trace element geochemistry suggest that the Whiskey Gulch sill formed differently than the other sills. Compared with the other two sills, the Whiskey Gulch sill is not geochemically differentiated, does not appear to have intruded into wet sediments, has lower average SiO₂, more copper, and exhibits other differences in trace element concentration. Figures 4a, 4b, and 4c show FeO^{*}-(Na₂O+K₂O)-MgO ternary diagrams for data from sample traverses of the Paradise, Plains, and Whiskey Gulch sills respectively. The traverse samples were collected by Steve Buckley, CSKT geologist. Differentiation trends of the Paradise and Plains sills are shown in Figures 4a and 4b. Differentiation is not apparent in the Whiskey Gulch data (Figure 4c).

In several areas where they are exposed, the Plains and correlative Moyie sills exhibit evidence of intrusion into wet sediments. These observations support

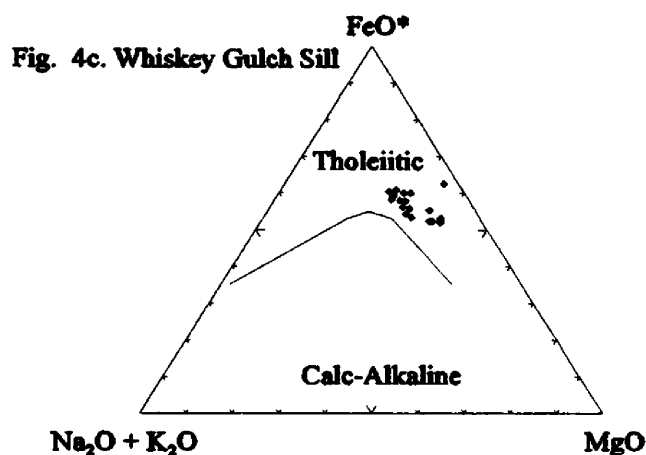
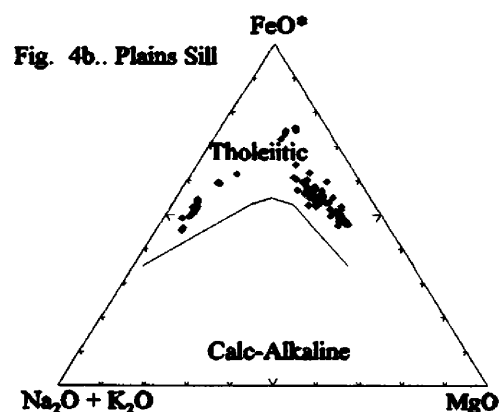
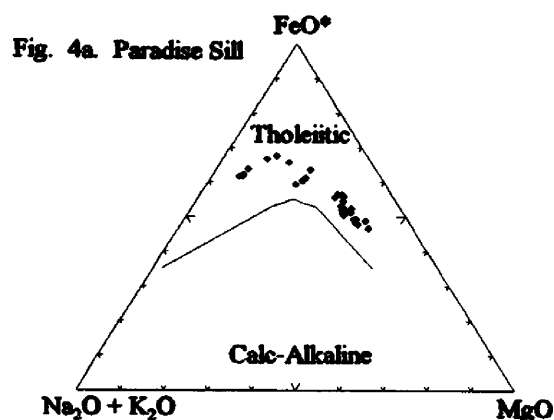


Figure 4. FeO*-Na₂O+K₂O-MgO ternary diagrams for the a)Paradise Sill, b)Plains Sill, and c) Whiskey Gulch Sill (Samples from this study and Buckley, 1993). Total iron recalculated as FeO*.

contemporaneous sedimentation and intrusion possibly near the paleo-surface (Höy, 1989; Buckley and Sears, 1992). The Plains sill shows the strongest evidence of wet sediment intrusion. Evidence along the upper contact of the Plains sill includes ovoid relict sedimentary structures, suggestive of boiling and soft-sediment deformation. Mirolitic cavities observed in the upper portion of the sill are also compatible with sill injection near the sediment-water interface (Höy, 1989; Buckley and Sears, 1992).

Younger dikes and related sill-like intrusions

The RCI is a mafic, PGE-bearing intrusion which cuts the Prichard sills and

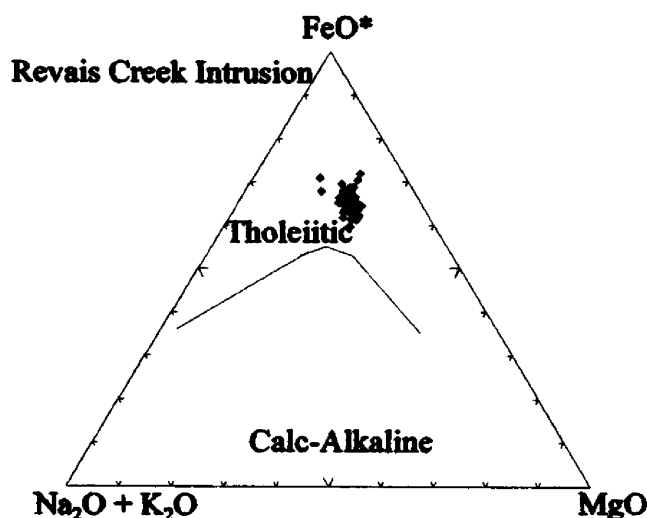


Figure 5. FeO^{*}-(Na₂O+K₂O)-MgO Ternary diagram of unmineralized samples from the Revais Creek Intrusive (This study and Kell, 1992). Total iron recalculated as FeO^{*}.

intrudes the Burke Formation in the Revais Creek area. Both dike and sill-like characteristics can be observed within the RCI. According to Kell (1992), the RCI is gabbroic and of continental tholeiite composition (Table 1). The FeO^{*}-(Na₂O+K₂O)-MgO ternary diagram in Figure 5 displays unmineralized RCI sample data from this study. These data support Kell's (1992) work and demonstrate that the dikes are quartz normative.

One sample from the RCI has been dated using Sm-Nd and Rb-Sr isotope geochronology. A five point mineral separate Sm-Nd isochron yields a late Proterozoic age of 745 ±23 Ma while a five point Rb-Sr isochron gives an age of 687 ±6 Ma (See Figure 10). Geologic relationships support that the RCI is younger than the Prichard Formation sills.

Sample (1942) reported that along Revais Creek the RCI strikes almost north and dips 45 degrees to the west. The RCI bends to the west on its southern end and continues

for seven to eight kilometers (Figure 2). The dip is difficult to discern along most of the body due to poor exposure. However, the straight map trace across the valleys and ridges demonstrates that there the dike is approximately vertical.

A significant change in the orientation of the RCI occurs up section as it enters the Burke and Revett formations (Figure 2). At this stratigraphic level, the RCI flattens and becomes more sill-like. While poor exposure in these areas makes it difficult to determine the exact relationship between the sedimentary host and the RCI, it appears that the intrusion cuts down-section.

The unaltered RCI gabbro is composed primarily of plagioclase and pyroxene with minor percentages of ilmenite, hornblende, orthoclase, biotite, apatite, microcline, and sulfide minerals (Table 3). This mineralogy and the fine to medium grain size is consistent throughout the body except in altered, mineralized areas. Samples that have been hydrothermally altered (propylitic) contain clinoamphibole, chlorite, sericite, serpentine, epidote, and quartz (Kell, 1992; Dahy, 1986; This Study). Table 2 shows major and trace element geochemistry variations for different rock types within the RCI.

Mapping, combined with grid soil sampling and magnetic and VLF surveys obtained by the CSKT during the summer of 1993, show that the RCI is more extensive than previously known. This intrusion has a mappable outcrop trace of at least 30 kilometers. The intrusion can be followed on the surface without major interruption along the entire trace (Figure 2).

The RCI, together with the Burke and Revett formations has been folded (Figure 2). These folds probably developed during Laramide compression. Mineralogy,

Table 2. Average Major and Trace element Geochemistry for different rock types within the RCI (see Appendix A for analytical information).

Rock Type*	UnAlt-UnMin	Alt-UnMin	Alt-Min	Ox-Min	HiCu-LoPGE
n	8	12	11	11	6
SiO ₂ Wt %	50.72	49.13	49.13	47.23	52.40
TiO ₂	2.69	3.08	2.54	2.41	3.03
Al ₂ O ₃	12.56	12.57	12.11	12.18	12.32
Fe ₂ O ₃	17.00	17.22	18.30	18.56	15.87
MnO	0.24	0.23	0.22	0.22	0.21
MgO	5.09	4.65	5.03	4.90	4.41
BaO	0.03	0.02	0.21	0.29	0.02
CaO	8.24	8.59	7.06	6.94	7.03
Na ₂ O	2.41	2.18	1.78	2.38	2.64
K ₂ O	0.84	0.67	0.60	0.63	0.42
LOI	0.03	1.50	3.05	4.29	1.65
Cr ₂ O ₃	0.01	0.01	0.01	0.01	<0.01
P ₂ O ₅	0.12	0.15	<0.02	<0.02	<0.02
TOTAL	100.00	100.00	100.00	100.00	100.00
Total Sulfur	0.01	0.01	0.61	0.18	<0.02
Au ppb	28	6	992	624	9
Pt ppb	27	21	1,681	1,013	20
Pd ppb	30	26	4,422	1,647	27
Pt:Pd	0.90	0.81	0.38	0.62	0.74
Rh ppb	nd	nd	65**	nd	nd
Os ppb	nd	nd	38**	nd	nd
Ir ppb	nd	nd	7**	nd	nd
Ru ppb	nd	nd	103**	nd	nd
Ag ppb	<0.2	<0.2	16.9	11.2	<0.2
Cu ppm	447	369	32,409	20,621	4,323
Pb	6	4	10	16	6
Zn	37	62	38	86	66
Mo	<0.3	<0.3	2	4	<0.3
Ni	24	25	260	240	87
Co	17	21	33	41	23
Cd	<1.0	<1.0	<1.0	<1.0	<1.0
Bi	<1.0	<1.0	<1.0	<1.0	<1.0
As	2	5	8.3	23	4.4
Sb	<0.2	0.5	2.1	2.5	1.4
Fe %	3.68	4.25	5.27	5.85	4.7
Mn ppm	298	396	416	581	402
La	9	8	6	5	10
Te	<0.2	<0.2	<0.2	<0.2	<0.2
Ba	101	108	378	235	49
Cr	29	28	39	52	35
Hg	<0.01	<0.01	0.03	0.03	nd

nd = not determined

n = number of samples

Combined data from this study and Kell (1992)

* Unalt-UnMin = Unaltered-Unmineralized, Alt-UnMin = Altered-Unmineralized, Alt-Min = Altered-Mineralized

** Data from 6 high grade samples

geochemistry, and cross-cutting relationships suggest that the dikes are compositionally similar to, but younger than, the sills in the Prichard Formation. And because the sills are pyroxene-free and contain amphibole formed by apparent hydration, emplacement conditions were different for the sills and the RCI. The age dating done in this study of the RCI (687 ± 6 Ma) compared to dating of the sills (1.1 - 1.6 Ga) agrees with the other geologic evidence.

Metal Concentration Within the Revais Creek Intrusion

Introduction

Sixty-four (64) of the 108 samples from the RCI used in this study were unmineralized. These samples yield average background levels of 50 ppb combined platinum and palladium and 409 ppm copper (Table 1). Concentrations of Pt+Pd and Cu in rocks from other deposits in the world of similar composition are typically much lower. Copper in basaltic rocks averages 100 ppm (Hodgsen, 1986). In quartz-normative continental tholeiite basalt copper averages 141 ppm (Prinz, 1967)(Table 1). Basalts in the Keweenawan Rift contain an average of 120 ppm Cu (Pirajno, 1992). Hooper (1988) analyzed 51 samples from Columbia River Basalts and associated volcanic rock. The average amount of copper in the Columbia River Basalts is 56.6 ppm. Quartz-normative continental tholeiite and Columbia River Basalts average 77 ppm and 53.4 ppm respectively.

It is difficult to compare the background PGE content of the RCI to other continental tholeiite rocks because of the paucity of PGE data. Crocket (1981), states that PGE in the Parana, Karroo, Deccan, and Columbia River continental tholeiite flood basalts contain an average 8.3 ppb Pd, and 0.092 ppb Ir. Crocket, (1981) also shows that the Pt+Pd concentrations for mafic rocks, in general, average between 10 and 20ppb.

Within the RCI, platinum group elements are concentrated, together with copper, gold, and silver in zones or pods. These zones seem to be small and somewhat evenly spaced along the outcrop trace of the RCI. Pt+Pd is concentrated to as much as 12,483 ppb within hand specimens from these zones. Varying amounts of hydrothermal

alteration, from pervasive rimming to complete replacement of all primary phases, affected the Cu-PGE-bearing zones. In some mineralized samples only partial alteration is observed; some contain pyroxene altered to clinoamphibole whereas the plagioclase is relatively fresh. In other samples all the primary minerals and textures have been replaced and obliterated by shearing and hydrothermal fluids. In some areas, specifically the Lucky Strike Pit, near the Green Mountain Mine area (Figure 2), there has been significant supergene alteration in the form of oxidation and weathering which has obscured aspects of the original hydrothermal alteration and mineralization. All of these partially altered to strongly altered samples, with or without superposed oxidation, may or may not contain anomalously high levels of PGE and copper.

Green Mountain Mine

The Green Mountain area was the principal site of historic mining activity in the district. Between 1910 and 1942, 2,700 tons of ore was shipped from veins 1 to 3 feet wide. This ore averaged 18% copper, 1 ounce per ton (opt) silver, 0.18 opt gold, 0.13 opt platinum (Sample, 1942). The operation, however, was not profitable during this period.

The ore is characterized by strong hydrothermal alteration, zones of oxidation, and shearing. All of the significant PGE mineralized zones occur within the RCI, near the gabbro-quartzite (Revett Formation) contact. The majority of the mine workings of the Green Mountain and adjacent mines appear to be along the footwall contact. Poor mine records and collapsed workings do not allow for a detailed evaluation of the spatial

location(s) or additional details of the ore distribution.

Bayhorse Prospect

Little is known about the extent of the Bayhorse workings. No records are known to exist and the shaft is not accessible. The opening of the shaft is approximately 20' wide and 20' deep and the small size of the tailings dump suggests that the shaft did not go much deeper. There are no mineralized outcrops of the RCI at the Bayhorse prospect so it is difficult to determine where the mineralization occurred spatially.

The tailings dump here yielded the highest PGE grades found in this study. The degree of hydrothermal alteration here is less than that at the Green Mountain Mine. No supergene alteration was observed at the Bayhorse prospect. In 1992, the CSKT drilled three reverse circulation holes (RC-92-1, RC-92-2, and RC-92-3) to determine the extent of the mineralization. Two of the holes intersected the footwall contact of the RCI and the Burke Formation but none intersected any rocks of comparable grade to the Bayhorse workings. This implies that the mineralized rocks found in the Bayhorse prospect are either erratic or confined to a small area.

Petrography of the Revais Creek Intrusion

Introduction

The petrographic characteristics of the RCI vary with location with respect to alteration and mineralization. Therefore, the petrography of the rocks of the RCI will be described according to the following groupings related to hydrothermal alteration and mineralization:

- Unmineralized gabbro
 - Weakly altered/Unaltered
 - Strongly altered
- Mineralized gabbro (contains elevated PGE, Au, Cu concentrations)
 - Partially altered
 - Strongly altered
 - Oxidized
 - High copper, Low PGE content.

No samples of completely unaltered gabbro were found in this study. The freshest sample collected from the RCI contains very minor amount of alteration which consists of pyroxenes altering to amphibole. This rock-type is described as weakly altered gabbro.

Unmineralized Gabbro

Weakly Altered

Weakly altered RCI is a fine to medium grained, quartz normative, continental tholeiite, gabbro (Figure 4) (Table 3). Thin-section study shows that plagioclase (An_{32} to An_{60}) accounts for 50 percent of the rock and typically occurs in interlocking subhedral/anhedral laths. Pyroxene, comprising 35 to 40 percent of the rock, occurs interstitially as irregular anhedral grains. In some cases, the pyroxene and plagioclase

grains form a sub-ophitic to ophitic texture. Augite, the most abundant pyroxene,

Table 3. Typical Mineralogy of partially altered samples from the RCI.

MINERAL	MODAL VALUE (%)
<u>Early Magmatic</u>	
Plagioclase (An ₃₅₋₆₀)	45-50
Clinopyroxene	
Augite	30-35
Pigeonite	4-6
<u>Late Magmatic</u>	
Hornblende	tr-5
Biotite	tr-3
Qtz.-Plag. intergrowths	tr-5
Magnetite	3-8
Sulfide	tr
Apatite	tr-1

Combined data from this study and Kell (1992)

coexists with lesser amounts of pigeonite. Trace to eight percent of the rock is hornblende which occurs as a late magmatic phase adjacent to and partially rimming pyroxene grains. Five to ten percent interstitial magnetite and/or ilmenite is also common. Trace amounts of biotite, quartz, needle-like apatite, and possibly clinozoisite also occur. Quartz, where observed, commonly occurs as a myrmekitic intergrowth with another mineral, possibly plagioclase.

The paragenetic crystallization sequence of the primary minerals from oldest to youngest include: 1) plagioclase, 2) clinopyroxene, 3) magnetite and hornblende, and 3) biotite, clinozoisite(?), and quartz intergrowths. The sub-ophitic to ophitic texture consisting of plagioclase and clinopyroxene aid in the determination that plagioclase

started to crystallize before clinopyroxene. Hornblende rims clinopyroxene demonstrating that hornblende is a later phase. Late-stage magnetite and the quartz intergrowths occur in the interstices of plagioclase and clinopyroxene. Biotite and clinozoisite appear to have formed at the expense of the clinopyroxene. It is difficult to tell where magnetite, hornblende, biotite, clinozoisite, and quartz intergrowths fit into the paragenetic sequence.

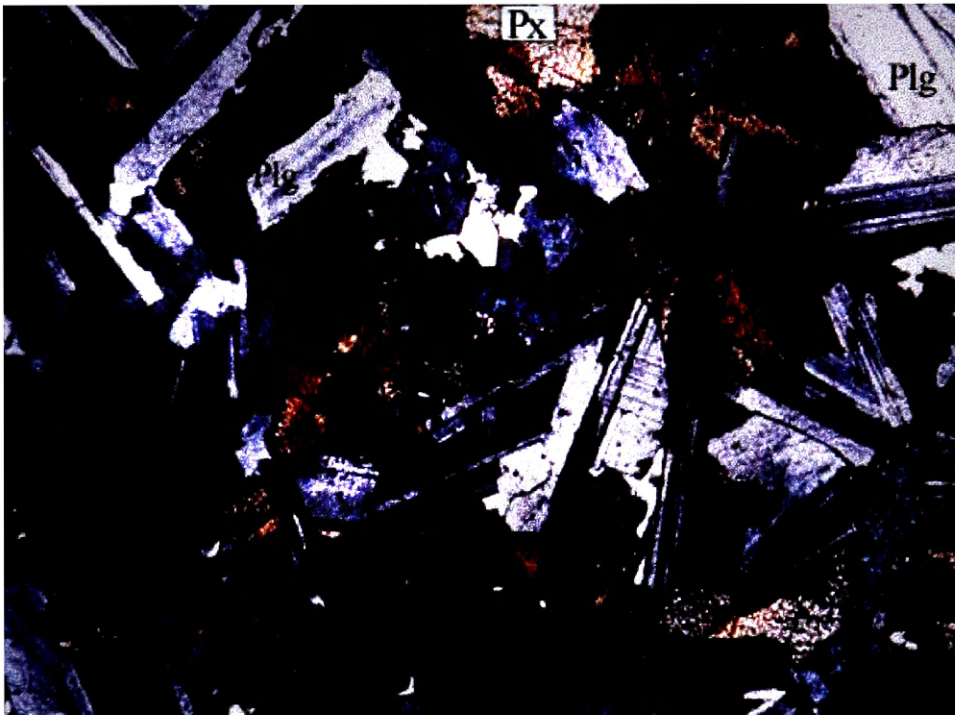


Figure 6. Photomicrograph of slightly altered Revais Creek Intrusion. Crossed nicols. Note grey plag (plg), laths, colored augite (px), and opaque magnetite. Width of photo is approximately 3.2mm.

Strongly altered RCI

The Green Mountain Mine and the Lucky Strike pit typically contain heavily sheared and altered gabbro. The Bayhorse prospect also contains strongly altered rock. The mineralogy of samples from different parts of the altered gabbro is highly variable due

Table 4. Typical Alteration Assemblage of Highly Altered RCI.

MINERAL	MODAL VALUE (%)	Host
Hornblende and other Clinoamphibole	20-25	Pyroxene
Clinzoisite	25-35	Plagioclase
Epidote	tr-5	Plagioclase
Chlorite	15-20	Plagioclase
Biotite	tr-1	Pyroxene
Sericite	tr-1	Plagioclase
Quartz	2-5	
Magnetite	1-2	
Sulfide	2-5	
Serpentine (?)	tr	Pyroxene

Combined data from this study and Kell (1992)

to varying degrees of hydrothermal alteration. A photomicrograph of a typical highly altered sample is shown in Figure 5. The alteration mineralogy and paragenetic sequence is outlined in Table 4. Primary pyroxenes were replaced by hornblende, other clinoamphiboles, chlorite, biotite, and possibly serpentine. Clinzoisite, zoisite, epidote, chlorite, and sericite replaced plagioclase. The degree of replacement of the primary pyroxene and plagioclase minerals varies from minor rimming to complete replacement and destruction of all primary minerals. The magnetite-ilmenite grains sometimes exhibit what appears to be skeletal replacement of magnetite by ilmenite. Most likely, ilmenite exolved from magnetite.

Mineralized Gabbro

Partially Altered

Figure 6 contains photomicrographs of partially altered, mineralized RCI. A few partially altered samples from the Revais dike-sill body contain elevated amounts of

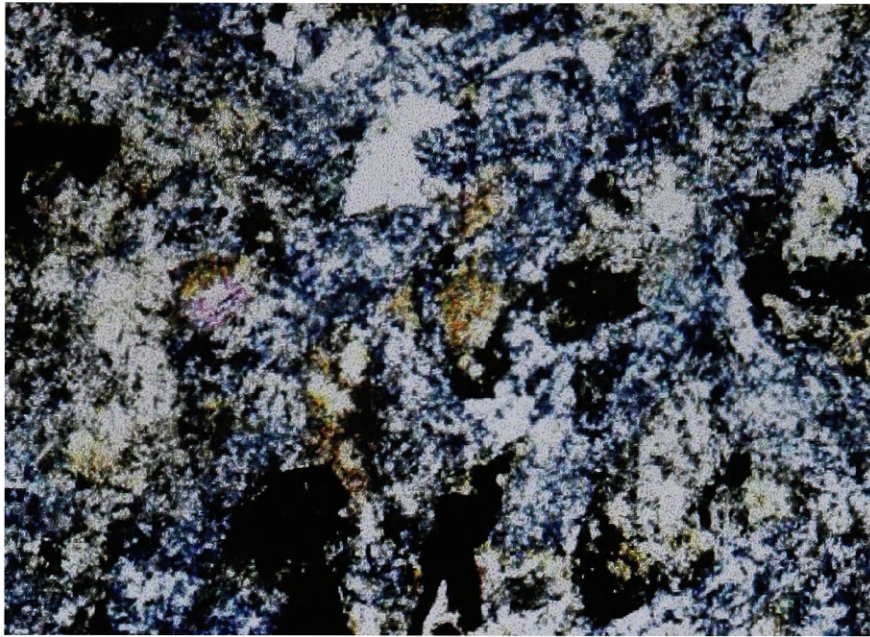


Figure 7. Crossed nicols photomicrograph of RCI gabbro that has undergone strong hydrothermal alteration. Blue mineral is probably chlorite and/or other hydrosilicate mineral. Width of photo is approximately 3.2mm.

copper, PGE, and gold. The majority of these samples come from the Bayhorse prospect. The Bayhorse samples were collected from the tailings dump near a collapsed shaft of unknown depth. The primary mineralogy of this rock type is essentially the same as the weakly altered, unmineralized rock type. In the partially altered, but mineralized samples, primary pyroxene is rimmed by secondary clinoamphiboles, chlorite, and biotite whereas the plagioclase is rimmed by fine-grained clinozoisite, zoisite, epidote, chlorite, and sericite. Small veins of chlorite are also common.

Sulfide grains are typically chalcopyrite with bornite exsolution lamellae and rimmed by supergene chalcocite. Sulfide grains commonly embay plagioclase, clinopyroxene and sometimes magnetite/ilmenite crystals. Figure 7 shows a sulfide grain embaying a plagioclase crystal while Figure 8 shows a sulfide grain embaying magnetite. Veinlets of chlorite (?) and other alteration minerals typically surround and cross-cut the

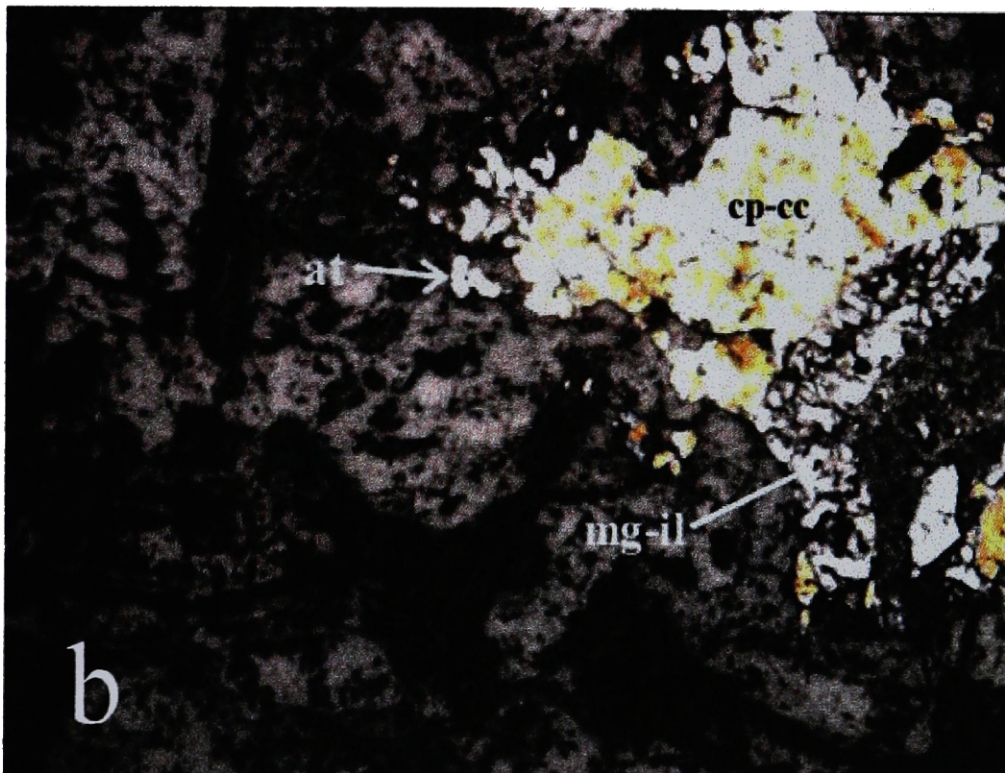
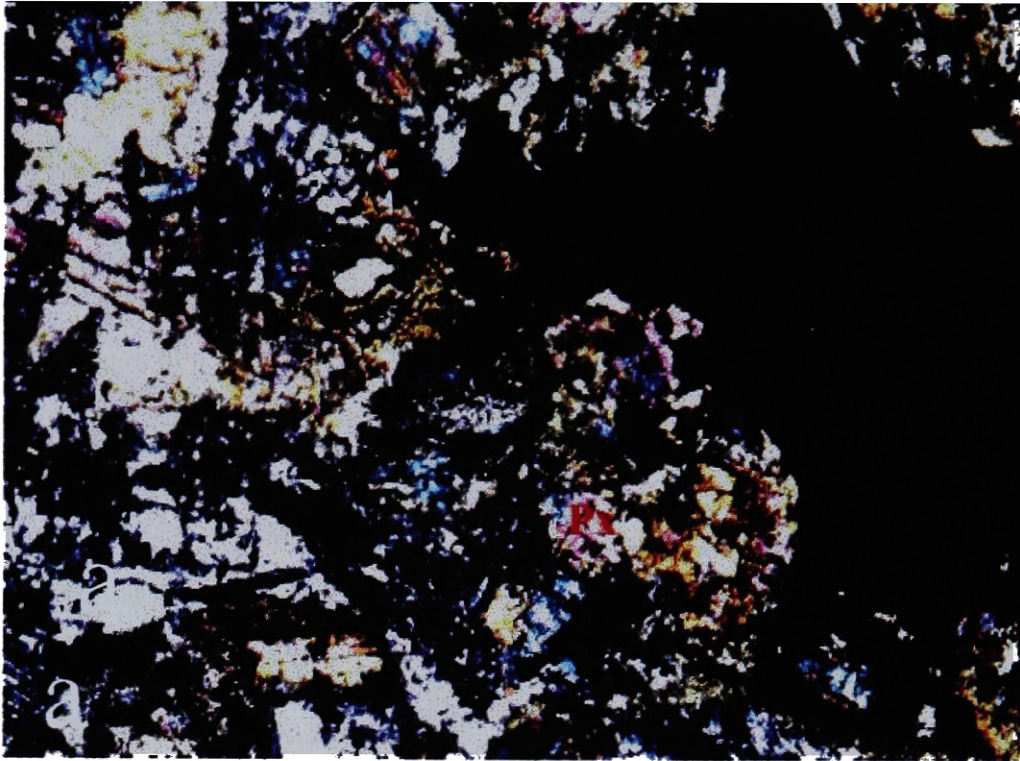


Figure 8. Two photomicrographs. a) Photomicrograph of partially altered, mineralized RCI. Note presence of partially altered clinopyroxene (cp). Crossed nicols. b) Reflected light photomicrograph of same region as 'a'. Note chalcopyrite-chalcocite (cp-cc) and atokite (Pt,Pd)₃Sn (at). Width of photos is approximately 2.2 mm.

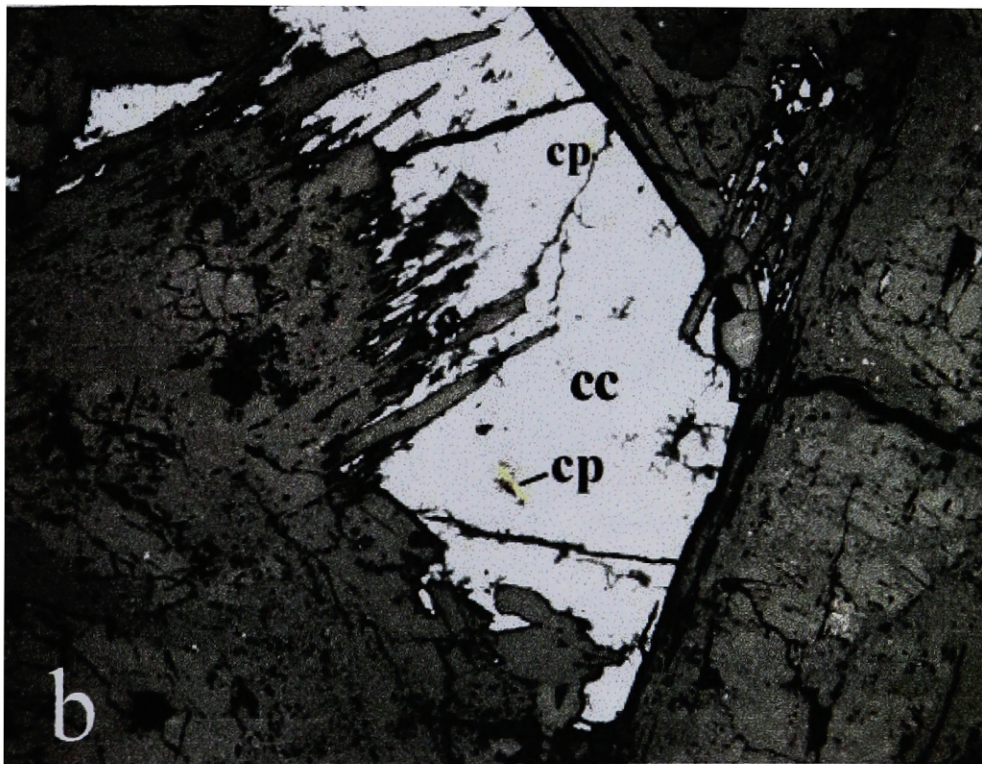


Figure 9. Two photomicrographs. a) Crossed nicols photomicrograph of relationship between relict plagioclase(plg) and chalcopyrite-chalcocite (cp-cc) grain. Note cp-cc grain infilling of 'tattered' end of plagioclase lath. b) Same view as 'a' in reflected light. Width of photos is approximately 1.2 mm.

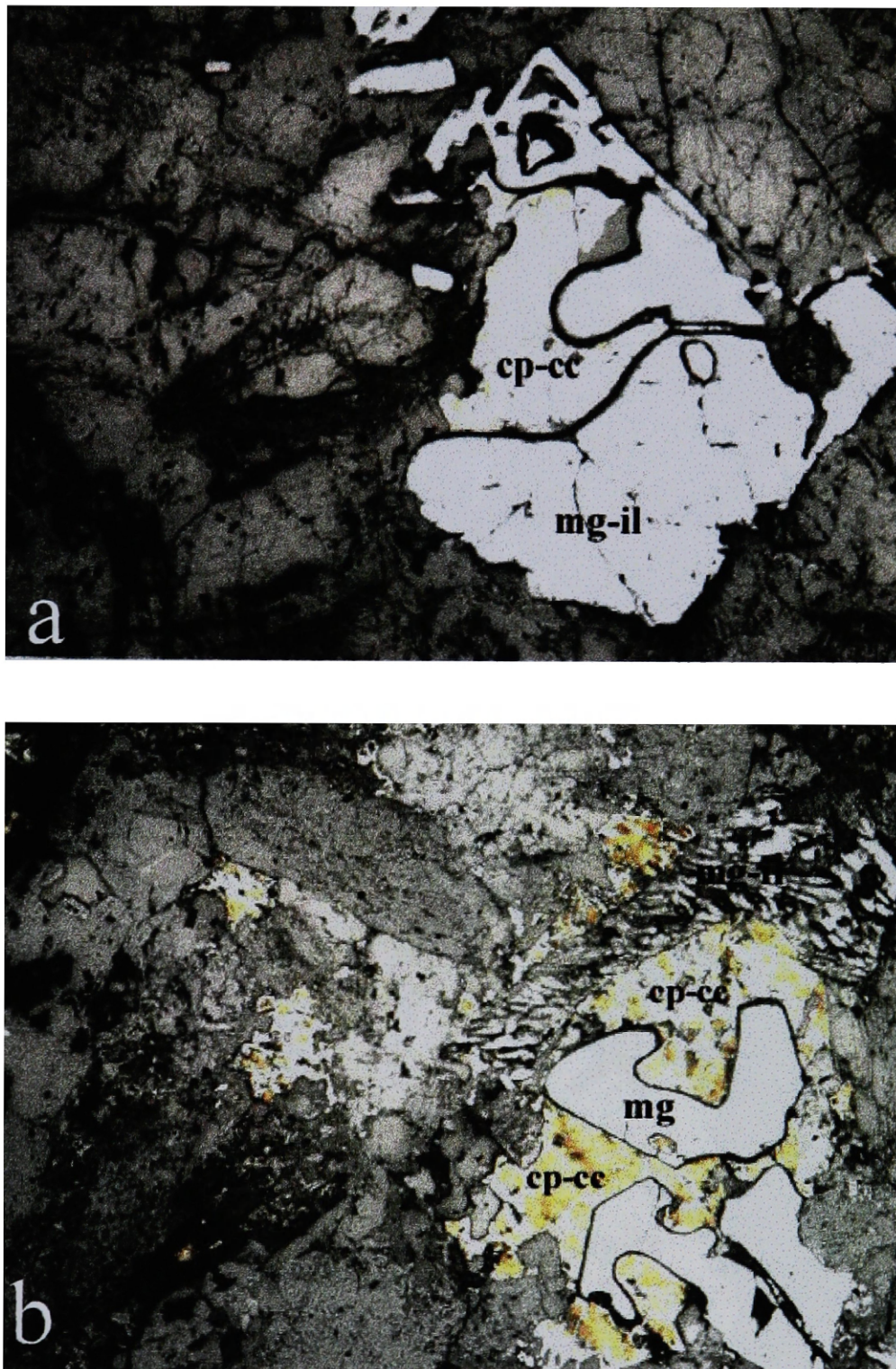


Figure 10. Two photomicrographs of examples (a & b) of magnetite(mg) embayed by chalcopyrite-chalcocite (cp-cc) grains. Note skeletal magnetite/ilmenite (mg-il) in upper right hand corner of 'b'. Both are reflected light photomicrographs. Photo 5a is approximately 1.2mm wide and 'b' is approximately 2.2mm wide.

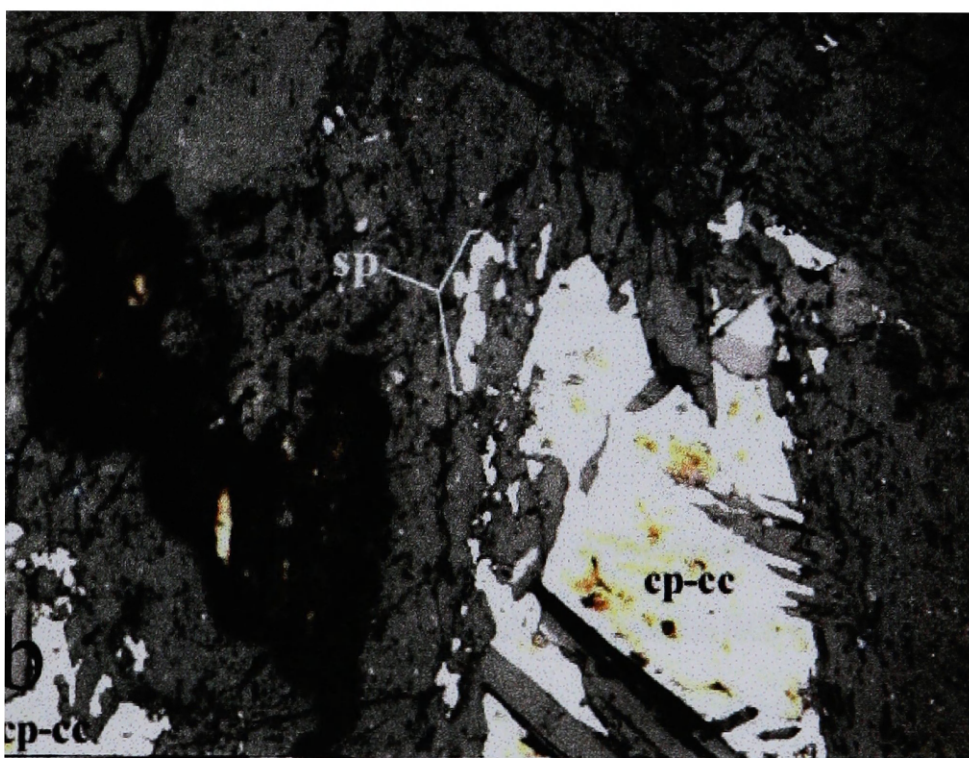
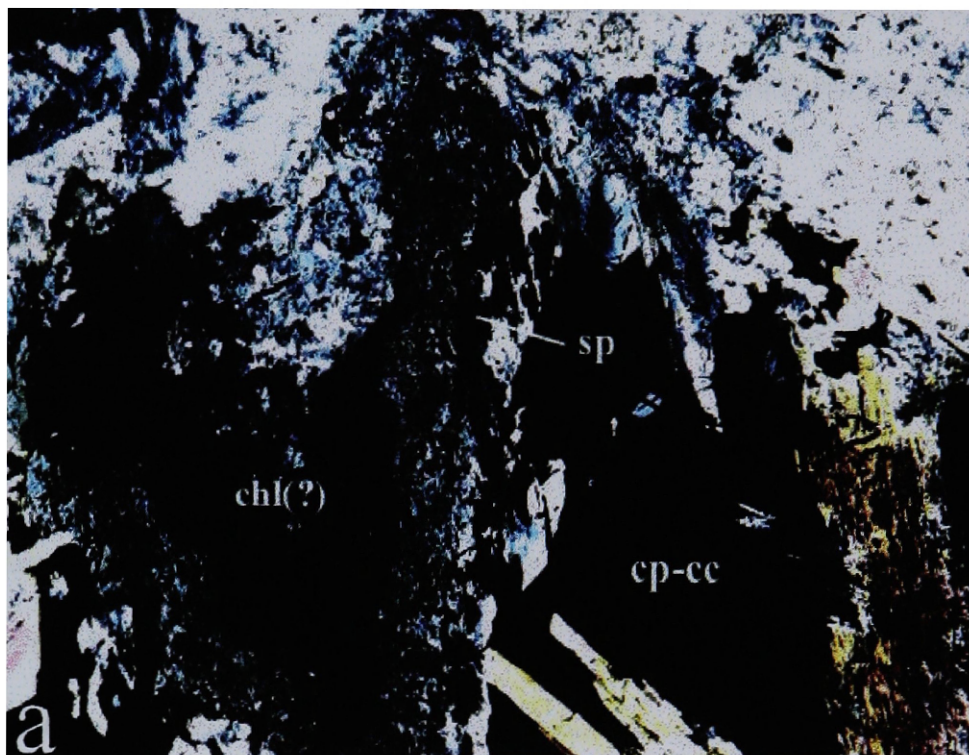


Figure 11. **a)** Crossed nicols photomicrograph of strongly altered, mineralized RCI. **b)** Same view as 'a' in reflected light. Note vein-like stibiopalladinite (sp) grain in the center of the photograph. This grain can also be seen in Figure 17. Photos are approximately 1.2 mm wide.

sulfide minerals. A SEM scan revealed that several platinum-group minerals (PGM) occur in these partially altered, sulfide-bearing samples. The SEM results will be discussed in more detail below.

Strongly Altered, Mineralized

Figure 9 contains photomicrographs of strongly altered, mineralized samples from the RCI. These samples contain much of the same mineralogy as the strongly altered, unmineralized samples. The degree of alteration is pervasive with complete replacement and obliteration of primary silicate minerals and textures.

Oxidized, mineralized

In some areas oxidation has produced an iron-rich gossan. Figure 10 shows a photomicrograph of oxidized RCI. The mineralogy of this gossan is similar to that of the strongly altered rocks except that the copper sulfides have been replaced by digenite, malachite, cuprite, and possibly goethite. These oxidized samples contain a higher average Pt:Pd ratio of 1:1.6 compared to the un-oxidized samples (1:2.6) (Table 2). Samples of oxidized gabbro from the Green Mountain area examined with the SEM contained only one small PGM grain.

High Copper, Low PGE bearing RCI

A few, partially altered to strongly altered, sulfide-bearing to sulfide-mineral-poor, and fine grained to coarse grained samples collected from the RCI contain elevated amounts of copper while the PGE content remains consistent at background values.

Table 5. PGE and other precious metal minerals in the RCI located and identified using the JEOL-6100 SEM at Montana State University.

<u>Name</u>	<u>Composition</u>	<u>Occurrence</u>	<u>Grain Size</u> <u>(μm)**</u>	<u>Figure #</u>
Atokite	(Pt,Pd) ₃ Sn	Sulfide/Sillicate	30 x 80	6,15
Isoferroplatinum (?)	(Pt,Pd) ₅ (Fe,Cu)	In chalcocite***	10 x 30	20
Kotulskite (?)	(Pd,Cu) ₂ TeBi	Sulfide/Sillicate	10	19
Mertieite (?)	Pd ₅ Sb ₂	Several in Sillicate	1 to 5	13,14,29
Michnerite (?)	Pd ₉ Bi ₄ Te ₄ Cu ₂	In chalcocite***	5 x 10	N/A
Michnerite (?)	Pd ₁₃ Bi ₅ Te ₄	Sulfide/Sillicate	4 x 10	22
Sperrylite*	PtAs ₂	Sulfide/Sillicate	8	12,13,14,16
Stibiopalladinite	(Pd,Cu) ₃ Sb ₂	In sillicate	100	17
Tulameenite	Pt ₈ Fe ₃ Cu ₅	Sulfide/Sillicate	3 x 8	21
Hollingworthite (?)*	Rh-As-Cu-Pt-S	Included in Sperrylite	10	11
Un-named Pd Min.	Pd ₆ (Cu,As) ₂ Te	In chalcocite***	10	23
Native Silver (?)	Ag ₇ Cu ₂ Au	In chalcocite***	3 x 7	23

* Grains of Hollingworthite and Sperrylite in figures 7a and 7b were located and tentatively identified by Oscar Robertson of the USGS.

** Each listing is of an individual grain except sperrylite (3 grains) and stibiopalladinite (grain conglomerate).

*** Supergene replacement of chalcopyrite and bornite by chalcocite

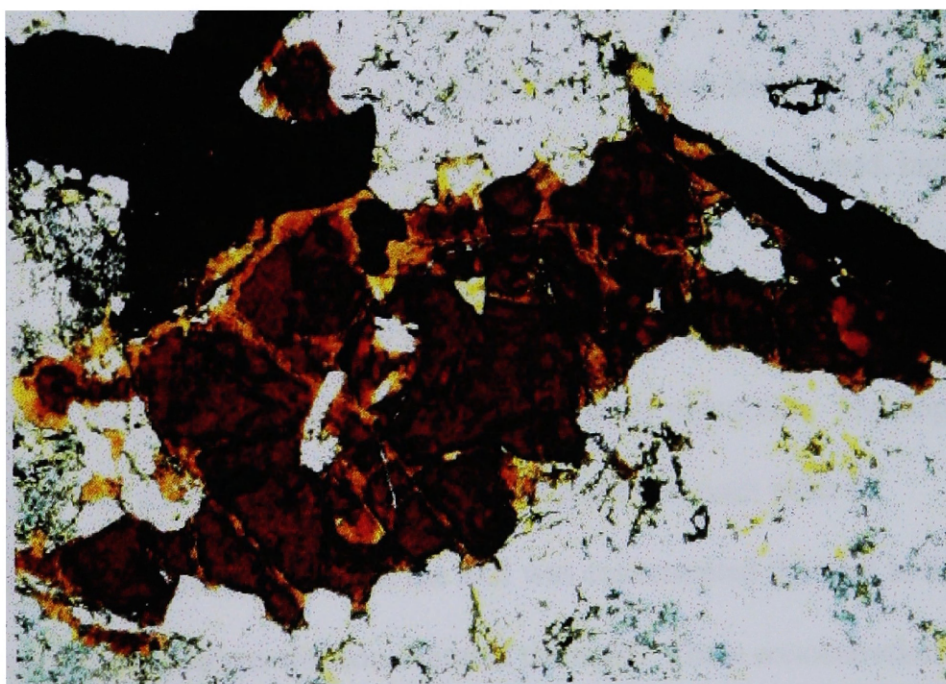


Figure 12. Crossed nicols photomicrograph of a strongly oxidized sample from the RCI. The red and orange grain dominating the photo is composed of cuprite and possibly goethite and was formerly a chalcopyrite-bornite mixture. The opaque masses are magnetite. Photo is approximately 3.2 mm wide

Geochemistry of the Revais Creek Intrusion

In this study 70 samples were analyzed for major element and base and precious metal whole-rock content. Data from 38 samples from Kell (1992) were combined with those in this study (total = 108 samples) for the purpose of identifying the geochemical relationships within the RCI. All 108 samples contain varying degrees of mineralization and hydrothermal alteration. Analyses for Ni, Cu, S, Pb, Au, Pt, and Pd were obtained from samples taken along the entire length of the RCI including the highest-grade zones. Ni, Cu, S, Pb, Au, Pt, and Pd all partition strongly into sulfide minerals. These metals behave, in the presence of a sulfide melt, as chalcophile elements. Therefore, it was expected that there might be a correlation between sulfur and these metals if the sulfides were formed during magmatic processes. The majority of the unaltered and altered RCI samples, however, do not contain detectable amounts of sulfur. The detection limit was 0.02%.

The sulfur versus metal plots in Figures 13a-f illustrate that there is a low correlation between the two. There is not enough data on partially altered, high-grade rocks to determine if a stronger correlation exists.

Figure 14 contains logarithmic palladium versus metal plots. Palladium correlates well with gold, copper and platinum as indicated by linear regression. The slopes of these plots, indicate that the order of fractionation with respect to each other is Ni<Pt<Cu<Au<Pd. That is, Ni within the RCI was concentrated the least in the zones of mineralization and palladium was concentrated the most. These concentration trends can

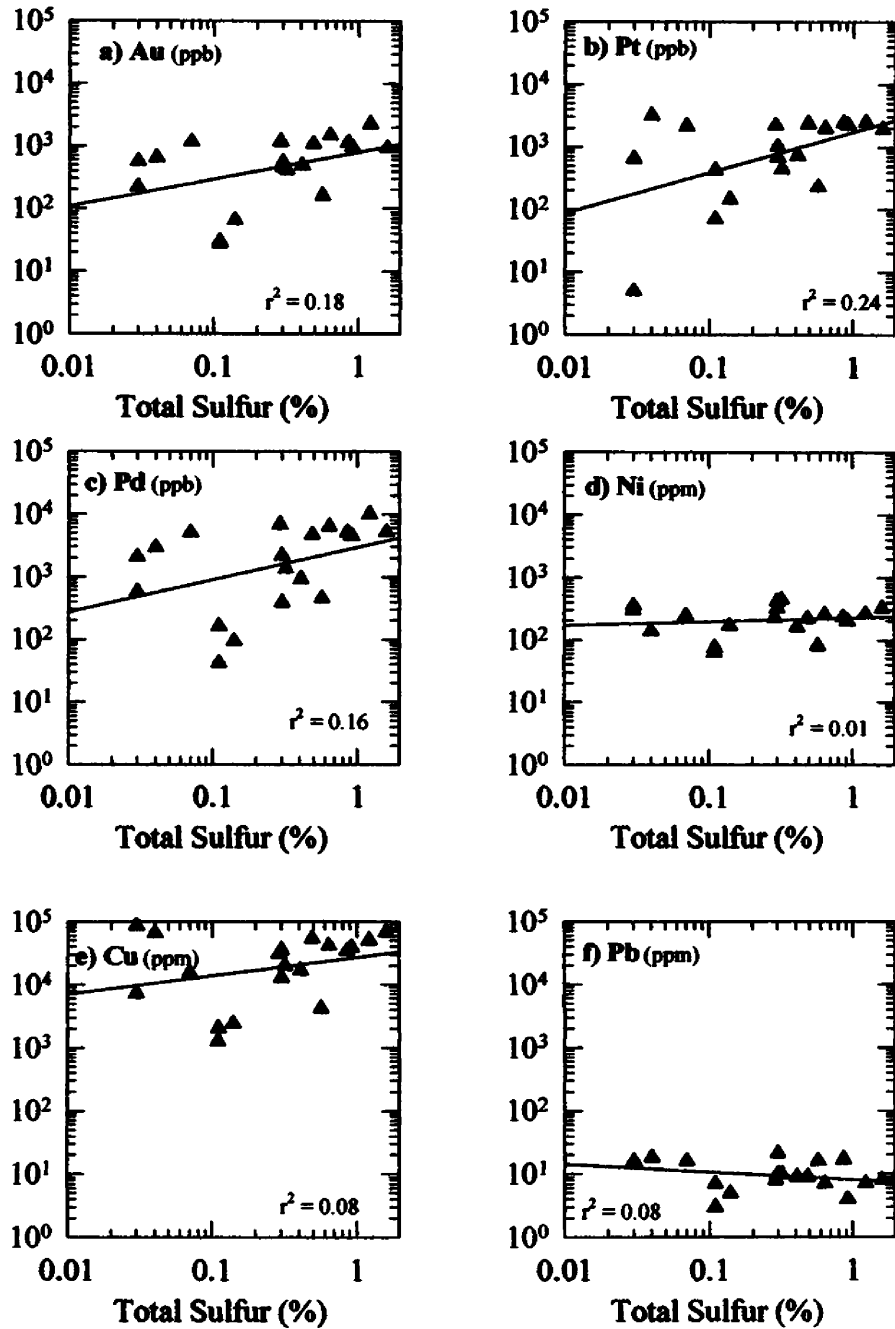


Figure 13a-f. Sulfur log vs. metal log plots. Lines and r^2 values are from linear regression. All samples are mineralized. (See Appendix A for analytical information).

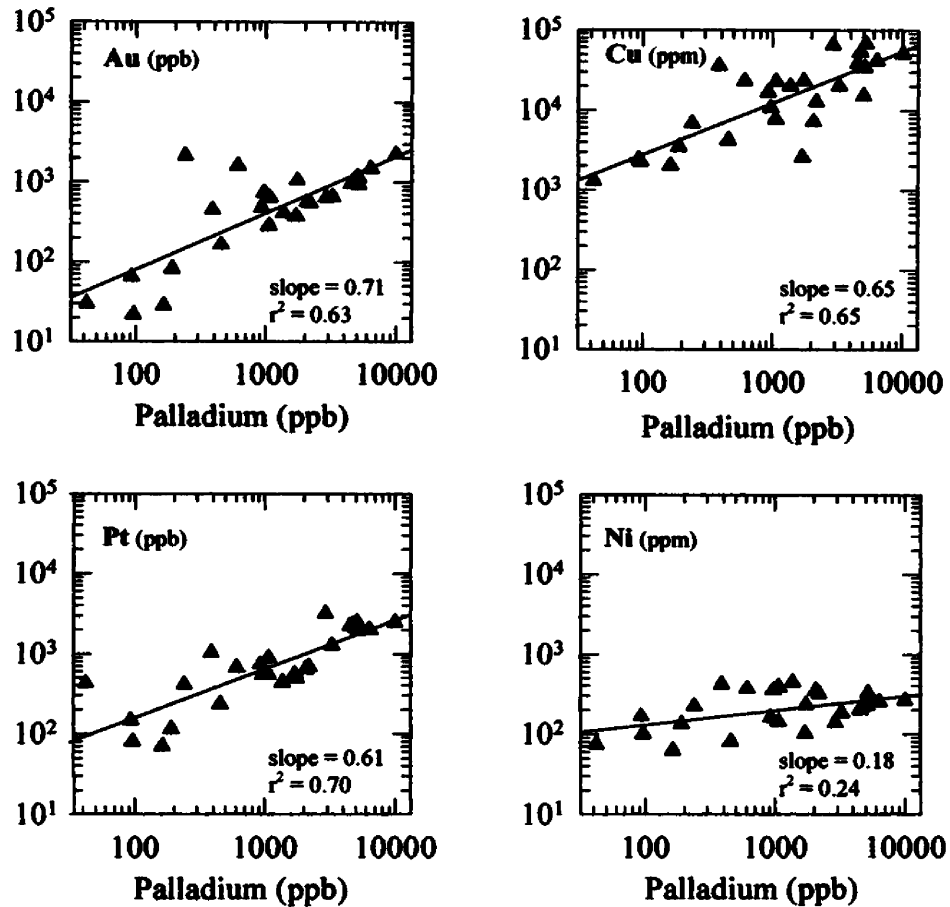


Figure 14. Palladium vs. Au, Cu, Pt, and Ni log plots of mineralized samples from the RCI. All samples are mineralized. (See Appendix A for analytical information).

also be seen in the ratio of concentrated metal/background metal in Table 2. Gold, copper, and platinum show moderate positive correlations with palladium whereas nickel does not.

Scanning Electron Microscope Study

Introduction

Five polished thin sections of samples from the RCI were examined using the JEOL-6100 Scanning Electron Microscope (SEM) at Montana State University. Three thin sections were examined by Robert Oscarson of the USGS (Menlo Park) using an SEM. Three of the thin sections were from oxidized samples from the Green Mountain Mine area containing higher grades of PGE. The other five thin sections were from partially to strongly hydrothermally, but not supergene, altered RCI from the Bayhorse Prospect. All examined thin sections were from samples chosen for their high content of PGE and the likelihood that platinum-group minerals (PGM) would be present.

Backscatter electron images (BEI) for most of these PGM grains were obtained (Figures 15-27). These images show the textural and spatial relationships of the PGM grains.

SEM Findings

Sulfide-bearing, high-grade samples exhibiting varying degrees of hydrothermal alteration from the Bayhorse tailings dump provided the best data on the occurrence of PGM. All of the thin sections examined with the SEM from the Bayhorse contain PGE-bearing minerals (Table 5). The PGM occur in three different textural environments:

- at the grain boundaries of sulfides and silicates/hydrosilicates
- entirely enclosed in silicates or hydrosilicates
- entirely enclosed within sulfides

Most commonly, the PGM are euhedral to sub-euhedral and occur along small veins of chlorite (?) within sulfide grains or on the contacts between the copper sulfide and

silicate/hydrosilicate minerals.

Several PGE minerals were semi-quantitatively identified using X-ray electron dispersion scans (EDS). Figures 15-27 are backscatter electron images of PGE and other precious metal-bearing mineral grains. Some of these PGM are palladium-bismuthotelluride minerals such as michnerite (Figure 22), kotulskite (Figure 23), and some were not identified. Other PGE mineral species include mertieite (Figures 17 & 18), stibiopalladinite (Figure 21), sperrylite (Figures 15, 16, 17, & 20), atokite (Figure 19), isoferroplatinum (Figure 24), tulameenite (Figure 25), hollingworthite (?) (Figure 15), and Pt-Au-Ag-Cu, and Ag-Cu-Au compounds (Figure 27).

Some of the PGM grains, specifically mertieite (?) (Figures 17 & 18) and stibiopalladinite (Figure 21) exhibit textures indicative of a hydrothermal origin. About eighteen grains of Pd_3Sb_2 (mertieite?), ranging in size from 5 to about 20 microns, were found in granoblastic quartz (Figures 17, 18, and 33). Also, a vein-like, grain "conglomerate" of stibiopalladinite, about 120 microns long, was located in a hydrosilicate groundmass, possibly chlorite or clinozoisite (Figure 21).

The oxidized samples contain fewer PGM grains than in the fresher samples. Only one PGM grain was located in the three oxidized samples. This grain, an unidentified Pd-Sb mineral, is associated with ilmenite in a hydrothermally altered and subsequently oxidized sample.

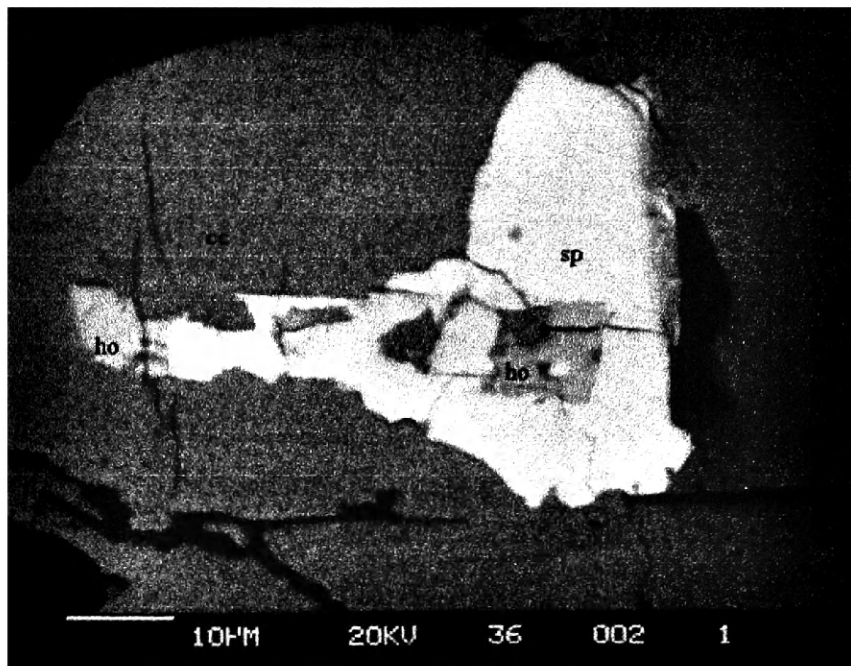


Figure 15. SEM BEI showing sperrylite (sp) grain with hollingworthite (ho) in the center. Note that the PGM grain is surrounded by supergene chalcocite (cc) after chalcopyrite and/or bornite .

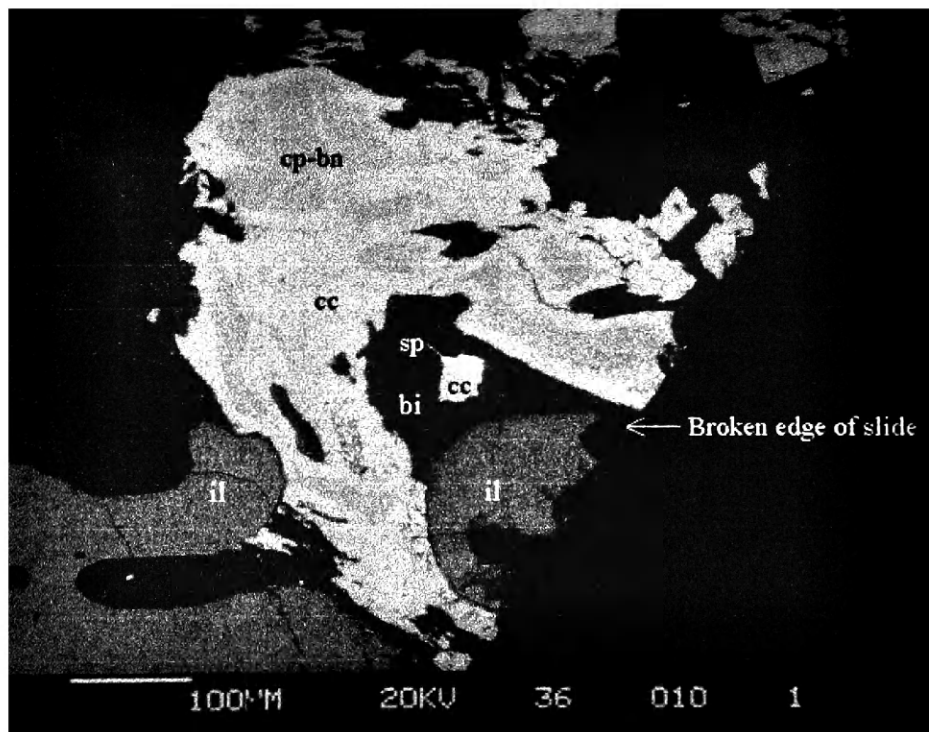


Figure 16. SEM BEI showing small sperrylite (sp) grain on supergene chalcocite (cc) grain boundary. Dark area surrounding sperrylite is possibly biotite (bi) or another hydrosilicate. Also note chalcopyrite-bornite (cp-bn) and ilmenite (il).

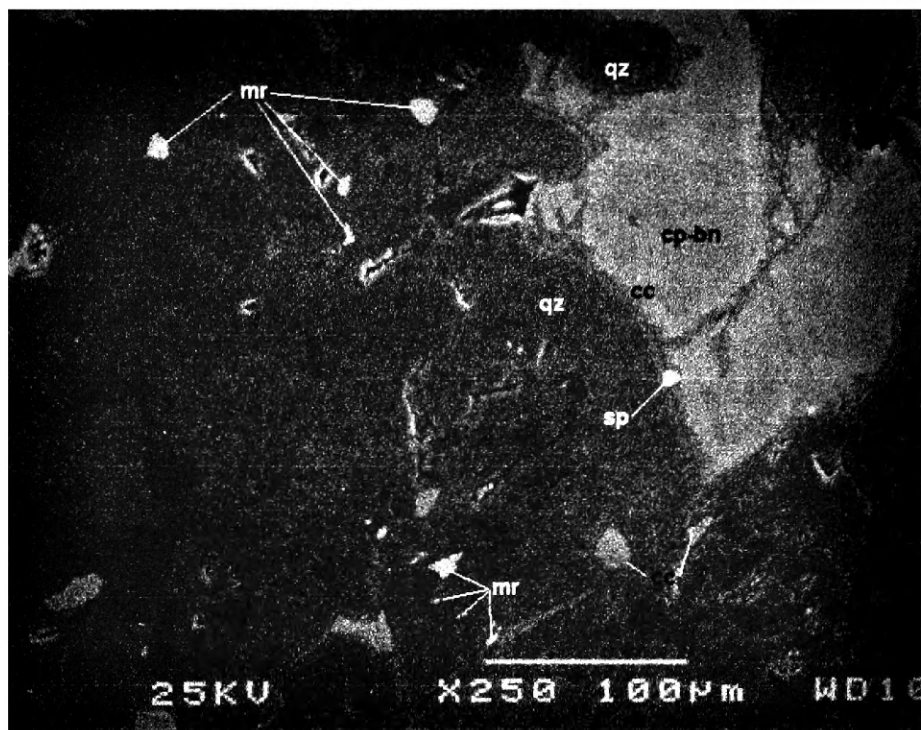


Figure 17. SEM BEI of same area as in Figure 33a & b. Note chalcopyrite-bornite (cp-bn) grain rimmed with chalcocite (cc) with sperrylite (sp) grain on boundary. Also note abundance of bright mercieite (mr) grains scattered in the center of the photo. Much of the dark area is quartz (qz) with granoblastic texture. White box is approximate area of Figure 18.

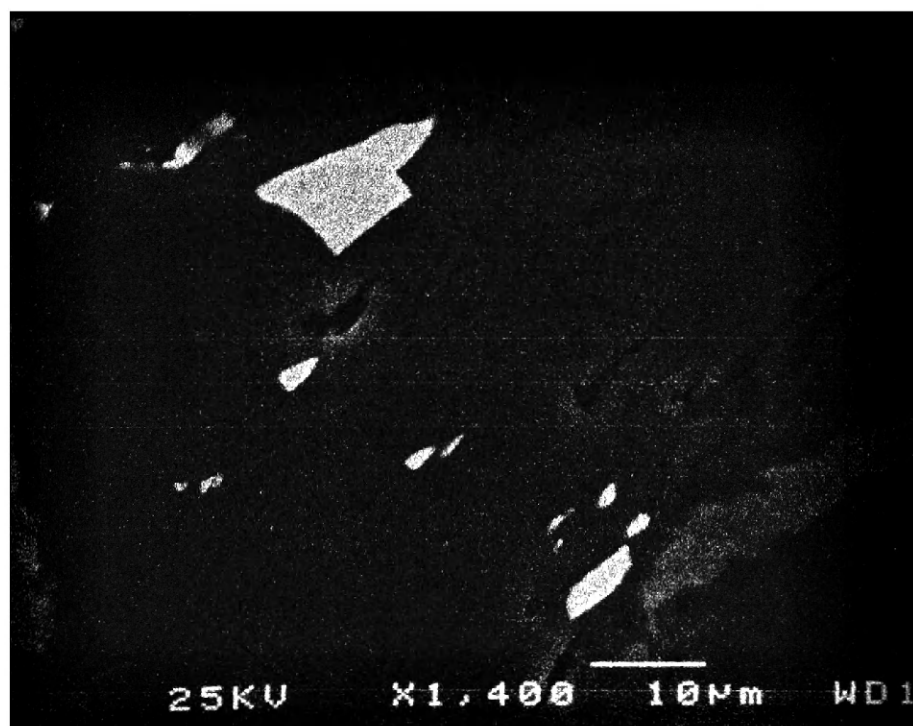


Figure 18. SEM BEI closeup of bright mercieite grains seen in Figure 17.

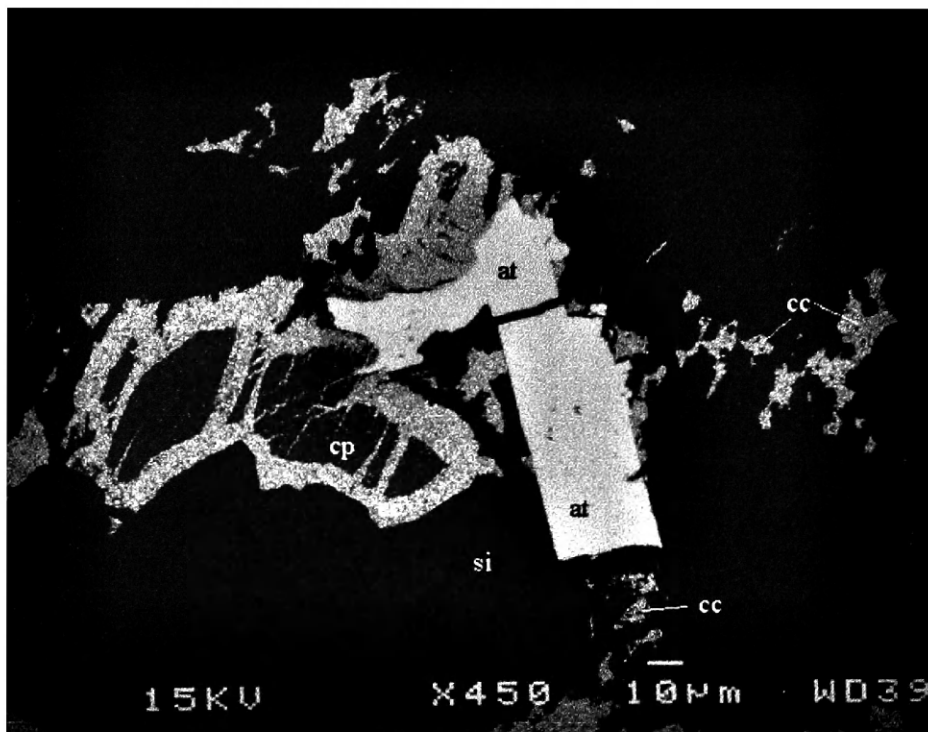


Figure 19. SEM BEI of large double grain of atokite (at) adjacent to chalcopyrite (cp) grain rimmed by chalcocite (cc). This atokite grain can also be seen in Figure 8. Surrounding dark area is silicate (si), possibly pyroxene.

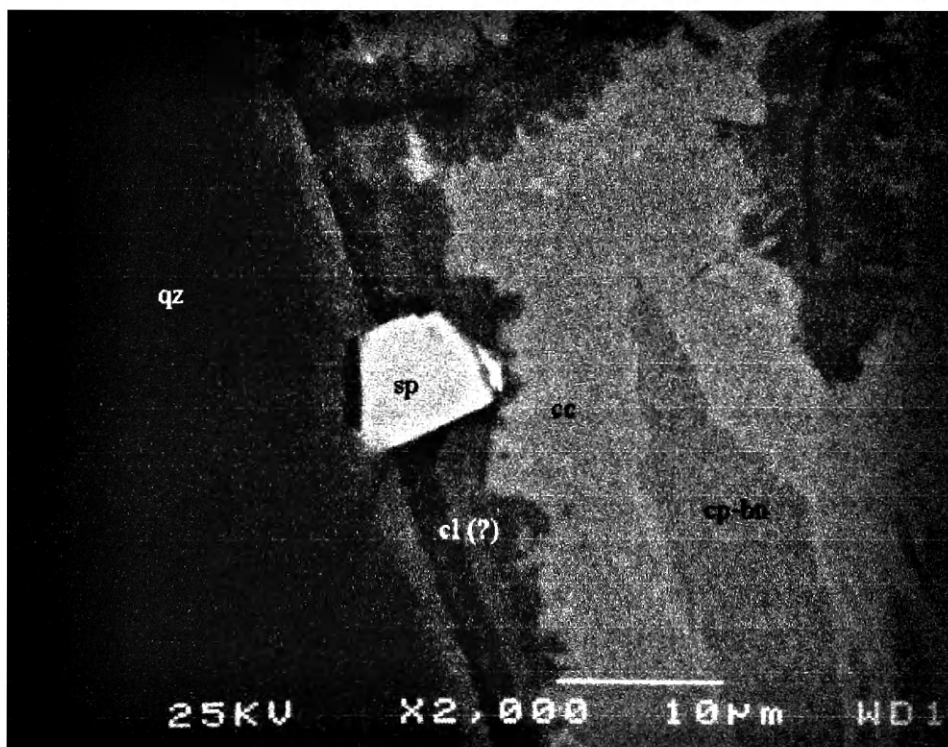


Figure 20. SEM BEI closeup of sperrylite (sp) grain along chalcocite (cc)-quartz (qz) grain boundary. Along this boundary is a hydrosilicate possibly chlorite (cl) or epidote. This grain can also be seen in Figure 17.



Figure 21. SEM BEI showing long vein-like stibiopalladinite (st) grain in mass of very fine grained hydrosilicate minerals (chlorite and or epidote). This grain conglomerate can also be seen in Figure 11. Note chalcopyrite (cp) rimmed by secondary chalcocite (cc).



Figure 22. SEM BEI showing mertieite (mr) grain in hydrothermal quartz.

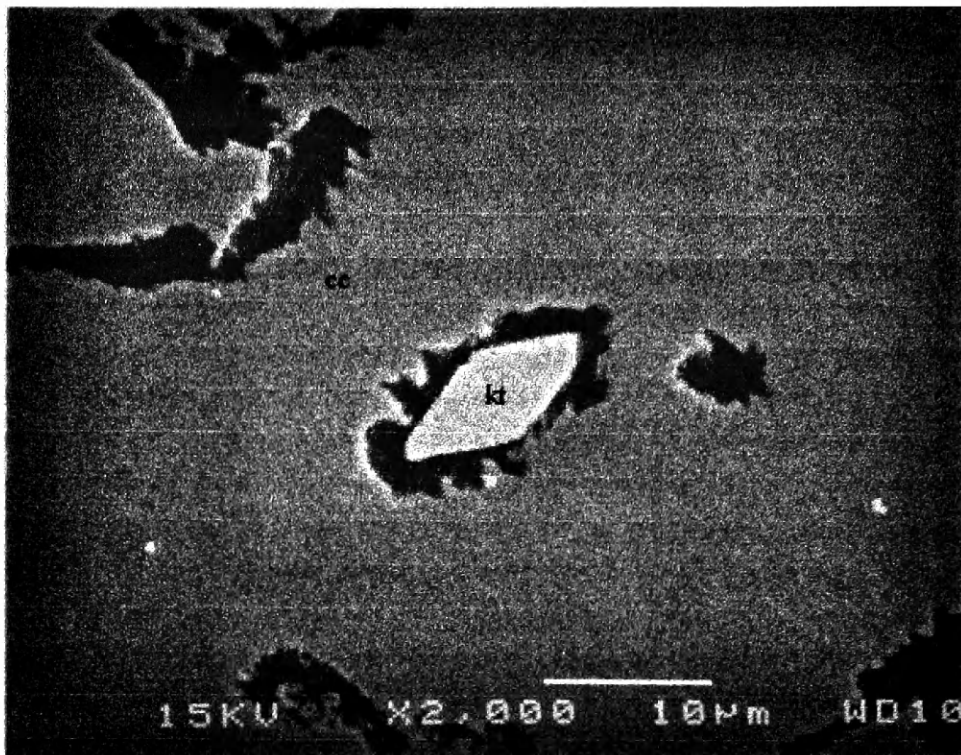


Figure 23. SEM BEI showing diamond shaped kotulskite (kt) grain in chalcocite (cc). Dark rim around diamond is an unidentified silicate mineral, possibly chlorite.

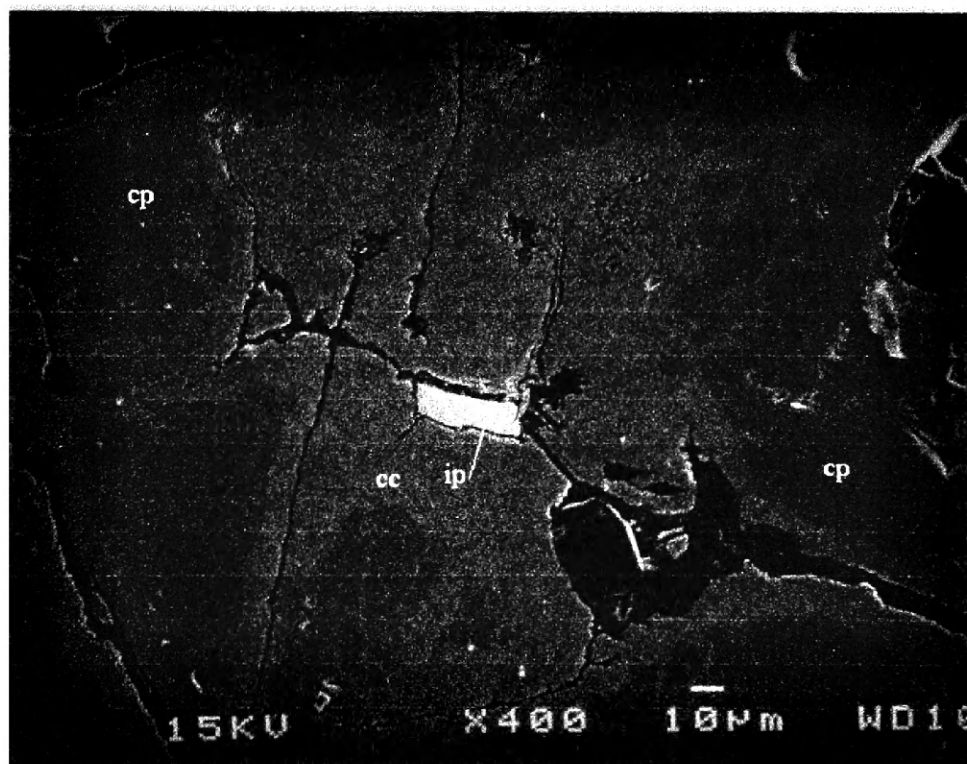


Figure 24. SEM BEI showing isoferroplatinum (ip) grain in chalcocite (cc) altered from chalcopyrite (cp). Dark veins are unidentified silicate mineral, possibly chlorite.

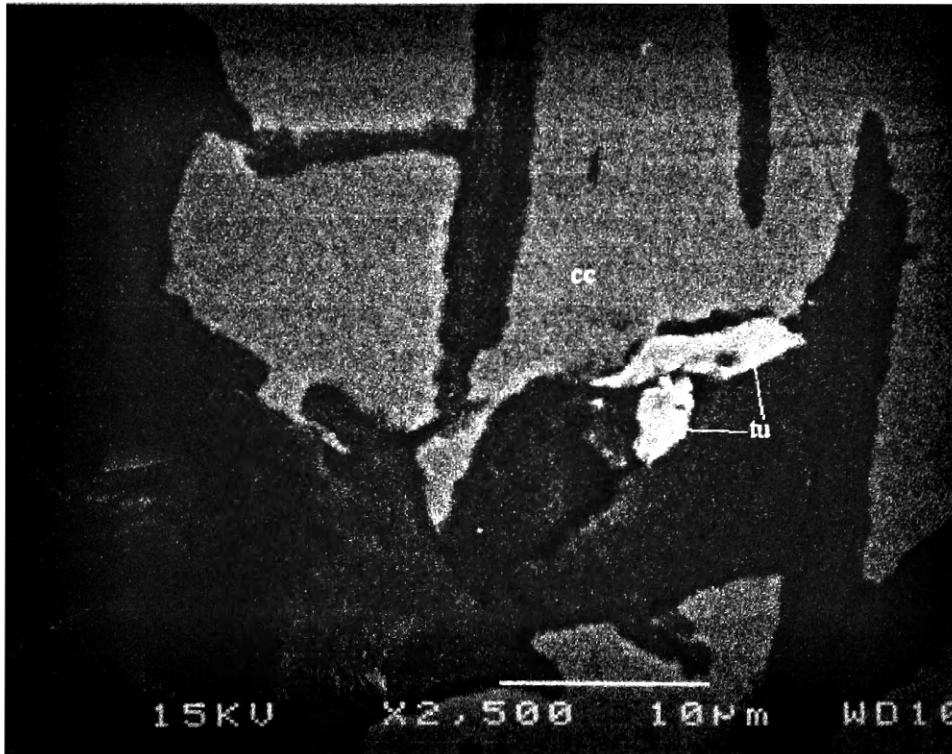


Figure 25. SEM BEI showing two small tulameenite (tu) grains on secondary chalcocite (cc)-silicate grain boundary. Silicate mineral(s) was/were not identified due to small size.



Figure 26. SEM BEI showing a michnerite (mi) grain in quartz (?) (qz) between chalcocite (cc) and magnetite (?) (Mg). Note small amount of remaining chalcopyrite (cp)

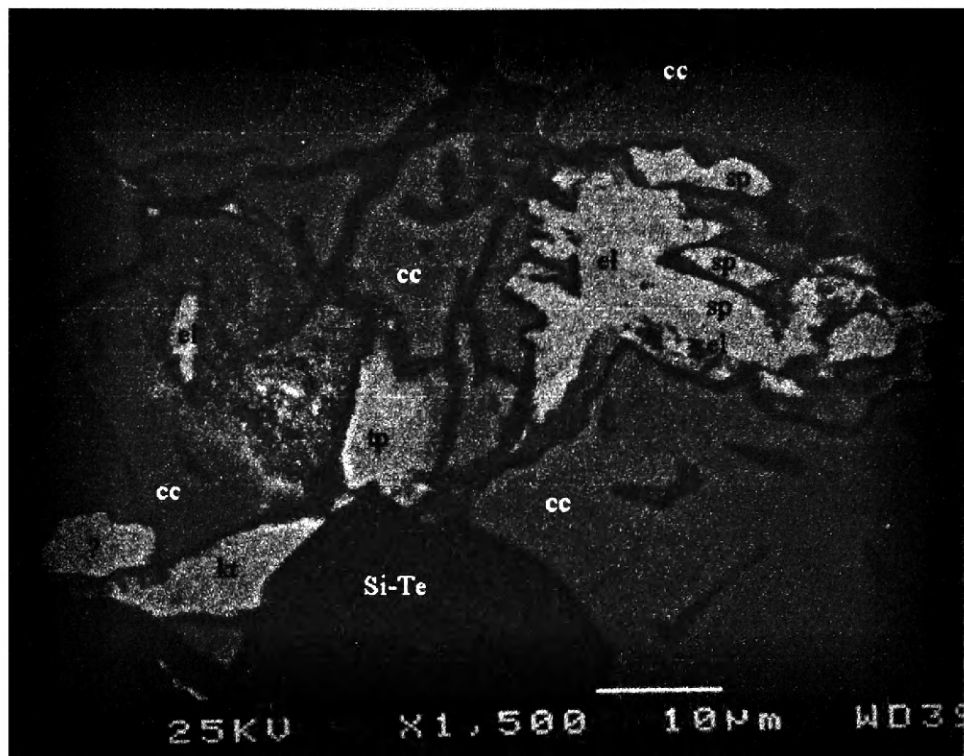


Figure 27. SEM BEI showing collection of at least four different precious metal phases including Sperrylite (?) (Sp), silver-rich electrum (el), kotulskite (kt) and telluropalladinite (?) (Tp). Most surrounding material is chalcocite (cc) with veins of unidentified silicate (chlorite or epidote). Note "Si-Te" grain, this grain contains silicon and tellurium. These elements were identified in an x-ray map.

Sulfur Isotope Study of the Revais Creek Mining District

Twelve samples from the Revais Creek mining district and surrounding area were analyzed by Dr. Ed Ripley at Indiana University for their sulfur isotopic composition to help determine the source of the sulfide mineral sulfur (Table 6). The rationale for a sulfur isotope study is that sulfur of primary magmatic origin in mafic and felsic rocks generally has $\delta^{34}\text{S}$ values that cluster around 0‰ \pm 5‰ (Faure, 1986); non-magmatic sources commonly are enriched, depleted, or have wide ranges relative to 0‰. Sulfur isotope compositions are commonly expressed as $\delta^{34}\text{S}$, as seen in Equation 1.

$$\delta^{34}\text{S}_{spl} = \left[\frac{\left(\frac{^{34}\text{S}}{^{32}\text{S}} \right)_{spl} - \left(\frac{^{34}\text{S}}{^{32}\text{S}} \right)_{std}}{\left(\frac{^{34}\text{S}}{^{32}\text{S}} \right)_{std}} \right] \times 10^3 \quad \text{Eqn. 1 (Faure, 1986)}$$

Where spl = sample, and std = standard.

A $^{32}\text{S}/^{34}\text{S}$ ratio of 22.22 from the iron meteorite Canyon Diablo is used as a standard in this calculation.

Mafic igneous rocks typically have isotopic compositions of sulfur similar to those of the earth's mantle and meteorites (Faure, 1986). Therefore, the $\delta^{34}\text{S}$ value of a mafic igneous rock will generally be close to 0‰ and significantly positive or negative variations commonly suggest contamination by sulfur from surrounding crustal rocks. Depending on their history, sedimentary, felsic, and mafic igneous rocks may have highly variable $\delta^{34}\text{S}$ values.

Table 6. Sulfur isotope analysis results from the Revais Creek district and selected other mineralized areas for comparison. Sample analysis performed by Dr. Ed Ripley at the University of Indiana

Sample	Sample type	$\delta^{34}\text{S}$ (‰)
Sediment samples		
Revais Creek area		
PF1	Prichard F Fm. sediment	0
PE-1	Prichard E Fm. sediment	+5.8
RC-1	Revett Fm. (copper rich)	-1.1
RC-2	Revett Fm. (copper rich)	-1.4
RC-3	Revett Fm. (copper rich)	-7.2
Avg.(Standard dev.)	Revett Formation samples (n=3)	-3.2 (2.81)
Avg.(Standard dev.)	All sedimentary samples (n=5)	-0.78 (4.14)
Igneous samples		
Revais Creek area		
PARS-1	Paradise Sill	-2.5
AA-2	RCI (high grade, part. alt.)	+1.1
F93-3531	RCI (high grade, part. alt.)	+1.3
F93-3570	RCI (high grade, part. alt.)	+1.1
GMVS-1B	RCI (low grade, str. alt.)	+3.2
GMIS-7	RCI (low grade, str. alt.)	+1.3
TT-3	RCI (low grade, str. alt.)	+2.0
Avg.(Standard dev.)	RCI Samples (6)	+1.67 (0.75)
Noril'sk (Gorbachev and Grinenko, 1973)		
Avg.	Gabbro	+12
Avg.	Sed.	+16.4
Stillwater (Zientek <i>et al.</i> , 1982; Zientek, 1983)		
Avg.	Igneous	0
Avg.	Hornfels	+2.7
Avg.	Mineralized Hornfels	-1.03
Avg.	Massive Sulfide	-1.33
Belt Supergroup (Rye <i>et al.</i> , 1984)		
Spar Lake-Troy	pyrite (n = 12)	+3.8 to +23.1
	galena (n = 4)	+2.2 to +18.1
	chalcopyrite (n = 10)	+8.5 to +19
	chalcocite-bornite-digenite (n = 9)	+5.0 to +23.3

Biogenic fractionation is the most common means of changing $\delta^{34}\text{S}$ values in sedimentary rocks. Sulfate reducing anaerobic bacteria, due to kinetic considerations, preferentially break $^{32}\text{S-O}$ relative to $^{34}\text{S-O}$ bonds in the sulfate ion during reduction. This fractionates the sulfur isotopes enriching the H_2S produced in ^{32}S while leaving an isotopically heavy SO_4 residue. This fractionation mechanism can produce highly negative $\delta^{34}\text{S}$ values in sulfide minerals formed from the isotopically lighter H_2S . Felsic igneous rock, such as granite, may have been created through crustal anatexis, giving it $\delta^{34}\text{S}$ values of the protolith average (Faure, 1986).

Sulfur isotopes have been used to identify sulfurization (the introduction of foreign sulfur) of some mafic magmas. One such example is in the Noril'sk region in Siberia. In Noril'sk, Gorbachev and Grinenko (1973) found that rocks from the Talnakh gabbro have an average $\delta^{34}\text{S}$ value of +12.0‰ whereas adjacent sedimentary rocks average +16.4‰.

Zientek *et al* (1982) and Zientek (1983) studied S-isotopic composition in the Stillwater complex in Montana. In the complex, average $\delta^{34}\text{S}$ values were 0.0‰ for igneous bodies, 2.7‰ for unmineralized hornfels samples, -1.03‰ for mineralized hornfels, and -1.33‰ for massive sulfide zones within the hornfels. Zientek suggests that these data provide evidence that:

- pre-igneous sulfide minerals with positive $\delta^{34}\text{S}$ values occur in hornfels protoliths.
- mineralized zones in the hornfels are of igneous origin.
- magmatic sulfur entered hornfels near igneous bodies.
- assimilation of sedimentary sulfur within the igneous complex was not significant.

Sulfur isotope data for the Revais Creek area are limited, but the data are similar to those from the Stillwater Complex. Six samples from the RCI, two from the Prichard Formation, three from zones of Cu-Ag mineralization within the Revett Formation proximal to the RCI, and one from the Paradise sill were analyzed for their $\delta^{34}\text{S}$ values (Table 6). The average RCI sample has a $\delta^{34}\text{S}$ value of 1.67‰ and a standard deviation of ± 0.75 (range: 1.1‰ to 3.2‰, n=6). The sedimentary samples have an average of $\delta^{34}\text{S} = 0.78$ ‰ with a standard deviation of ± 4.14 (range: +5.8‰ to -7.2‰, n=5) (Table 6).

Data from sulfur isotopy of the Spar Lake deposit (Rye *et al.*, 1984) hosted by the Revett Formation about 200 Km northwest of the RCI show that the $\delta^{34}\text{S}$ values there are higher than those from the Revett Formation adjacent to the RCI (Table 6). This suggests that there might have been some interaction between the RCI and the sedimentary rocks that it intruded. The sparse data in this study does not statistically show that there was gabbro-sediment interaction. The $\delta^{34}\text{S}$ averages of the RCI and the sedimentary rocks are quite similar and their standard deviations overlap. Therefore, the data here are inconclusive as to the significance of the isotopic values.

Fluid Inclusions in the Revais Creek Intrusion

Fluid inclusions were examined microscopically in three quartz vein samples from the RCI. Two samples were from strongly altered, mineralized zones in the Green Mountain and Lucky Strike areas. The third sample was from a small quartz vein in an unmineralized section of the RCI.

Homogenization temperatures of fluid inclusions from all three samples were determined at the University of Montana using a U.S. Geologic Survey-type gas flow heating and freezing stage mounted on a microscope. Determining of freezing temperatures was difficult due to the small size of the inclusions. These inclusions were identified as being primary due to their relatively larger size, isolated locations, and lack of associated fractures.

The inclusions from the two samples in the mineralized areas did not contain any daughter minerals and had oblong shapes and CO₂ vapor bubbles. Some of the inclusions from the unmineralized area contained halite and possibly sylvite daughter crystals and CO₂ vapor bubbles indicating at least 23 weight percent NaCl equivalent.

All primary inclusions examined in the mineralized area homogenized over a temperature range of 203°C to 380°C. The mean homogenization temperature of the inclusions from the two samples is 305.5°C. Only one inclusion from the unmineralized sample was large enough to see the vapor homogenize. The vapor in this inclusion homogenized at about 142°C whereas the halite crystal disappeared at 174°C.

It is difficult to estimate the depth of burial of the RCI during hydrothermal alteration because the age of alteration is not known. Burwash (1993) developed four

Table 7. Fluid inclusion data from 2 mineralized samples.

Sample	Inclusion	Homogenization Temp. (°C)	Return Temp. (°C)
1	1	309	292
1	2	323	312
1	3	292	273
1	4	337	N/D
1	5	203	191
2	1	321	274
2	2	309	291
2	3	322	271
2	4	308	270
2	5	380	367
2	6	307	297
2	7	235	220
2	8	325	282
Range		203 - 380	
Mean		305.5	

age-sedimentation models for the Belt Supergroup. All of Burwash's models suggest that Belt sedimentation terminated prior to 900 Ma. Winston and Link (1986) show that the thickness of the Belt sedimentary rocks in the Plains area is about 15 kilometers. The highest stratigraphic level attained by the RCI is approximately 7.5 kilometers below the top of the Belt Supergroup in this area. Therefore, 7.5 kilometers is probably a maximum depth of burial possible during hydrothermal alteration.

While this is a very limited study of fluid inclusions in the RCI, it presents an estimate of the range of temperatures of the hydrothermal fluids that altered and mineralized the intrusion. In the mineralized area, it appears that the rock was altered by solutions with at least 23 wt% NaCl equivalent at trapping temperatures above 305°C,

depending on the lithostatic and hydrostatic pressure. Trapping temperatures, however, are probably much higher than the temperature of homogenization ($\sim 305^{\circ}\text{C}$) because it is likely that pressure was higher during the hydrothermal event.

Rb-Sr and Sm-Nd Isochron Dates of the Revais Creek Intrusion

Introduction

An age date of the RCI was acquired to help differentiate the RCI from the other mafic bodies in the Belt Supergroup as well as to determine genetic models. One sample from the RCI was analyzed for Sm, Nd, Rb and Sr concentrations by isotope dilution and for $^{87}\text{Sr}/^{86}\text{Sr}$ and $^{143}\text{Nd}/^{144}\text{Nd}$ ratios. The analytical procedures used are described in Foland and Allen (1991).

The medium-grained sample was obtained from where the RCI dike feeds the sill-like body. This sample was selected because it is the least altered gabbro found in this study. The sample is comprised of 43 percent augite with some pigeonite, 48 percent plagioclase, 4 percent hornblende, 1 percent biotite, and 3 percent magnetite/ilmenite. Trace amounts of micrographic/myrmekitic quartz-potassium feldspar/plagioclase intergrowths, alteration and weathering products also occur. The Sm-Nd relationships, however, should not be disturbed by this minor amount of alteration (Foland 1995).

Procedures

Dr. Ken Foland of Ohio State University performed the separations and isotope analyses. Pyroxene, plagioclase, and hornblende were separated from crushed rock using conventional magnetic and heavy-liquid procedures together with hand picking. To analyze apatite, a portion of the whole rock sample was leached with dilute HCl which preferentially dissolved the apatite. Therefore, the whole-rock leachate represents apatite. The plagioclase fraction yielded suitable Rb-Sr, but not Sm-Nd data. The results and

analytical uncertainties are given in Table 8. Figures 28, 29, and 30 show plots of the Sm/Nd and Rb/Sr data. Linear regression of these data provided Rb-Sr and Sm-Nd internal isochrons.

Table 8. Rb-Sr and Sm-Nd analytical data for sample of the RCI (analyses performed by Dr. Ken Foland at Ohio State University).

Sample	Sm ^a (ppm)	Nd ^a (ppm)	¹⁴⁷ Sm/ ¹⁴⁴ Nd ^a	¹⁴³ Nd/ ¹⁴⁴ Nd ^b	Rb ^a (ppm)	Sr ^a (ppm)	⁸⁷ Rb/ ⁸⁶ Sr ^a	⁸⁷ Sr/ ⁸⁶ Sr ^b
Whole rock	5.464	19.62	0.1683	0.512652(7)	23.9	143	0.4828	0.709561(21)
Whole rock residue ^c	4.289	13.37	0.1940	0.512675(11)	17.1	132	0.3737	0.708570(14)
Whole rock leachate ^c	2.048	8.978	0.1379	0.512487(5)	6.95	9.7	2.0790	0.725391(11)
Amphibole	9.21	28.99	0.1921	0.512761(7)	16.5	19	2.5040	0.729254(25)
Pyroxene	4.426	13.09	0.2045	0.512812(10)	16.2	21	2.2840	0.710778(15)
Plagioclase					3.99	441	0.0262	0.704990(8)

^a By isotope dilution, uncertainties are Nd, Sm, and Sr, $\pm 0.1\%$; Rb, $\pm 0.4\%$; ¹⁴⁷Sm/¹⁴⁴Nd, 0.1%; and, ⁸⁷Rb/⁸⁶Sr, $\pm 0.5\%$. (Foland and Allen, 1991)

^b Measured present day values normalized to ¹⁴⁶Nd/¹⁴⁴Nd = 0.721900 or ⁸⁷Rb/⁸⁶Sr = 0.119400.

Uncertainties in last digit(s), given in parentheses, are two standard deviations of the mean for in-run statistics. Reference value and one-sigma external reproducibility are 0.51184x $\pm 0.00000x$ for ¹⁴³Nd/¹⁴⁴Nd of the LaJolla standard.

^c The whole-rock sample was leached to remove and isolate the apatite fraction in a leachate fraction. Both the leachate and residue were treated quantitatively using highly purified materials and clean lab ware. Leaching was carried out as follows: 30 minute immersion in 3 ml of 2 N HCl; agitate and allow to stand for 30 minutes; repeat; decant off supernate; wash with high purity water and combine wash with supernate. Concentrations are reported as ppm for the original sample weight.

Results

A five point Sm-Nd isochron yields an age of 745 ± 23 Ma with a mean square of weighted deviations (MSWD) of 2.5 (Figure 28). The calculated initial ¹⁴³Nd/¹⁴⁴Nd ratio for this isochron is 0.511820 ± 0.000028 ($\epsilon_{Nd}[745 \text{ Ma}] = +2.8 \pm 0.6$). The

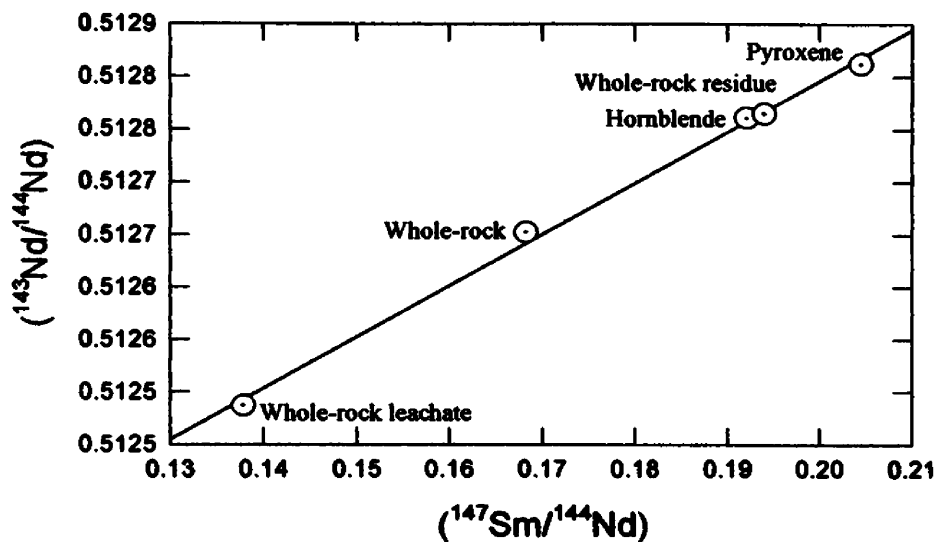


Figure 28. Sm-Nd isochron based on two mineral fractions, whole-rock leachate (apatite), whole rock residue, and whole rock from the RCI. The age calculated from this plot is 745 ± 23 Ma and the initial $^{143}\text{Nd}/^{144}\text{Nd}$ ratio is 0.511820 ± 0.000028 (Analyses performed by Foland, 1995).

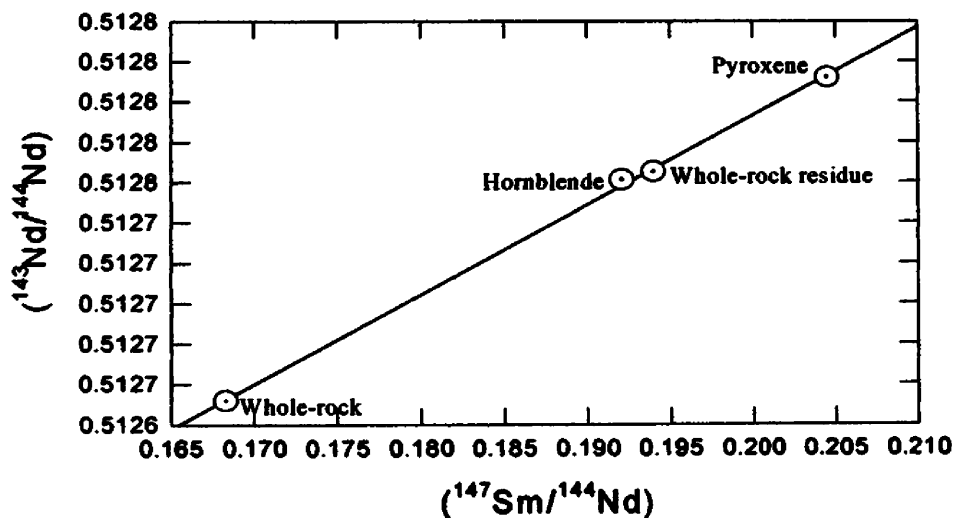


Figure 29. Sm-Nd isochron based on two mineral fractions, whole rock residue, and whole rock from the RCI. The age calculated from this plot is 676 ± 14 Ma and the initial $^{143}\text{Nd}/^{144}\text{Nd}$ ratio is 0.511907 ± 0.000018 (Analyses performed by Foland, 1995)

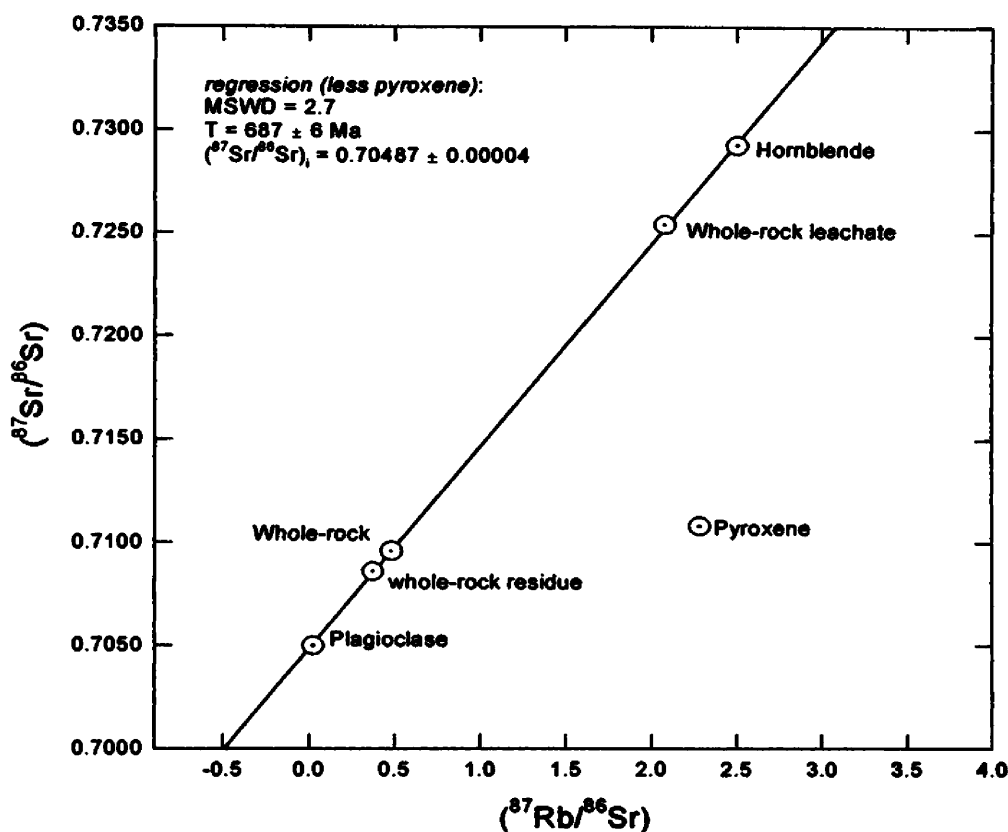


Figure 30. Rb-Sr isochron based on three mineral fractions, whole rock residue, and whole rock from the RCI (pyroxene excluded). The age calculated from this plot is 687 ± 6 Ma and the initial ($^{87}\text{Sr}/^{86}\text{Sr}$) ratio is 0.70487 ± 0.00004 (Analyses performed by Foland, 1995).

whole-rock leachate (apatite) deviates the most from a perfect fit. If this fraction is removed from the isochron, the results of the regression yield a MSWD of 0.23, an age of 676 ± 14 Ma, and an initial $^{143}\text{Nd}/^{144}\text{Nd}$ ratio of 0.511907 ± 0.000018 ($\epsilon_{\text{Nd}}[676 \text{ Ma}] = +2.7 \pm 0.4$) (Figure 29). The Rb-Sr isochron in Figure 30 is in close agreement with the Sm-Nd data with a MSWD of 2.7, and age of 687 ± 6 Ma, and an initial $^{87}\text{Sr}/^{86}\text{Sr}$ of 0.70487 ± 0.00004 . The first pyroxene separate analysis was excluded from the Rb-Sr internal isochron because it greatly deviates from the linear fit. Because the pyroxene sample was subsequently lost, it could not be re-run to check the anomalous result from

the initial run (Foland, 1995). The Rb-Sr date of 687 ± 6 Ma has the greatest precision, therefore, it is probably closest to the actual age of the RCI (Figure 29).

Implications of the 687 ± 6 Ma - 676 ± 14 Ma ages of the RCI

The Rb-Sr and Nd ages of the RCI roughly correspond with Windermere time. This was during a time when large-scale rifting, sedimentation, and volcanism affected western North America. Windermere age strata extend from the Mackenzie Mountains in northwestern Canada to southeastern British Columbia and northeastern Washington State. Rocks of similar age and stratigraphy crop out discontinuously in other areas of the western United States.

Many other Windermere age igneous rocks have been dated. In the Mackenzie Mountains, a quartz diorite plug and diabase sills yielded ages of 777.7 ± 2.5 Ma (U-Pb) and $766-769 \pm 27$ Ma (Rb-Sr), respectively (Jefferson and Parrish, 1989). Evenchick *et al.* (1984) dated zircons from granitic rocks of the southern Cordillera. A range of 728 to about 760 Ma for these rocks suggests that they are temporally similar to those from the Mackenzie Mountains (Jefferson and Parrish, 1989). Near Revelstoke, British Columbia, zircons from an alkalic nepheline syenite yielded an age of about 740 ± 36 Ma (Parrish and Scammell, 1988), and in northeastern Washington State preliminary Sm-Nd data from a metabasalt at the base of the Windermere Supergroup suggest an age of 762 ± 44 Ma (Devlin *et al.*, 1988). All of these temporally similar occurrences within the Windermere Supergroup show that diverse igneous activity occurred between about 780 and 730 Ma (Jefferson and Parrish, 1989).

Table 9. Geochemistry of Windermere Age Rocks Including the RCI.

Sample	SiO ₂	TiO ₂	Al ₂ O ₃	Fe ₂ O ₃	MnO	MgO	CaO	Na ₂ O	K ₂ O	P ₂ O ₅	Age(Ma)
<i>Average RCI (Unaltered)</i>	50.6	2.78	12.5	16.7	0.23	4.9	8.4	2.4	0.7	0.11	687±6 ¹
Avg Little Dal Basalt*	50.3	2.23	13.2	17.7	0.18	6.1	4.8	3.5	1.7	0.18	
Little Dal Basalt JP-77-398*	49.2	2.00	14.0	19.3	0.22	5.7	3.6	3.9	1.9	0.11	
Quartz Diorite*	52	1.4	14	13	0.2	5.7	7.6	3.2	2.9	0.2	777.7±2.5 ²
Diabase Sills*											
77LBA19-4	50	2.5	12	18	ND	4.9	8.6	2.3	1.3	0.2	766-769±27 ³
43A	48	2.4	14	18	ND	5.5	9.7	1.7	0.5	0.2	
Diabase Dikes*											
42	49	1.4	16	13	ND	6.5	9.8	2.7	1.5	0.2	
44	45	2.9	14	19	ND	6.1	8.8	2.2	1.4	0.2	

* Geochemical data from Jefferson and Parrish, (1989).

1 Rb-Sr isochron (This study).

2 U-Pb zircon upper intercept (Jefferson and Parrish, 1989)

3 Rb-Sr isochron (Armstrong *et al.*, 1982)

Similarities, with respect to major element geochemistry, of selected igneous rocks from the Mackenzie Mountains and samples from the RCI are listed in Table 9. Despite the fact that Windermere age sedimentary rocks are absent in western Montana and the rocks of the RCI are 45 to 95 million years younger, it seems that there could be some relationship between the RCI and Windermere age rifting, sedimentation and volcanism. The age date from this study has some interesting implications for the Belt basin. It appears from this date that there was a significant period of partial melting of the mantle at about 687 ± 6 Ma. Further implications are beyond the scope of this study.

Environment of Formation and Genetic Model of the Revais Creek Intrusion

The Revais Creek Intrusion differs from average gabbroic, quartz-normative, continental tholeiites because it contains anomalously high levels of copper, palladium, and possibly platinum, and relatively low amounts of nickel in unaltered rocks (Table 1). Also, the RCI has higher TiO₂, Fe₂O₃*, and lower Al₂O₃ than average continental tholeiites. Windermere age extension of the region is probably related to the formation of the RCI. Normal continental tholeiite in extensional environments is most likely the result of partial (5-10%) melting of mantle material that either fractionated in a magma chamber, or has been subsequently contaminated by crustal rock (Barnes *et al*, 1985).

However, the anomalously high background concentrations of copper, palladium, and possibly platinum in the Revais Creek Intrusion require further explanation. Possible mechanisms of creating these anomalous concentrations include:

- Degree of partial melting of source material.
- Deriving the RCI magma from a source already enriched in Cu, Pd, Pt and depleted with respect to Ni, and possibly Ir, Rh, and Os.
- Crustal contamination of the RCI magmas with selected metals.

Partial Melting

The degree of partial melting in the mantle affects the concentrations of PGE in a melt. Naldrett and Duke (1980), citing data from Ross and Keays (1979), and Crocket (1979), suggest that, nickel has a strong affinity for olivine. Partition coefficients (K_D) On the other hand, copper, palladium, and platinum are concentrated in sulfide minerals. Mantle sulfide minerals melt before the more refractory olivine phase during partial melting. Therefore, the (Pd +Pt)/(Ir + Rh + Os) ratio of a partial melt will decrease and

the Ni/Cu ratio will increase with increasing partial melting. The RCI geochemistry is compatible with a partial melt origin because of its high (Pd +Pt)/(Ir + Rh + Os) ratio. However, this does not explain why there is more Cu, Pd, and Pt in the Revais Creek intrusion than similar continental tholeiite rocks.

An uncontaminated melt will have geochemical characteristics similar to its source. If the source is already enriched in Cu, Pd, and Pt while depleted of Ni, Ir, Rh, and Os, the melt will assume, if not accentuate, these traits. Relative amount of these elements in the source, and the degree of melting of that source, control the resulting amounts of the elements in a melt. If the RCI magma was a second generation partial melt, Cu, Pd, and Pt would be further enriched while Ni, Ir, Rh, and Os would be further depleted.

Crustal Assimilation

Crustal assimilation by a magma can introduce foreign metals into the system. However, geochemical and textural differences will reflect magmatic assimilation of crustal rocks. Such evidence of crustal assimilation would include contained inclusions, elemental variations (like increased SiO₂ content), or isotopic data. There is, however, no evidence supporting crustal assimilation by the RCI magma such as documented in the Plains sill by Buckley and Sears, (1992).

Partial Melting of an Enriched Source

It is possible that the RCI magma might have resulted from partial melting of a source that was already enriched in Cu, Pd, and Pt perhaps by an earlier partial melting

event. Rifting during the time of Belt Supergroup sedimentation produced a partial melt, like the sills in the Prichard Formation, that was possibly again partially melted during Windermere rifting to produce the RCI magma. However, this process would produce a melt enriched in SiO_2 , K_2O and depleted in MgO . Therefore, partial melting of an enriched source to produce the RCI seems unlikely.

The general east-west striking trend of the RCI and the Revett-hosted Cu-Ag mineralization coincides roughly with the Jocko Line, a proposed syndepositional fault (Winston, 1996; Ryan & Buckley, 1993). The RCI may have intruded along this proposed structural weakness. Therefore, partial melting of mantle peridotite produced a gabbroic magma enriched in Cu, Pd and Pt and depleted with respect to Ni. The resulting magma, intruded the Belt sedimentary rocks, possibly along an existing structural weakness. The whole sedimentary pile and the igneous rocks within it were subsequently folded by Laramide-age compression.

Discussion

The two most documented processes of PGE concentration in rocks worldwide are: (1) silicate melt saturation and subsequent segregation of magmatic sulfide and (2) deposition of metals from hydrothermal solution. The data obtained in this study indicate that the zones of metal concentration in the RCI may be the result of a combination of the two processes. Table 9 shows the pros and cons of whether magmatic or hydrothermal processes could have been responsible for the zones of metal concentration in the RCI.

Table 10. Evidence for magmatic vs. hydrothermal concentration in enriched zones within the RCI.

Magmatic concentration	
Pros	Cons
<ul style="list-style-type: none">• Some sulfide mineral textures might be interpreted as magmatic by some workers.• The close association of PGM and sulfide minerals suggests sulfide scavenging.	<ul style="list-style-type: none">• Small size of the RCI.• Small zones of mineralization
Hydrothermal concentration	
Pros	Cons
<ul style="list-style-type: none">• PGM association with hydrosilicate minerals.• PGM exhibiting vein-like, epigenetic textures.• Some sulfide minerals exhibit hydrothermal textures.• PGE and Cu ratios similar to known hydrothermal deposits.• High Pd/Ir ratio suggests hydrothermal mobilization.	<ul style="list-style-type: none">• No apparent correlation between degree of alteration and grade of mineralization.

Magmatic Concentration Processes

The magmatic concentration process is shown schematically in Figure 31.

Magmatic sulfide droplets form in silicate magma when the amount of sulfur in the magma exceeds the silicate magma's sulfur-saturation point. The sulfide droplets scavenge the group VIII transition, siderophile elements, specifically Ni, Cu, Co and PGE. The PGE also exhibit chalcophile tendencies. These transition metals may be concentrated 100 to 100,000 times in sulfide droplets relative to the parent silicate magma (Naldrett, 1989). As the sulfide liquid cools and crystallizes, the PGE partition into platinum group minerals that crystallize last along sulfide-silicate grain boundaries (Zientek, 1993). If the intrusive body crystallizes slowly, a density contrast between the sulfide liquid and the silicate liquid may allow the sulfide droplets to sink and pool at the footwall of the structure. This

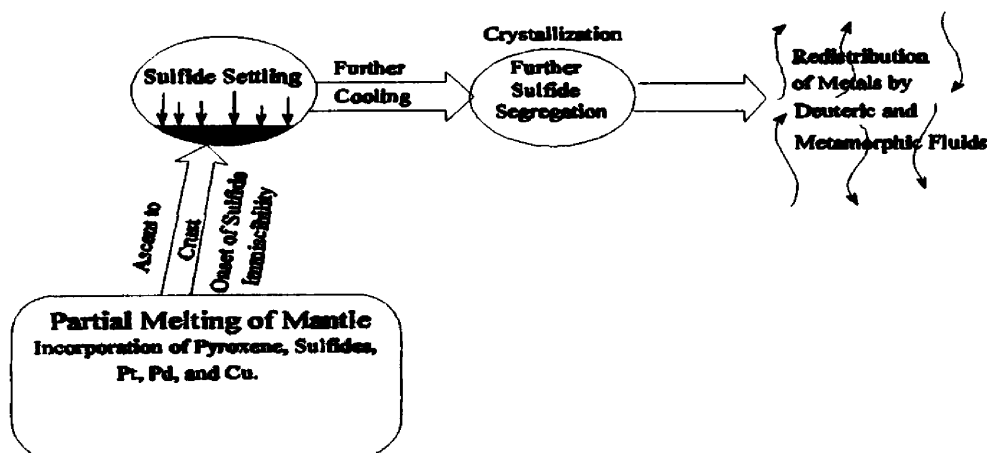


Figure 31. Stages in the formation of a typical magmatic ore and subsequent remobilization (Naldrett, 1989).

process further concentrates the sulfides and PGE and can result in footwall magmatic sulfide deposits (Naldrett, 1989).

In the RCI, some sulfide mineral textures can be interpreted as the result of magmatic sulfide segregation. Also, many PGM are spatially associated with sulfide minerals suggesting sulfide scavenging. Producing an immiscible sulfide liquid phase in a silicate magma can be accomplished by one or more of the following processes:

- Assimilation of sulfur
- Assimilation of a silic material
- Decreasing temperature
- Decreasing Fe^{2+} content
- Increasing the fugacities of O_2 and S_2
- Increasing load pressure

In the RCI, some sulfide mineral textures might be interpreted by some workers as the result of magmatic sulfide segregation. Also, many PGM are spatially associated with sulfide minerals suggesting sulfide scavenging.

Sulfur assimilation

The data from a sulfur isotope study of the RCI and wallrock are inconclusive as to whether or not sulfur assimilation occurred. The average RCI sample has a $\delta^{34}\text{S}$ value of $1.67\text{‰} \pm 0.75$. The average $\delta^{34}\text{S}$ for sedimentary samples is -0.78‰ of ± 4.14 (Table 6). At first glance, the difference in the average $\delta^{34}\text{S}$ between the RCI and sedimentary rocks suggests that the sulfur in each came from different sources. The lower average $\delta^{34}\text{S}$ for sedimentary samples suggests that the sulfur in the RCI and sedimentary rocks come from different sources. However, the standard deviations are large and they overlap. Therefore, the data are inconclusive. Additional sulfur isotope work might statistically

resolve a difference or similarity in the two rock types.

Sialic Assimilation

Irvine (1975), using data from the Muskox Intrusion in the Canadian Northwest Territories, proposed sialic contamination of a mafic magma as a means of lowering its capacity to carry sulfur. Naldrett and Macdonald (1980) proposed that silica-rich wallrock contamination of the Sudbury mafic magma caused sulfide liquation. The silica-contamination model developed by Naldrett and Macdonald (1980) is shown in Figure 32. The FeO-SiO₂ side of the ternary diagram is equivalent to silicate melts and the FeS corner is equivalent to sulfide magmas. A magma at a composition indicated by Point A is a one phase, homogeneous FeO-SiO₂-FeS liquid. If SiO₂ is added so that the composition

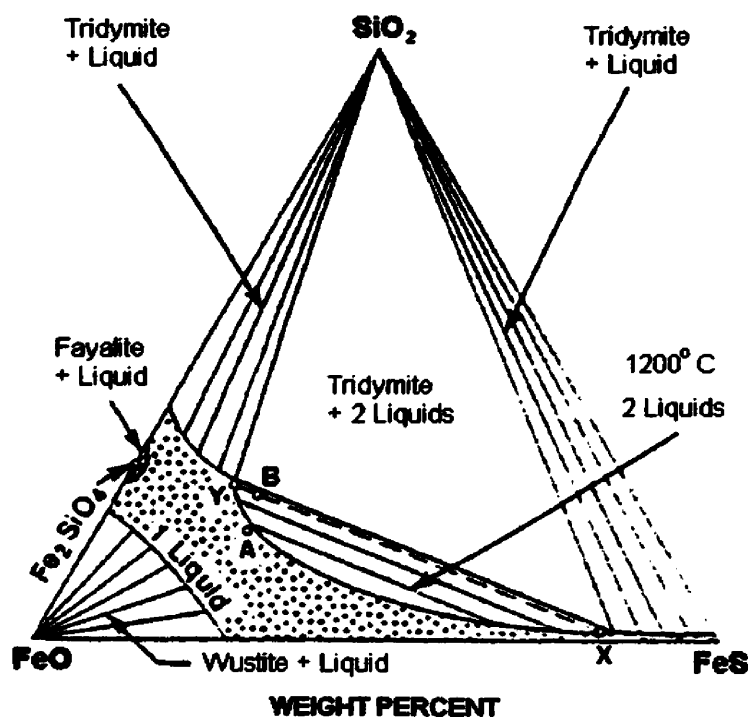


Figure 32. Ternary diagram illustrating the hypothetical effect of silica contamination of a FeO-FeS melt. (Macdonald, 1987)

changes to that of Point B, the magma now consists of a two-phase, silicate-rich liquid (Y) and co-existing sulfide liquid (X) (Macdonald 1987).

In the Muskox Intrusion, Irvine (1975) demonstrated sialic contamination of the magma by roof-rock stoping and melting. He described 1.5 meter blocks of quartzite along a contact zone cemented by the granophyre at the top of the intrusion, and large amounts of embayed fragments of quartzite throughout the granophyre. Also, the granophyre is highly potassic, whereas the lower part of the intrusion is not. Irvine (1975) shows that partial melting of the hornfelsed schist roof-rock would produce a highly potassic melt as seen in the Muskox Intrusion. Naldrett and Macdonald (1980) cited a high percentage of normative quartz, partially digested inclusions in the host rocks, high $^{87}\text{Sr}/^{86}\text{Sr}$ ratio, and lack of cyclical units as evidence of sialic contamination at the Sudbury.

In contrast to the Muskox Intrusion and the Sudbury Irruptive, the RCI appears to have had limited interaction with sedimentary country rocks. The intrusion/wall-rock contacts are typically sharp to only slightly gradational, and no inclusions of any kind have been found in the gabbro. Even where the RCI becomes more sill-like, there is very little apparent geochemical differentiation from the hanging wall to the footwall of the structure. Also, no granophyre is evident in the RCI. Finally, there is no marked difference in SiO_2 content anywhere throughout the RCI to indicate wall-rock assimilation or differentiation.

Fe⁺⁺ effect

Experimental studies by Wentlandt (1982) suggest that the capacity of a silicate magma to dissolve sulfur increases with increasing Fe^{2+} content. Also, the bonding of

sulfur with Fe^{2+} dictates the solubility of sulfur in the melt (Irvine, 1975; Richardson and Fincham; 1954). One way to lower the amount of Fe^{2+} , and therefore the amount of sulfur dissolved in a magma, is through oxidation and the subsequent formation of magnetite. Within the RCI, magnetite is present in similar percentages throughout, including zones of unmineralized gabbro. The observation that there is no change in magnetite percentage in the mineralized zones indicates that crystallization of magnetite and changes in Fe^{2+} content may not be responsible for sulfide saturation in the RCI.

S₂ and O₂ Fugacities (f)

Wentlandt, (1982) and Haughton *et al.*, (1974) have shown that increasing $f\text{S}_2$ and $f\text{O}_2$ decreases a silicate magma's capacity to carry dissolved sulfur. However, it is not possible to quantify these systems with the limited data available on the RCI.

Pressure and Temperature Variation

Increasing load pressure or temperature also decreases sulfur solubility within a magma (Wentlandt, 1982). If some process increases pressure or temperature of a magma and the sulfur content is near saturation, a sulfide liquid could be formed. However, it seems unlikely that such a process occurred within the RCI. All of the zones of concentrated metals and sulfur are located in the more sill-like section of the RCI which was presumably emplaced higher in the stratigraphic section and under less load pressure and perhaps temperature relative to the rest of the body. Therefore, increasing pressure was probably not responsible for sulfur saturation of the silicate magma in the sill-like section of the RCI. In fact, the opposite was more likely the case.

Not enough data are available to discuss the temperature variations and their effect

on sulfur solubility. However, it seems unlikely that the PGE concentration-bearing, sill-like section of the RCI was hotter than the dike-like portion where no concentrations of these elements have been discovered.

Hydrothermal Concentration of Precious Metals

PGE's may also be concentrated in rocks by hydrothermal processes. There are several known occurrences of hydrothermally concentrated PGE in the world. Some of the most well studied areas include the Salt Chuck Intrusion in Alaska (Watkinson & Melling, 1992; McCallum *et al*, 1976), the New Rambler deposit in Wyoming (Nyman *et al*, 1990), the Two Duck Lake Intrusion, Ontario (Watkinson & Ohnenstetter, 1992), the Messina Mine in South Africa (Mihálik *et al*, 1974), and Rathbun Lake in Northeastern Ontario (Rowell & Edgar, 1986).

Evidence cited by these authors and found in the RCI that a post-magmatic hydrothermal processes concentrated metals in the include: 1) High Cu/(Cu+Ni) ratios and low Pt/(Pt+Pd) ratios comparable to known hydrothermal PGE deposits, 2) the behavior of Cu, Pd, and Pt versus Ni, Ir, Os, Ru, and Rh in hydrothermal solutions, 3) ore and gangue textures including vein-like PGE minerals, hydrothermal alteration minerals and, 4) alteration assemblages that include (clinoamphibole, clinozoisite, epidote, chlorite, sericite and quartz).

All of these data suggest that hydrothermal fluids invaded and altered primary magmatic silicate minerals of the RCI. At the same time, these fluids leached, transported, and concentrated metals. The most likely source of the PGE is the RCI itself which

contains high background levels of the metals (Table 1).

Comparisons to PGE Deposits of Documented Hydrothermal Origin

Copper and PGE ratios can be indicative of the origin of PGE deposits. Compared to PGE deposits of magmatic origin, deposits of hydrothermal origin have higher ratios of $\text{Cu}/(\text{Cu}+\text{Ni})$, $(\text{Pt}+\text{Pd})/(\text{Os}+\text{Ir}+\text{Rh})$, and $\text{Pd}:\text{Pt}:(\text{Os}+\text{Ir}+\text{Rh}+\text{Ru})$ and generally lower ratios of $\text{Pt}/(\text{Pt}+\text{Pd})$ (Table 11). However, the Stillwater contains $\text{Pt}/(\text{Pt}+\text{Pd})$ values that are similar to the RCI. Hydrothermal deposits have a higher $\text{Cu}/(\text{Cu}+\text{Ni})$ ratio than magmatic deposits because copper is more soluble in hydrothermal solutions than nickel. The differences in PGE ratios result because Pt and Pd are more mobile in hydrothermal fluids than Os, Ir, and Rh (McCallum *et al*, 1976) and Pd is more soluble than Pt.

The copper and platinum group element ratios listed in Table 11 support a hydrothermal origin of the metal concentrations in the RCI. A six sample suite that covers both partially hydrothermally altered and strongly hydrothermally altered rock has an average Pd:Pt ratio of 2.5:1. This same set of samples was analyzed for the total PGE suite. The ratio of $\text{Pd}:\text{Pt}:(\text{Ir}+\text{Os}+\text{Ru}+\text{Rh})$ is approximately 25:10:1. The Pd:Pt ratio of the partially altered ores of the RCI is about 3:1, and it appears that the stronger the hydrothermal alteration, the lower the ratio.

A study of the New Rambler mine in Wyoming by McCallum *et al* (1976) compared the Pd:Pt and $\text{Pd}:\text{Pt}:(\text{Ir}+\text{Os}+\text{Ru}+\text{Rh})$ ratios of several PGE deposits. The study showed that PGE deposits of hydrothermal origin have much larger $\text{Pd}:\text{Pt}:(\text{Ir}+\text{Os}+\text{Ru}+\text{Rh})$ ratios than deposits of magmatic origin. The data in Table 11 indicate that the ratios from the RCI are similar to ratios from hydrothermal deposits.

Table 11. Comparison of Ratios of Cu, Pt and Pt+Pd with selected other elements in the Revais Creek Intrusion and other Platinum-Group Element Deposits. Selected magmatic sulfide (Class I), komatiitic (Class II), and hydrothermal (Class III) occurrences are considered.

Deposit	Class	Cu/ (Cu+Ni)	Pt/ (Pt+Pd)	(Pt+Pd)/ (Os+Ir+Rh)	Pd:Pt: (Rh+Os+Ir+Ru)	Ref.
Pechenga, Kola Peninsula.	I	0.35	0.55	nd	nd	1
JM Reef, Stillwater Complex	I	0.36	0.20	nd	nd	2
Discord. Chromitite, Stillwater Complex	I	0.11	0.48	nd	nd	2
A-Chromitite, Stillwater Complex	I	nd	0.30	nd ⁱ	nd	2
Leka Ophiolite chromitite, Norway (n = 10)	I	nd	0.61	4.6	1.4:2.3:1	3
Merensky Reef, Bushveld *	I	0.3	0.72	13.0	5:19:1	4
Sudbury	I,II	0.46	0.94	13.7	2:2:1	1
Noril'sk-Talnakh W. Sibera*	I,II	0.59	0.27	10.6	5.8:2.2:1	4
Donaldson West, Ungava Quebec *	II	0.17	0.21	7.3	4.4:1.2:1	4
Katniq, Ungava Quebec *	II	0.23	0.33	5.2	2.6:1.3:1	4
New Rambler, Wyoming	III	nd	0.05	nd	~1800:100:1	5
Two Duck Lake, Ontario (n = 22)	I, III	0.92	0.32	nd ⁱⁱ	nd	6, 7
Rathbun Lake, N.E. Ontario	III	>0.9	0.31	1120	560:236:1	8
Messina Mine, South Africa	III	nd	0.17	nd ⁱⁱⁱ	22:4.5:1	9
Salt Chuck Intrusion, Alaska	III	nd	0.027	216.6 ^{iv}	163:12:1	10
Revais Creek Intrusion, Montana	III	0.99 ^v	0.28 ^v	68 ^{vi}	41:23:1	This study

nd = not determined

* Denotes that ratios were calculated from values normalized to 100% sulfide.

ⁱ (Pt+Pd)/(Rh+Ru+Ir) = 2.5 (Page *et al.*, 1985).

ⁱⁱ (Pt+Pd)/(Ir+Rh) = 60.7 (Good and Crocket, 1994)

ⁱⁱⁱ (Pd+Pt)/(Ir+Ru+Rh) = 31.8 (Mihálik *et al.*, 1974).

^{iv} Average of two samples: SC29 & SC21 from Watkinson and Melling (1992).

^v Data averaged from eleven altered, mineralized samples (This study).

^{vi} Data from six samples analysed for PGE suite both partially and strongly altered (This study).

Reference guide for Table 11:

1. Naldrett and Cabri, 1976.
2. Page *et al.*, 1985.
3. Pederson *et al.*, 1993.
4. Naldrett and Duke, 1980.
5. McCallum *et al.*, 1976.

6. Watkinson and Ohnstetter, 1992.
7. Good and Crocket, 1994.
8. Rowell and Edgar, 1986.
9. Mihálik *et al.*, 1974.
10. Watkinson and Melling, 1992.

PGE deposits formed by magmatic processes, including chromitites and reefs (PGE zones) in the Stillwater complex, and the Merensky Reef in the Bushveld Complex, typically contain low (<0.5) $\text{Cu}/(\text{Cu}+\text{Ni})$ ratios, high (0.2-0.94) $\text{Pt}/(\text{Pt}+\text{Pd})$ ratios, and low (4.6-13.7) $(\text{Pt}+\text{Pd})/(\text{Os}+\text{Ir}+\text{Rh})$ ratios. Most of the hydrothermal PGE deposits contain high (>0.9) $\text{Cu}/(\text{Cu}+\text{Ni})$ ratios, low (0.027-0.31) $\text{Pt}/(\text{Pt}+\text{Pd})$ ratios, and high (68-1120) $(\text{Pt}+\text{Pd})/(\text{Os}+\text{Ir}+\text{Rh})$ ratios. The strong similarity between the RCI and other deposits of presumed hydrothermal origin, in terms of these ratios, is evident in Table 11. These ratios reflect a preferred hydrothermal mobilization of Cu versus Ni (Table 2), and Pd rather than Pt. For example, assuming that the unaltered-unmineralized rocks (Table 1) represent the background Cu and PGE concentrations of the RCI, the altered-mineralized rock contains elevated metal concentrations. Copper in mineralized rock is concentrated to seventy-two times background whereas nickel is concentrated ten times.

Ore-gangue textures

PGM occur in three textural modes in the RCI: 1) PGM completely surrounded by sulfide minerals, 2) PGM on sulfide-silicate grain boundaries, and 3) in hydrothermally formed silicate minerals. The sulfide mineral grains do not appear to be immiscible-looking, rounded droplets. However, the textures in the RCI could be interpreted as magmatic because, in some cases, the sulfide minerals appear to be filling interstices between the euhedral pyroxene and plagioclase crystals. Textures suggesting that the RCI high-grade zones were formed by hydrothermal processes include sulfide grains that embay, and possibly replace, primary magmatic silicates and oxides.

Figure 33 contains photomicrographs showing annealed quartz with 120° grain intersections that is of submagmatic, recrystallized or, hydrothermal origin. Grains of mertieite (Pd,Sb₂) surrounded by the hydrothermal quartz are also evident in these photomicrographs. All of the hand specimens containing the highest-grades of Cu, Pd, and Pt are at least partially hydrothermally altered while the sulfide minerals are commonly associated with and sometimes rimmed and embayed by chlorite, recrystallized quartz and other alteration minerals (See Figures 33 a & b).

The depositional textures of some platinum-group minerals also support a hydrothermal origin. Within the RCI, vein-like stibiopaladinite ((Pd,Cu)₂Sb₂) in a hydrosilicate groundmass and associations of mertieite (Pd,Sb₂) with hydrothermal minerals such as recrystallized quartz are indicative of a hydrothermal origin. These PGM, however, might be the result of hydrothermal reworking of PGM formed by another, earlier process.

The types of platinum group minerals that occur in the RCI also are compatible with a hydrothermal concentration process. The presence of palladium bismuthotellurides, and palladium antimony compounds observed in the RCI (Table 5) tend to be more common than other PGM in known hydrothermal PGE deposits (McCallum *et al*, 1976).

Hydrothermal alteration

Within the RCI, copper sulfides and PGM occur in rocks that have undergone at least partial greenschist facies propylitic hydrothermal alteration. The assemblage of

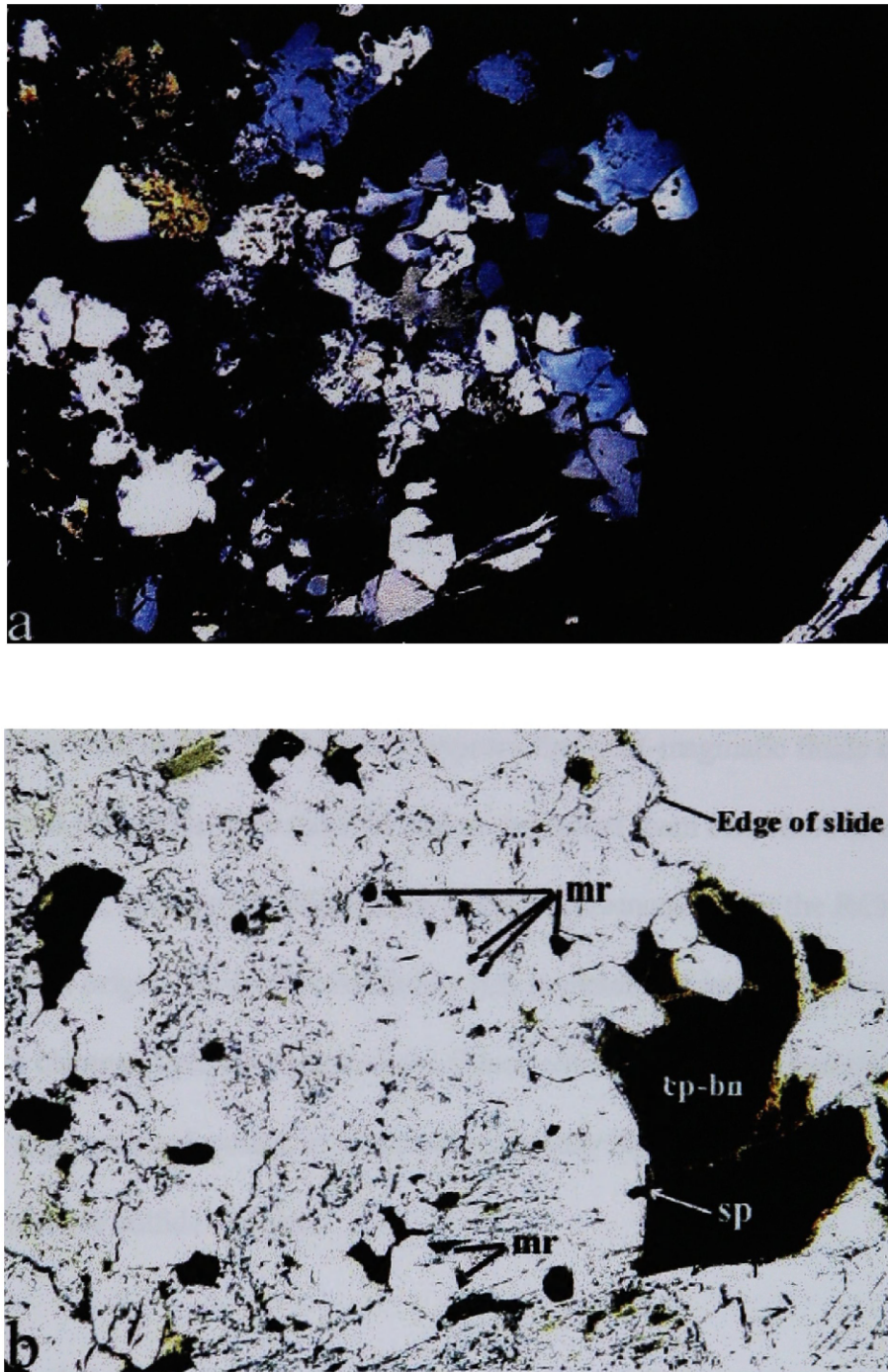


Figure 33. a) Crossed nicols photomicrograph of recrystallized quartz. Note 120° annealed quartz grain intersections. b) Same view as 'a' in plane light. Large opaque grain on right side of photo is chalcopyrite and bornite (cp-bn). Several of the small opaque grains dotting the photo are mertieite (Pd_5Sb_2) (mr). Note the small grain of sperrylite (sp) on the boundary of the cp-bn grain. These PGM grains can also be seen in Figures 17 and 18. Width of photos is approximately 2.5mm.

clinoamphibole, chlorite, sericite, quartz, and epidote is the result of hydration of the primary pyroxene and plagioclase. Small chlorite-epidote veins are common, and all primary silicate minerals are rimmed by clinoamphibole and chlorite. Also, the sulfide minerals which commonly appear to replace magnetite are typically spatially associated with chlorite and epidote. However, there is no apparent correlation between degree of hydrothermal alteration and PGE grade (Kell, 1993; This study). Poor exposure and paucity of mine records make it difficult to obtain a detailed look at the extent of the alteration and the spatial distribution of the ore within the RCI.

The RCI contains anomalously high background PGE values in unaltered rock. Sulfur isotopy in this study, while inconclusive, does not discount that the sulfur in the RCI is of magmatic origin. Therefore, it appears that post-magmatic fluids could have leached metals and sulfur from the RCI and re-deposited them elsewhere in the same body. The small, zone or pod-like nature of the occurrences within the RCI also suggests a hydrothermal origin. Hydrothermal fluids, rich in metal-bearing complex ions that encounter a change in physio-chemical conditions commonly deposit metals in such zones. Magmatic segregation deposits, in contrast, are usually layered due to settling out of denser immiscible sulfide droplets.

Hydrothermal Transport

If hydrothermal processes are responsible for metal concentrations in the RCI, how were the metals transported? Pan and Wood, (1994), Wood *et al.*, (1989), Mountain and Wood (1988a; 1988b), and Wood, (1987) present thermodynamic constraints on the

transport of platinum and palladium by complexing with hydroxide (OH⁻), bisulfide (HS⁻), chloride (Cl⁻), or ammonia complex ions in hydrothermal solutions. They apply their thermodynamic results to the hydrothermally introduced PGE concentrations at the New Rambler mine, Wyoming and the Rathbun Lake occurrence, Ontario. At New Rambler (McCallum et al, 1976) and Rathbun Lake (Rowell and Edgar, 1986), the mafic host rocks have undergone propylitic alteration to greenschist facies. Ore deposition occurred between 300°C and 335°C at New Rambler and between 300°C to 400°C at Rathbun Lake. Mountain and Wood (1988) and Wood *et al.* (1989) suggest that, under these temperatures and alteration conditions, bisulfide complexing is responsible for transporting Cu, Pt, Pd and, possibly, Ni (I am unaware of any experimental investigations into the solubility of Ni in bisulfide complexes. However, lower Ni-bisulfide stability could be responsible for the lack of Ni concentration in the RCI.).

If the metals at these deposits were transported by bisulfide complexation in hydrothermal solutions, the most likely cause of deposition would be the interaction of the solutions with magnetite, chlorite, and epidote within sheared metagabbro (Mountain and Wood, 1988a). A sulfur-rich solution bearing Cu-, Pt-, Pd-, and, possibly, Ni-bisulfide complexes could react with the iron-bearing magnetite, chlorite, and/or epidote to form iron-sulfides. This reaction would decrease the concentration of reduced sulfur in the fluid by oxidizing it, thereby decreasing the stability of the bisulfide complexes. The result is the precipitation of the Cu and PGE metals (Mountain and Wood, 1988a). Experimental stabilities of Pt-chloride, Pd-chloride, Pt-bisulfide, and Pd-bisulfide, are shown in Figure 34.

Cu, Pd, and Pt concentrations within the RCI are similar to those in the New Rambler mine, the Rathbun Lake occurrence and, the Salt Chuck intrusion in Alaska (Pan and Wood, 1994). Similarities include, associated with propylitic or greenschist facies alteration and the apparent replacement of magnetite by copper-iron-sulfides. The respective authors concluded that bisulfide complexation of Cu, Pt, and Pd was important in each of these deposits.

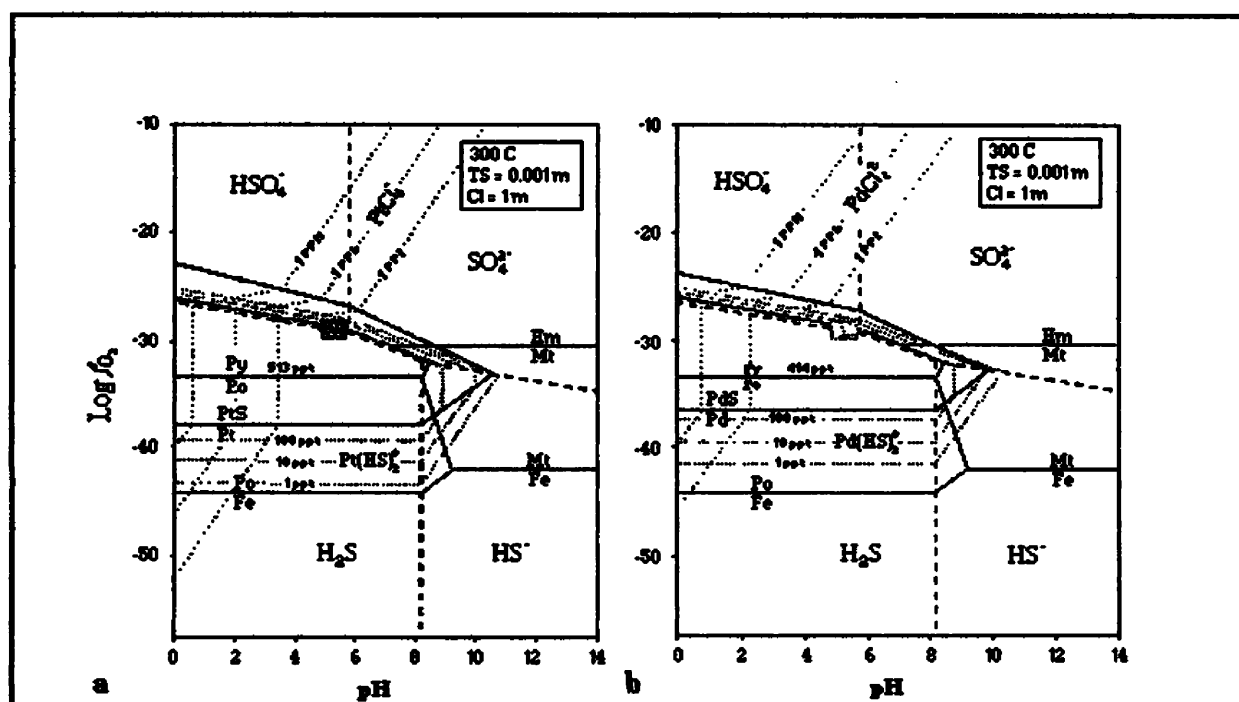


Figure 34. $\text{Log } f_{O_2}$ - pH diagrams for the system Pt(Pd)-H-O-S showing the stability of various Pt(Pd) phases and their solubility as bisulfide complex. a) The Pt-H-O-S system. b) The Pd-H-O-S system. (Adapted from Pan & Wood, 1993)

Pan and Wood (1994), cite the Salt Chuck intrusion in Alaska as an example of bisulfide-complex transport of Pt and Pd. The alteration mineralogy in the Salt Chuck is similar to that of the RCI, consisting of epidote, actinolite, chlorite, titanite and calcite. Pan and Wood (1994) conclude that the presence of epidote and chlorite at 300°C

indicates that the pH of the hydrothermal fluids must be greater than 4. The presence of sulfide and not sulfate in the RCI indicates that the fluids were reducing. A system with a pH greater than 4 under reducing conditions would support Pt and Pd-bisulfide complexes (Figure 34). The solubility of Pt and Pd as bisulfide complexes is dependent on several factors. Temperature, ΣS , pH, and eH all affect how much Pt and Pd can be carried in solution.

Copper, Nickel and PGE behavior in hydrothermal solutions

Wood *et al.*, (1989), Mountain and Wood, (1988), Pan and Wood, (1994), and Gammons and Bloom (1993) present thermodynamic and experimental data on the solubility of platinum and palladium in hydrothermal solutions. Mountain and Wood, (1988) show that platinum and palladium-chloride ($PtCl_4^{2-}$ and $PdCl_4^{2-}$) complex ions reach solubilities of more than 1 ppm in oxidizing solutions at 300°C, 0.005 molal sulfur, and a pH range of <2 to 6. However, under reducing conditions at 300°C, 0.1 molal sulfur, and pH's between 7 and 9, platinum and palladium-bisulfide complexes ($Pt(HS)_4^{2-}$ and $Pd(HS)_4^{2-}$) are stable in solution only in amounts up to 100 part per trillion (ppt). Pan and Wood (1994) in a similar study suggest that the concentrations approach 0.5 ppb under similar conditions (Figure 34).

Copper occurs in various complexes that are stable in oxidizing fluids at temperatures less than 350°C including $Cu(OH)_2$, $Cu(CO_3)_2^{2-}$, $CuSO_4$, and $CuCl^+$. In reducing, weakly acidic solutions, chloride complexing dominates at 250-350°C while at temperatures below 250°C bisulfide complexing becomes more important (Barnes, 1979). This observation suggests that either there is a problem with transporting Pt and Pd as

bisulfide complexes in the RCI or that copper is more mobile than previously thought under neutral, reducing conditions.

Comparison of the RCI with the Two Duck Lake Intrusion

Controversy continues over the origin of many PGE deposits and occurrences; both hydrothermal and magmatic processes have been proposed. The Two Duck Lake Intrusion of the Port Coldwell Alkalic Complex in Ontario, Canada is a good example of a controversial deposit. Copper and PGE mineralization within the Two Duck Lake Intrusion is hosted by the Two Duck Lake Gabbro. Disseminated chalcopyrite and pyrrhotite with lesser amounts of pentlandite and pyrite characterize the mineralized rock (Good and Crocket, 1994). Gabbroic rocks containing Cu-PGE rich assemblages have been partially altered to actinolite + chlorite + epidote + sericite + calcite (Watkinson and Ohnenstetter, 1992).

Watkinson and Ohnenstetter (1992), conclude that PGE mineralization is the result of hydrothermal processes while Good and Crocket (1994) counter that the same deposits result from magmatic processes. Watkinson and Ohnenstetter (1992) suggest that late magmatic deuteric fluids altered primary sulfides, transported PGE, Cu and other metals, possibly as chloride complexes, and precipitated the metals. This suggestion is based upon field, petrographic, and mineral-chemical data such as:

- spatial association of PGM with chalcopyrite
- chalcopyrite replacing plagioclase and pyrrhotite
- spatial association of PGM and chalcopyrite with Cl- and F-bearing minerals and chlorite, epidote, actinolite, sericite, and calcite

- the occurrence of zoned hollingworthite

Good and Crocket (1994) contend that Watkinson and Ohnenstetter (1992) are incorrect and that the metal concentrations in the Two Duck Lake gabbro are the result of magmatic processes with possible deuteric mobilization of chalcophile elements at a hand-sample scale. Their evidence for this includes:

- significant correlation between sulfur and chalcophile element concentrations (They suggest that hydrothermal processes would disperse the data)
- coherent geochemical behavior for Ni and Ir (Ni should be strongly fractionated from Ir in hydrothermal systems)
- good preservation of primary gabbro minerals and an absence of extensive alteration of these minerals

Copper-PGE concentrations in the RCI are very similar to those in the Two Duck Lake Intrusion. Both have similar $\text{Cu}/(\text{Cu}+\text{Ni})$ and $\text{Pt}/(\text{Pt}+\text{Pd})$ ratios, similar PGM and ore textures, and similar alteration assemblages. The Two Duck Lake Intrusion differs from the RCI in that it is coarser grained and it contains olivine, xenoliths of surrounding rock, and granophyre. Also, there is no extensive alteration of primary minerals within the Two Duck Lake gabbro (Good and Crocket, 1994) whereas, mineralized rocks of the RCI have been subjected to partial to strong hydrothermal alteration.

Strong correlations between sulfur and the chalcophile elements, coherent geochemical behavior of Ni and Ir, and lack of extensive alteration of primary silicate minerals within the Two Duck Lake gabbro suggest that the concentration process was primarily magmatic (Good and Crocket, 1994).

The data in Figures 13a-f indicate that little or no correlation exists between sulfur

and the chalcophile elements in the strongly mineralized rocks of the RCI. Good and Crocket (1994) state that within the Two Duck Lake Intrusion, the significant correlation between sulfur and the chalcophile elements is indicative of magmatic control. Therefore, the lack of correlation in the RCI suggests that hydrothermal processes were involved in transporting metals. Unfortunately, lack of data on the minor PGE's (Ir, Os, Ru, and Rh) within the RCI to determine whether there is any correlation between these and the other metals.

Combined Magmatic and Hydrothermal Processes

The data from this study do not prove or disprove the existence of a magmatic concentration process. It has been argued that some of the sulfide mineral grains might be of a magmatic origin. Despite this possibility, most of the evidence presented supports the contention that hydrothermal processes were responsible for a significant part of the metal concentration. A model where more than one process is responsible for the concentration of the high grade metal zones in the RCI could explain the lack of strong sulfur-metal and metal-metal correlations in Figures 13 and 14. This could also explain why there is little to no correlation between the degree of hydrothermal alteration and tenor. Of course, it would be difficult to suggest that magmatic and hydrothermal concentration occurred in the same places by pure coincidence.

Conclusions

The Revais Creek mining district contains anomalously high concentrations of copper, palladium, and platinum in a 687 ± 6 Ma, gabbroic, quartz-normative, continental tholeiite intrusion. Mineralized rocks occur in small zones or pods along the outcrop trace of the sill-like section of the RCI. Metals in the RCI vary from average “background” levels in unaltered samples of 57ppb Pt+Pd, and 447ppm copper to greater than 12,000ppb and 11 percent respectively in hydrothermally altered specimens containing copper-iron-sulfides. The primary process of Cu, Pd, and Pt concentration in the RCI is believed to be aqueous transport and deposition of Cu, Pd, and Pt as bisulfide complex ions in reducing, neutral, hydrothermal fluids within the RCI. Fluid inclusions in quartz demonstrate that the temperatures of the mineralizing hydrothermal fluids were in the range of 203°C to 380°C. The source of the Cu, Pd, Pt, and S is not determined, however geochemistry suggests that at least Cu, Pd, and Pt originated in the RCI.

Despite the small size of the pods of concentrated metals, the occurrence of copper and PGE is geologically significant. It is likely that there are undiscovered pods of mineralized rocks along the RCI and in bodies of similar age and composition throughout the area affected by Windermere extension. At present, the extent of the occurrences is unknown, and the grades of these pods warrant further examination and exploration along the Revais Creek Intrusion, and perhaps over a much larger area. Since all of the known significant concentrations of copper and PGE are located within the more sill-like section of the RCI, I recommended that any future exploration be focused in such areas. Locating the RCI and similar bodies can be accomplished through mapping, soil sampling, and

magnetic surveys. Tracer elements that aid in determining the location of the RCI include copper, palladium, platinum, and vanadium.

A detailed spatial alteration study of the known mineralized zones in the RCI might provide a better understanding of what process or processes were responsible for the metal concentrations. Also, further sulfur isotope analyses might statistically indicate whether the origin of sulfur was the RCI or the surrounding sediments.

Appendix A**Sample analysis methods performed by Bondar - Clegg of Vancouver B.C.**

Element	Lower Detection Limit	Extraction	Method
Gold	1ppb	Fire assay	Fire assay-DCP
Platinum	5ppb	Fire assay	Fire assay-DCP
Palladium	1ppb	Fire assay	Fire assay-DCP
Silver	0.2ppm	HCL:HNO ₃ (3:1)	Induc. Coup. Plasma
Copper	1ppm	HCL:HNO ₃ (3:1)	Induc. Coup. Plasma
Lead	2ppm	HCL:HNO ₃ (3:1)	Induc. Coup. Plasma
Zinc	1ppm	HCL:HNO ₃ (3:1)	Induc. Coup. Plasma
Molybdenum	1ppm	HCL:HNO ₃ (3:1)	Induc. Coup. Plasma
Nickel	1ppm	HCL:HNO ₃ (3:1)	Induc. Coup. Plasma
Cobalt	1ppm	HCL:HNO ₃ (3:1)	Induc. Coup. Plasma
Cadmium	1.0ppm	HCL:HNO ₃ (3:1)	Induc. Coup. Plasma
Bismuth	5ppm	HCL:HNO ₃ (3:1)	Induc. Coup. Plasma
Bismuth	1ppm	HCL:HNO ₃ (3:1)	Atomic absorption
Arsenic	5ppm	HCL:HNO ₃ (3:1)	Induc. Coup. Plasma
Arsenic	1.0ppm		Neutron activation
Antimony	5ppm	HCL:HNO ₃ (3:1)	Induc. Coup. Plasma
Antimony	0.2ppm		Neutron activation
Mercury	0.010ppm	HCL:HNO ₃ (3:1)	Cold vapor AA
Iron	0.01%	HCL:HNO ₃ (3:1)	Induc. Coup. Plasma
Manganese	1ppm	HCL:HNO ₃ (3:1)	Induc. Coup. Plasma
Tellurium	10ppm	HCL:HNO ₃ (3:1)	Induc. Coup. Plasma
Tellurium	0.2ppm	Multi-acid/MIBK	Atomic absorption
Barium	2ppm	HCL:HNO ₃ (3:1)	Induc. Coup. Plasma
Chromium	1ppm	HCL:HNO ₃ (3:1)	Induc. Coup. Plasma
Vanadium	1ppm	HCL:HNO ₃ (3:1)	Induc. Coup. Plasma
Tin	20ppm	HCL:HNO ₃ (3:1)	Induc. Coup. Plasma
Tungsten	20ppm	HCL:HNO ₃ (3:1)	Induc. Coup. Plasma
Lanthanum	1ppm	HCL:HNO ₃ (3:1)	Induc. Coup. Plasma
Aluminum	0.01%	HCL:HNO ₃ (3:1)	Induc. Coup. Plasma
Magnesium	0.01%	HCL:HNO ₃ (3:1)	Induc. Coup. Plasma
Calcium	0.01%	HCL:HNO ₃ (3:1)	Induc. Coup. Plasma
Sodium	0.01%	HCL:HNO ₃ (3:1)	Induc. Coup. Plasma
Potassium	0.01%	HCL:HNO ₃ (3:1)	Induc. Coup. Plasma
Strontium	1ppm	HCL:HNO ₃ (3:1)	Induc. Coup. Plasma
Yttrium	1ppm	HCL:HNO ₃ (3:1)	Induc. Coup. Plasma
Silica (SiO ₂)	0.01%	Borate fusion	Induc. Coup. Plasma

Titanium (TiO ₂)	0.01%	Borate fusion	Induc. Coup. Plasma
Alumina (Al ₂ O ₃)	0.01%	Borate fusion	Induc. Coup. Plasma
Total Iron (Fe ₂ O ₃)	0.01%	Borate fusion	Induc. Coup. Plasma
Manganese (MnO)	0.01%	Borate fusion	Induc. Coup. Plasma
Magnesium (MgO)	0.01%	Borate fusion	Induc. Coup. Plasma
Barium oxide (BaO)	0.001%	Borate fusion	Induc. Coup. Plasma
Calcium (CaO)	0.01%	Borate fusion	Induc. Coup. Plasma
Sodium (Na ₂ O)	0.01%	Borate fusion	Induc. Coup. Plasma
Potassium (K ₂ O)	0.05%	Borate fusion	Induc. Coup. Plasma
Loss on ignition (LOI)	0.05%		Gravimetric
Chromium oxide (Cr ₂ O ₃)	0.01%	Borate fusion	Induc. Coup. Plasma
Phosphorous (P ₂ O ₅)	0.03%	Borate fusion	Induc. Coup. Plasma
Whole rock total	0.01%		
Sulfur (total)	0.02%		LECO

References

- Armstrong, R.L., Eisbacher, G.H. , and Evans, P.D., 1982, Age and stratigraphic-tectonic significance of Proterozoic diabase sheets, Makenzie Mountains, northwestern Canada. *Canadian Journal of Earth Sciences*, v. 19, pg. 316-323.
- Barnes, H. L., 1979, Solubilities of ore minerals. *in* Barnes, H.L. (ed) *Geochemistry of hydrothermal ore deposits 2nd Edition*. John Wiley & Sons, Inc. New York, Chichester, Brisbane, Toronto, pg. 404-460.
- Barnes, S.-J., Naldrett, A.J., and Gorton, M.P., 1985, The origin of the fractionation of platinum-group elements in terrestrial magmas, *Chemical Geology*, v. 53 pg. 303-321
- Best, M.G., 1982, *Igneous and Metamorphic Petrology*: New York, W.H. Freeman and Company, 620 p.
- Buckley, S.N. 1993, Personal communication regarding mapping and sample analyses in the Revais Creek area.
- Buckley, S.N., Sears, J.W., 1992, Evidence for emplacement of mafic sills into wet sediments in the Prichard Formation, Middle Proterozoic Belt Supergroup, Perma area, Western Montana. *GSA Abstracts with Programs, Rocky Mountain Section, Ogden, Utah*. v. 24 (6) pg. 4-5.
- Burwash, R.A., 1993, Overview of Belt geochronology and problems of dating the Belt-Purcell Supergroup. *in* *Programs and Abstracts, Belt Symposium III, August 14-21, 1993*.
- Burwash, R.A. and Wagner, P.A.. 1989, Sm/Nd geochronology of the Moyie Intrusions, Moyie Lake map area, British Columbia: British Columbia Ministry of Energy, Mines and Petroleum Resources, *Geological Fieldwork, Paper 1989-1*, p. 45-48.
- Cressman, E.R., 1989, Reconnaissance stratigraphy of the Prichard Formation (Middle Proterozoic) and the early development of the Belt Basin, Washington, Idaho, and Montana: U.S. Geological Survey Professional Paper 1490, 79p.
- Crocket, J.H., 1981, Geochemistry of the Platinum-Group Elements, *in*: Cabri, L. (ed.), *Platinum Group Elements: mineralogy, geology, and recovery*. Canadian Institute of Mining and Metallurgy Special Volume 23, pg. 47-64.
- Crocket, J.H., 1979, Platinum group elements in mafic and ultramafic rocks: A survey. *Canadian Mineralogist*, v. 17, pg. 391-403.

- Dahy, J.P., 1986, A preliminary investigation of the Revais Creek dike. Unpublished thesis for the Montana College of Mineral Science and Technology. 10 p.
- Devlin, W.J., Brueckner, H.K., and Bond, G.C., 1988, New isotopic data and a preliminary age for volcanics near the base of the Windermere Supergroup, northeastern Washington, U.S.A., *Canadian Journal of Earth Science*, v. 25, pg. 1906-1911.
- Evenchick, C.A., Parrish, R.R., and Gabrielse, H., 1984, Precambrian gneiss and Late Proterozoic sedimentation in north-central British Columbia. *Geology*, v. 12, pg. 233-237.
- Faure, G., 1986, *Principals of Isotope Geology*: New York, Chichester, Brisbane, Toronto, Singapore, John Wiley and Sons, 589 p.
- Foland, K.A. and Allen, J.C., 1991, Magma sources for Mesozoic anorogenic granites of the White Mountain magma series, New England, USA. *Contributions to Mineralogy and Petrology* v. 109, pg.195-211.
- Foland, K.A., 1995, Personal communication regarding procedure and results of Sm-Nd and Rb-Sr age dating of the Revais Creek Intrusion.
- Gammons, C.H. and Bloom, M.S., 1993, Experimental investigation of the hydrothermal geochemistry of platinum and palladium: II. The solubility of PtS and PdS in aqueous sulfide solutions to 300°C, *Geochimica et Cosmochimica Acta*, v. 57, pg. 2451-2467.
- Good, D.J., and Crocket, J.H., 1994, Genesis of the Marathon Cu-platinum-group element deposit, Port Coldwell Alkalic Complex, Ontario: a midcontinent rift-related magmatic sulfide deposit, *Economic Geology* v. 89, pg. 131-149.
- Gorbachev, N.S. and Grinenko, L.N., 1973, The sulfur isotope ratios of the sulfides and sulfates of the Oktyabr'sk sulfide deposit, Noril'sk region, and the problem of its origin: *Geokhimiya* v. 8, pg. 1127-1136.
- Haughton, D.R., Roeder, P.L., and Skinner, B.J., 1974, Solubility of sulfur in mafic magmas: *Economic Geology*, v. 69, p. 451-467.
- Herberger D., 1990 Unpublished mapping.
- Höy, T., 1989, The age, chemistry, and tectonic setting of the Middle Proterozoic Moyie sills, Purcell Supergroup, southeastern British Columbia, *Canadian Journal of*

- Earth Sciences v. 26, pg. 2305-2317.
- Irvine, T.N., 1975, Crystallization sequences in the Muskox intrusion and other layered intrusions--II. Origin of chromitite layers and similar deposits of other magmatic ores: *Geochimica et Cosmochimica Acta*, v. 39, pg. 991-1020.
- Irvine, T.N., and Barager, W.R.A., 1971, A guide to the chemical classification of the common volcanic rocks, *Canadian Journal of Earth Sciences*, v. 8, pg. 523-549.
- Jefferson, C.W. and Parrish, R.R., 1989, Late Proterozoic stratigraphy, U-Pb zircon ages, and rift tectonics, Mackenzie Mountains, northwestern Canada. *Canadian Journal of Earth Sciences*, v. 26, pg. 1784-1801.
- Kell, R., 1992, Summary of petrographical and geochemical study Revais Creek gabbro-hosted copper-palladium-platinum-gold deposit Dixon area - Flathead Indian Reservation Sanders County, Montana. Unpublished report for the Confederated Salish and Kootenai Tribes.
- Lange, I. M., and Sherry, R.A., 1983, Genesis of the sandstone (Revett) type of copper-silver occurrences in the Belt Supergroup of northwestern Montana and northeastern Idaho. *Geology*, v. 11, pg. 643-646.
- Macdonald, A.J., 1987, The platinum group element deposits: classification and genesis. *Geoscience Canada Reprint Series 3*. Originally published in *Geoscience Canada* v. 14 Number 3 (September 1987).
- Mauk, J.L., 1983, Stratigraphy and sedimentation of the Proterozoic Burke and Revett Formations, Flathead Indian Reservation, western Montana [M.S. thesis]; Missoula, University of Montana 106 p.
- McCallum, M.E., Loucks, R.R., Carlson, R.R., Cooley, E.F. and Doerge, T.A., 1976, Platinum metals associated with hydrothermal copper ores of the New Rambler Mine, Medicine Bow Mountains, Wyoming: *Economic Geology*, v. 71, pg.1429-1450.
- Mihálik, P., Jacobsen, J.B.E., and Hiemstra, S.A., 1974, Platinum-group minerals from a hydrothermal environment: *Economic Geology*, v. 69, pg. 257-262.
- Mountain, B.W., and Wood, S.A., 1988a, Chemical controls on the solubility, transport, and deposition of platinum and palladium in hydrothermal solutions: a thermodynamic approach: *Economic Geology*, v.83, pg. 492-510.
- Mountain, B.W., and Wood, S.A., 1988b, Solubility and transport of platinum-group

- elements in hydrothermal solutions: Thermodynamic and physical chemical constraints, in Prichard, H.H., Potts, P.J., Bowles, J.F.W., and Cribb, S.J., eds., Proceedings of the symposium "Geo-Platinum 87" held at Open University, Milton-Keynes, Great Britain, April 22-23, 1987: Basking, Essex, Great Britain, Elsevier, p. 57-82.
- Mudge, M.R., Harrison, J.E., Kleinkopf, M.D., and Ingersoll, R.G., 1976, Status of mineral resource information for the Flathead Indian Reservation, Montana. U.S. Geological Society and U.S. Bureau of Mines Administrative Report BIA-22 73 pg.
- Naldrett, A.J., 1989, Magmatic sulfide deposits: Oxford Monographs on Geology and Geophysics No. 14, Oxford University Press, New York, 186 p.
- Naldrett, A.J., and Cabri, L.J., 1976, Ultramafic and related mafic rocks: Their classification and genesis with special reference to the concentration of nickel sulfides and platinum-group elements: *Economic Geology*, v. 71, pg. 1131-1158.
- Naldrett, A.J., and Duke, J.M., 1980, Platinum metals in magmatic sulfide ores: *Science*, v. 208, Num. 4451, pg. 1417-1424.
- Naldrett, A.J. and Macdonald, A.J., 1980, Tectonic settings of some Ni-Cu sulfide ores: their importance in genesis and exploration, in Strangway, D.W., ed., *The Continental Crust and its Mineral Deposits: Geological association of Canada, Special Paper 20*, pg. 633-657.
- Norwick, S.A., 1972, The regional Precambrian metamorphic facies of the Prichard Formation of western Montana and northern Idaho, PhD Dissertation University of Montana. 129 pg.
- Nyman, M.W., Sheets, R.W., and Bodnar, R.J., 1990, Fluid-inclusion evidence for the physical and chemical conditions associated with intermediate-temperature PGE Mineralization at the New Rambler Deposit, Southeastern Wyoming: *Economic Geology*, v. 28, pg. 629-638.
- Page, N.J., Zientek, M.L., Czamanske, G.K., and Foose, M.P., 1985, Sulfide mineralization in the Stillwater Complex and underlying rocks, in Czamanske, G.K., and Zientek, M.L. eds., *The Stillwater Complex, Montana: Geology and Guide: Montana Bureau of Mines and Geology Special Publication 92*, pg. 93-96.
- Pan, P. and Wood, S.A., 1994, Solubility of Pt and Pd sulfides and Au metals in aqueous bisulfide solutions, *Mineral. Deposita*, v. 29 pg. 373-390.

- Parrish, R.R. and Scammell, R.J., 1988, The age of the Mount Copeland syenite gneiss and its metamorphic zircons, Monashee Complex, southeastern British Columbia, *in* Radiogenic Age and Isotopic Studies: Report 2. Geological Survey of Canada, Paper 88-2, pg. 21-28.
- Pederson, R.-B., Johannesen, G.M., and Boyd, R., 1993, Stratiform Platinum-group element mineralizations in the ultramafic cumulates of the Leka Ophiolite Complex, Central Norway. *Economic Geology*, v. 88, pg. 782-803.
- Pirajno, F., 1992, *Hydrothermal Mineral Deposits - principles and fundamental concepts for the exploration geologist*: Berlin, Heidelberg, New York, London, Paris, Tokyo, Hong Kong, Barcelona, Budapest. Springer-Verlag, 702 pg.
- Poage, M. A., 1997, Hydration, metamorphism and diabase-granophyre relations in a thick basaltic sill emplaced into wet sediments, western Montana, M.S. thesis, University of Montana, 132 p.
- Porder, S.J. 1997, Metamorphism and metasomatism of the Lower Prichard Formation: A petrologic, geochemical and thermobarometric study of the lowermost member of the Belt/Purcell Supergroup, M.S. thesis, University of Montana.
- Richardson, R.D. and Fincham, C.J.B., 1954, Sulfur in silicate and aluminate slags. *J. Iron Steel Inst. London*, v. 178, pg. 4-14.
- Ross, J.R., and Keays, R.R., 1979, Precious metals in volcanic-type nickel sulfide deposits in Western Australia. Part 1: Relationship with the composition of the ores and their host rocks: *Canadian Mineralogist*, v. 17 pg. 417-436.
- Rowell, W.F., Edgar, A.D., 1986, Platinum-Group Element mineralization in a hydrothermal Cu-Ni sulfide occurrence, Rathbun Lake, Northeastern Ontario: *Economic Geology* v. 81 pg. 1272-1277.
- Ryan, P.C., and Buckley, S.N., 1993, Stratabound Cu-Ag mineralization and implications for Revett Formation deposition, Flathead Indian Reservation, Western Montana, *in*: Program and Abstracts, Belt Symposium III, August 14-21, 1993.
- Rye, R.O., Whelan, J.F., Harrison, J.E., and Hayes, T.S., 1984, The origin of copper-silver mineralization in the Ravalli Group as indicated by preliminary stable isotope studies., Montana, Bureau of Mines and Geology, Special Publication 90, p. 104-107.
- Sahinen, U.M., 1936, The Revais Creek mining district, Sanders County, Montana. Unpublished Montana Bureau of Mines and Geology Manuscript. 17 p.

- Sample, R.D., 1942, Report on the Green Mountain Copper Mine (formerly Drake or Dixon Mine) Revais Creek district, near Dixon, Sanders County, Montana. Unpublished U.S.G.S. War Minerals Investigation. 14 p.
- Sears, J.W, Chamberlain, K.R. and Buckley, S.N., 1998, Structural and U-Pb geochronological evidence for 1.47 Ga rifting in the Belt basin, western Montana, *Canadian Journal of Earth Sciences*, v. 35 pg. 467-475.
- Sears, J.W, 1990, Unpublished mapping.
- Sims, J.L., Jacob, J.P., Lauer, D., Skinner, L.L., and Sears, J.W., 1994, Petrogenesis of a sill-sediment complex, lower Belt Supergroup, Perma, Montana, *GSA Abstracts with Programs*, v. 26 (6), pg. 63.
- Watkinson, D.H. and Melling, D.R., 1992, Hydrothermal origin of platinum group mineralization in low-temperature copper sulfide-rich assemblages, Salt Chuck Intrusion, Alaska: *Economic Geology*, v. 87, pg. 175-184.
- Watkinson, D. H. and Ohnenstetter, D., 1992, Hydrothermal origin of platinum-group mineralization in the Two Duck Lake Intrusion, Coldwell Complex, Northwestern Ontario: *Canadian Mineralogist*, v. 30, pg. 121-136.
- Wentlandt, R.F., 1982, Sulfide saturation of basalt and andesite melts at high pressures and temperatures: *American Mineralogist*, v. 67, pg. 877-885.
- Winston, D., 1986, Sedimentation and tectonics of the Middle Proterozoic Belt Basin and their influence on Phanerozoic compression and extension in western Montana and northern Idaho, *in* Pederson, J.A., ed., *Paleotectonics and sedimentation in the Rocky Mountain Region, United States: American Association of Petroleum Geologists Memoir*. v. 41 pg.3-20.
- Winston, D. and Link, P.K., 1986, Middle Proterozoic rocks of Montana, Idaho, and Eastern Washington: The Belt Supergroup. *In* *Precambrian: conterminous U.S. Edited by J.C. Reed et al.* Geological Society of America, *The Geology of North America*, v. C-2 pg. 487-517.
- Wood, S.A., Mountain, B.W., and Fenlon, B.J., 1989, Thermodynamic constraints on the solubility of platinum and palladium in hydrothermal solutions: Reassessment of hydroxide, bisulfide, and ammonia complexing: *Economic Geology* v. 84, pg.2020-2028
- Wood, S.A., 1987, Thermodynamic calculations of the volatility of the platinum group elements (PGE): The PGE content of fluids at magmatic temperatures, *Geochimica*

et *Cosmochimica Acta*, v. 51, pg. 3041-3050.

Zartman, R.E., Peterman, Z.E., Obradovich, J.D., Gallego, M.D., and Bishop, D.T., 1982, Age of the Crossport sill near Eastport, Idaho: in Reid, R.R. and Williams, G.A., eds., Society of Economic Geologists, Coeur d'Alene Field Conference, Idaho, 1977: Idaho Bureau of Mines Bulletin 24, p. 61-69.

Zientek, M.L., 1993, Personal communication.

Zientek, M.L., Ripley, E.M., 1990, Sulfur isotopes of the Stillwater Complex and associated rocks, Montana, *Economic Geology*, v.85, pg. 376-391.

Zientek, M.L., Ripley, E.M., and Cooper, R.W., 1982, Sulfur isotopic studies of the Stillwater Complex, Montana: *Geological Society of America Abstracts with Programs*, v. 14, p.652

Zientek, M.L., 1983, Petrogenesis of the Basal zone of the Stillwater Complex, Montana [Ph.D. Thesis]: Stanford University, Stanford, California, 246 p.